

EXAMINING THE IMPACTS OF BEAVER DAM ANALOGUES AND  
GROUNDWATER STORAGE ON MINERS CREEK, CALIFORNIA

By

Miles Munding-Becker

A Thesis Presented to

The Faculty of California State Polytechnic University, Humboldt

In Partial Fulfillment of the Requirements for the Degree

Master of Science in Environmental Systems: Geology

Committee Membership

Dr. Laura Levy, Committee Chair

Dr. Margaret Lang, Committee Member

Dr. Hillary Jenkins, Committee Member

Dr. Margaret Lang, Program Graduate Coordinator

December 2022

## ABSTRACT

### EXAMINING THE IMPACTS OF BEAVER DAM ANALOGUES AND GROUNDWATER STORAGE ON MINERS CREEK, CALIFORNIA

Miles Munding-Becker

Beavers have been altering streams in North America for millions of years by impounding water behind their dams. The recent historical removal (intensely throughout the 18<sup>th</sup> and 19<sup>th</sup> century) of these dams altered the hydrology in low gradient streams from dynamic anastomosing streams and wet meadow complexes to incised channels with little structural diversity. Anthropogenic structures called Beaver Dam Analogues (BDAs) are used as a restorative process by mimicking natural beaver dams that can reverse channel incision, increase ponded and groundwater storage, and provide low velocity habitat for aquatic species and vegetation. A system of four original BDAs were installed on Miners Creek and monitoring data was collected over the course of six years from water year 2016-2021. Here, monitoring data from water year 2021 is used to determine reach-scale storage dynamics and BDA recharge, ponded storage, and habitat suitability for juvenile Coho (*Oncorhynchus kisutch*) based on ponded depth. The reach on Miners Creek was found to be predominantly a losing reach with BDA recharge only occurring during the onset of the wet season. At their maximum, ponds were found to increase storage by up to ~36 m<sup>3</sup>. During the dry summer months, however, there was not sufficient habitat to support recruitment of juvenile Coho. This was shown to be

predominantly due to issues stemming from a combination of issues pertaining to BDA structural integrity, water availability, and seasonal changes in water usage within the watershed.

## ACKNOWLEDGEMENTS

I would like to thank the many people who have guided me throughout my research. Guidance has been provided to me by my advisers Laura Levy, Margaret Lang, and Hillary Jenkins. Others in academia who have provided me with guidance have included but are not limited to Jasper Oshun, James Graham, and Christopher Dugaw. Early in my research I enjoyed the openness of the BDA community and people such as Ellen Wohl, Julianne Scamardo, and Michael Pollock provided me with their time to discuss my project and the stream restoration world in general. Paul Powers dedicated several hours to aid me in my understanding of Relative Elevation Modeling. While it was not included in my project, I am grateful for his insight.

Alongside my academic support I received support both fiscally and emotionally from the Scott River Watershed Council (SRWC). Members included: Erich Yokel, Charnna Gilmore, Betsy Stapleton. I must specifically acknowledge Erich Yokel for showing me how to use and operate the data loggers and instruments I used for my research. Additionally, I thank him for friendship during some uncertain times. Without the members of the (SRWC) this research would not be possible.

I received the motivation needed to complete this project through the support of my friends and family. Without them, I would not have finished, and I thank them for their patience and support over the past several years.

They include but are not limited to: Madeline McNerthney, Wyeth Wunderlich, Risa Okuyama, Hannah Joss, Clark Stevenson, Bri Tiffany, Pete and Malia Duin, Jesse



Clapoff, Noah Lashley, Matt Gustavson, Dylan Harper, Ben Swank, Joesept Eastman, Micah Cotton, Hunter Stone, Hannelore Polito, Peter Munding-Becker, Joyce Tuttle, Ashley Becker-Whipple, David Whipple, Uncles, Aunts, Cousins, Grandparents!

I would like to thank the California Department of Fish and Wildlife for their funding, as well as the Humboldt Geology Department for their support in sending me to SRF (Salmon Restoration Federation). The most significant contribution to my research was made by my father Peter Munding-Becker and my Aunt Hannelore Polito. I love you both and thank you. In memory of Daphne Reynolds.

## TABLE OF CONTENTS

ABSTRACT	ii
ACKNOWLEDGEMENTS	iv
LIST OF TABLES	ix
LIST OF FIGURES	x
LIST IF APPENDICES	xvi
1. INTRODUCTION	1
1.1 The North American Beaver	1
1.2 Beaver Dam Analogues	4
1.3 Miners Creek BDA Study	6
1.4 Study Site	7
2. METHODS	19
2.1 Data Collection & Processing	19
2.1.1 Shallow Groundwater Well Network	19
2.1.2 Rain Gauge	21
2.1.3 Discharge Measurements	22
2.2 Water Balance	27
2.3 Reach Scale Storage Dynamics and Ground Water Storage	28
2.3.1 Reach Scale Dynamics	29
2.3.2 Ground Water Storage	30
2.4 Beaver Dam Analogues Storage Dynamics	32
2.4.1 Beaver Dam Analogues Water Surface Elevation	32
2.4.2 Beaver Dam Analogue Poned Volume Estimates	33
3. RESULTS	35

3.1 Miners Creek Hydrology	35
3.1.1 Shallow Groundwater Well Network	35
3.1.2 Discharge and Precipitation	37
3.1.3 Water Balance	39
3.2 Miners Creek Storage	42
3.2.1 Reach Scale and Ground Water Dynamics	43
3.2.2 BDA Water Surface Elevation	48
3.2.3 BDA Poned Water Volume Estimates	49
3.2.4 Storage Comparisons	51
4. DISCUSSION	55
4.1 Shallow Groundwater Well Network	55
4.2 Water Balance	60
4.3 Reach Scale and Ground Water Storage Dynamics	63
4.3.1 Reach Scale Storage	63
4.3.2 Groundwater Storage	66
4.4 BDA Storage Dynamics	67
4.4.1 BDA Structure	67
4.4.2 Sediment Aggradation	70
4.4.3 Hydraulic Conductivity	72
4.4.4 Precipitation	75
4.4.5 BDA Poned Volume Estimates	76
5. NATURAL BEAVER DAMS CASE STUDY	78
6. RECOMMENDATIONS	83

7. CONCLUSIONS	85
REFERENCES	88

## LIST OF TABLES

Table 1. Summary statistics for WY 21 water balance on Miners Creek broken down by Wet, Dry, and Total season values. *US = upstream **DS = downstream.....	41
Table 2. Data sheet for Well 4 used to compare field WSE to WSE calculated by data loggers.....	97
Table 3. Summary results for developing Sensor Stage vs Discharge relationship and associated uncertainties at upstream station. ....	107
Table 4. Summary results for developing Stage vs Discharge relationship and associated uncertainties at downstream station. ....	108

## LIST OF FIGURES

Figure 1. Geographical location of the Scott River watershed located within the greater Klamath watershed. (Madeline McNerthney, CPH, Miles Munding-Becker CPH). Inset map provides the location of the Scott Valley within the State of California. .... 8

Figure 2. The ~20 km<sup>2</sup> Miners Creek watershed. In the hillshade, white represents areas of higher elevation while beige represents lower lying valley floor topography. The line cutting across the southwestern corner of the watershed indicates where snow may accumulate. .... 10

Figure 3. Miners Creek study site. Flow direction is from south to north and there are two seasonally active side channels depending on flow conditions. The upstream side channel is located west of the triple BDA configuration and the downstream side channel is west of well 2. Labels 1.1,1.2,1.3 corresponded to BDA numbers..... 11

Figure 4. Number of Coho Redds on lower Miners Creek during Water Year 2020. Twenty-two Redds were observed along with four carcasses. Redds and carcasses were flagged both upstream and downstream of the BDAs. (Erich Yokel, SRWC)..... 13

Figure 5. BDA labels and outlined ponded areas on December 18<sup>th</sup>, 2022. Image is meant for visual purposes and is not used for quantitative values. .... 15

Figure 6. Underlying geology of the Miners Creek Watershed: gr<sup>Mz</sup> - Mesozoic granite, quartz monzonite, granodiorite, and quartz diorite. Sch - Schists of various types; mostly Paleozoic or Mesozoic age; some Precambrian. Pz - Undivided Paleozoic metasedimentary rocks. Includes slate, sandstone, shale, chert, conglomerate, limestone, dolomite, marble, phyllite, schist, hornfels, and quartzite. um - Ultramafic rocks, mostly serpentine. Minor peridotite, gabbro, and diabase; chiefly Mesozoic. SO - Sandstone, shale, conglomerate, chert, slate, quartzite, hornfels, marble, dolomite, phyllite; some greenstone (California Department of Conservation)..... 17

Figure 7. Photos of the upstream and downstream gauging stations on Miners Creek. (Erich Yokel) ..... 24

Figure 8. Graph of WSE vs time for study duration (11/06/20-06/20/21). Each line represents the WSE for a well with its corresponding number. Wells on river right (RR), river left (RL), and in-stream proximal (~IS) show that all wells decline after the onset of irrigation season shown by the red rectangle. Additionally, all RR wells receive return flow depicted by the blue ovals. For spatial representation of each well please refer to Figure 4. .... 36

Figure 9. Graph of WSE vs. time for all wells on the same transect from 03/27/21-05/14/21. This period highlights irrigations impact on Wells. Each line is labeled to represent location (i.e., dotted = river left, solid line = instream proximal, dashed = river right). Lines are also numbered with corresponding Well number. Minor gridlines represent 0.05 m and major gridlines are 0.25 m. Wells 11 and 12 show a reverse trend compared to other wells where river left wells are higher in elevation than river right wells. This could be due to differences in hydraulic conductivity, substrate, or groundwater flow vectors. .... 37

Figure 10. Graph of discharge vs. time for study duration (11/06/20-06/20/21). Lines represent variation in upstream and downstream discharge. Rectangles show precipitation (mm) by day with a secondary y-axis. The data indicated that there are notable differences in discharge between upstream and downstream gauging stations depending on the time of year. .... 38

Figure 11. Graph of percent of county in drought index vs time (2020-2022). Water year 2021 is outlined by the black rectangle. (NIDIS) ..... 39

Figure 12. Graph of the temporal changes in water storage (mm) from the water balance during the study period (11/06/20-06/20/21). ET, evapotranspiration, represents water lost due to plant uptake or evaporation. P is precipitation (mm) from the onsite tipping bucket and downstream is runoff which is Q scaled by the upstream contributing area. Miners Creek maximum dynamic storage was in mid-February and the runoff ratio remained low even as dynamic storage increased by 167 mm from December 2020 to February 2021. \*Upstream runoff is accounted for in dynamic storage, it is not shown as it almost identically follows the trend of the downstream gauging station. Overall, this deficit really depicts the lack of precipitation..... 40

Figure 13. Graph of accumulation of water (mm) for all components of the Water Balance ( $\sum ET$ ,  $\Delta S$ ,  $\sum$ Downstream Runoff,  $\sum$ Precipitation) and groundwater storage from 11/06/20-06/20/21. For the purposes of this figure the sum of upstream runoff is excluded because it very closely resembles upstream runoff..... 41

Figure 14. Graph of discharge (Q) vs time from 10/01/20-11/26/20. Precipitation (mm) is on the secondary y-axis. Upstream discharge is shown prior to the study period to provide a sense of the antecedent conditions. The red square highlights the window where flow became continuous..... 44

Figure 15. Graph of WSE vs time from 10/01/20-11/26/20. Precipitation (mm) is on the secondary y-axis. Well 3 is instream proximal, with Wells 5 and 7 directly instream. Even under xeric conditions, there is dry season recharge (over 1 m at Well 7)..... 45

Figure 16. Groundwater storage, Precipitation, and  $\Delta Q$  over the course of the study (11/6/20-06/20/21). Storage stages are broken into four categories: Initial=Initial Storage, Steady=Steady State, Secondary=Secondary Storage, Baseflow. .... 46

Figure 17. Gaining and losing stream reach conditions between upstream and downstream gauging stations for water year 2021. Gaining stream conditions are shown in red with positive values. Losing conditions are represented by blue with negative values. The bounds of uncertainty provide support for the characterization of reach scale storage dynamics. The gaining period in mid-April can either represent contributions from groundwater storage to the stream or return flow during irrigation. .... 47

Figure 18. Weekly WSE (m) from Well 9 vs time (water year 2019-2021). Secondary y-axis shows daily precipitation (mm) during the same period. Pond bottom was only surveyed in water year 2021, therefore WSE (m) is used relative to masl (meters above sea level) instead of ponded depth. This is because pond morphometry can vary by year depending on the movement of sediment. .... 49

Figure 19. Conceptual model of ponded volume relative to BDA average crest elevation (left y-axis) and percent full (right y-axis). Volumes are separated into maximum, wet season average, and dry season average volumes with dashed lines. The brown horizontal cylinders represent the horizontal willow weaves that make the BDA structure. Bottom spheres represent cobbles that support the base of the BDA structure leading down to the pond bottom. These cobbles support the upstream section of each BDA. .... 50

Figure 20. The relationship between BDA storage vs upstream discharge. Each data point represents a daily time step separated by storage stages. Blue circles show a shift in BDA storage and upstream discharge at the onset of irrigation which overlap partially with *Secondary Storage* into *Baseflow* conditions. The drop in both BDA storage and upstream flow indicate how changes in water use effect Miners Creek. .... 53

Figure 21. The relationship between BDA storage vs GW Storage. Each data point represents a daily time step separated by storage stages. Blue circles show a shift in BDA storage and GW Storage at the onset of irrigation which overlap partially with *Secondary Storage* into *Baseflow* conditions. There is large decline in BDA storage during the onset of irrigation, but only minor changes in groundwater storage, which highlight BDAs dependency on surface flows. .... 54

Figure 22. Well WSE (m) rise (primary y-axis) upstream discharge (secondary y-axis) over water year 2021. Numbers on the graph indicate Well number while change in line pattern indicates whether the well is instream proximal (~IS), river right (RR) or river left (RL). Peak discharge events, regardless of magnitude, generally produce a similar rise in head throughout the shallow groundwater well network. .... 56



Figure 23. Well WSE and upstream discharge throughout the study. As discharge increased in an instream proximal well (Well 3) and a groundwater well (Well 11), increases in WSE became less significant as upstream discharge increased. In A), increases in upstream discharge resulted in an increase in WSE until ~8000 m<sup>3</sup>/day, after which there was no significant rise in WSE. In B), WSE increased rapidly under low discharge and maximum WSE occurred at ~2000 m<sup>3</sup>/day. Larger increases in discharge did not result in a greater WSE. .... 58

Figure 24. The relationship between total dynamic storage (x-axis) and runoff at the upstream and downstream gauging stations (y-axis). Generally, runoff only begins to increase once total storage exceeds 225 mm. However, this is unlikely to represent a maximum change in storage threshold. More precipitation would be needed to further establish this relationship. .... 63

Figure 25. Graph of WSE (m) vs time (03/28/21-5/15/21). A) Shows the increase in head at well 12 (river right) and B) shift from losing to gaining conditions along well 4, 5, and 6 transect. This change in conditions coincide with the shift from *Secondary Storage* to *Baseflow* conditions. .... 65

Figure 26. Change in WSE during *Baseflow* conditions. Overall, there is head stability, however, no recharge from groundwater sources or elsewhere. Meaning that none of these instream wells received gains throughout baseflow. .... 67

Figure 27. Survey photo of BDAs on Miners Creek 01/07/2019. Photo is looking Southwest towards well 9, slightly downstream of BDA 1.1. (Photo by Erich Yokel).... 68

Figure 28. Photo of BDA taken 01/12/2022. This photo does not overlap with the study period and is used to provide perspective on changes overtime. Photo is from almost the same perspective as Figure 27. This photo is taken slightly above BDA 1.1 still facing Southwest. (Photo by Dominic Schenone) ..... 69

Figure 29. Image of portion of BDA 1.1 that is always in direct wetted contact as stream stage fluctuates. All the BDA fill material has been washed out with the addition of several willow weaves. .... 70

Figure 30. Lidar data showing the difference between 2018 and 2010 imagery (2018 – 2010). This data only captures aggradation of sediment up until the reconfiguration of the BDAs in water year 2019. The aggradation shown west of river left Wells (1,4,13,8,11) is likely due to cattle grazing the adjacent hillside. .... 71

Figure 31. Elevation of surveyed well ground surface elevations from water year 2016 and water year 2021. Significant aggradation by wells is highlight by rectangles between survey points. Most instream wells, highlighted be blue squares, had significant

aggradation. Aggradation around Wells 3 and 6 is most likely due to external factors such as cattle grazing and is not associated with stream deposition. .... 72

Figure 32. Longitudinal profile of stream channel on Miners Creek on 7/1/21 in comparison to other times of the year. Below the bedrock boundary (Zb), shown by the solid black line, the material is assumed to match the fractured Serpentinite at the upstream (US) and downstream (DS) gauging stations. Between the Zb and the channel elevation in yellow with a light blue solid line, is the fill of decomposed granite. This figure makes assumptions on connectivity of Zb material based on where instream proximal wells reached a resisting layer. Here we see that groundwater quickly declines after the BDA pond dries out..... 74

Figure 33. Satellite imagery of Miners Creek and French Creek restoration sites, delineated by black rectangles. Red circles indicate the observed total Redds (spawning beds) during water year 2019 as surveyed by Erich Yokel (SRWC). .... 79

Figure 34. Rise in WSE at French Creek beaver dam from 09/01/21-10/04/21..... 80

Figure 35. Rise in WSE relative to initial values on 09/01/21- 10/01/21. Here we see an increase in WSE on Miners Creek in Wells 11,12,7, and 2. The increases in WSE in individual wells but not the system suggests that there was no regional pulse that may have caused an increase in stream stage on French Creek during the construction of the Beaver Dam. .... 81

Figure 36. Game camera photo of Beaver Dam construction on French Creek. There is a pair of Coho (bottom left) and a beaver (upper right). .... 82

Figure 37. Precipitation at both Callahan and Miners Creek stations from (11/06/20-9/31/21). .... 98

Figure 38. Miners Creek precipitation vs Callahan precipitation. The equation used to estimate precipitation is shown on the graph as well as the  $R^2$  value. .... 99

Figure 39. Upstream and Downstream rating curves, associated  $R^2$ , and equation..... 101

Figure 40. Upstream discharge (dashed line) and *Flowtracker2* Uncertainty (solid lines). The upper and lower estimates are estimated by making rating curves that are  $\pm$  the estimated uncertainty produced by the *Flowtracker2* (Table 3). .... 102

Figure 41. Downstream discharge (dashed line) and *Flowtracker2* Uncertainty (solid lines). The upper and lower estimates are estimated by making rating curves that are  $\pm$  the estimated uncertainty produced by the *Flowtracker2* (Table 4). .... 104

Figure 42. Each discharge measurement used to develop upstream and downstream rating curves plotted on their respective daily discharge value. .... 108

Figure 43. Well head for the furthest downstream transect (transect 1) throughout the study period and the system wide average. Precipitation is on the secondary y-axis. This shows that the system average will vary from individual well head. .... 110

Figure 44. Cross section of Transect 1 water surface elevation at each well (1,3,2), ground surface (GS) and boundary layer Zb. Flow would be going into the page and the overall cross-sectional gradient is from river left to river right Wells. Well 3 is an instream proximal Well..... 112

Figure 45. Cross section of Transect 2 water surface elevation at each well (4,5,6), ground surface (GS) and boundary layer Zb. Flow would be going into the page and the overall cross-sectional gradient is from the stream to RL and RR wells until baseflow conditions. Well 5 is an instream much of the year, however, becomes proximal sometime in spring as conditions dry out. .... 113

Figure 46. Cross section of Transect 3 water surface elevation at each well (8,9,10), ground surface (GS) and boundary layer Zb. Flow would be going into the page and the overall cross-sectional gradient is from RL and RR wells to the stream. Well 9 is instream proximal and is assumed to closely resemble river stage. .... 114

Figure 47. Cross-section of transect 4 water surface elevation at each well (11,15,12), ground surface (GS) and boundary layer Zb. Flow would be going into the page and the overall cross-sectional gradient is from the stream to RL and RR wells. Well 15 is instream stilling well, therefore, there is no estimate of Zb associated with this well. .. 115

## LIST OF APPENDICES

Appendix A: Water Surface Elevation .....	95
Appendix B: Precipitation.....	98
Appendix C: Discharge.....	100
Appendix D: Substrate Sampling.....	109
Appendix E: Ground Water Storage.....	110
Appendix F: Reach Scale Storage.....	111

## 1. INTRODUCTION

### 1.1 The North American Beaver

The North American Beaver, *Castor canadensis* has contributed to the creation of anastomosing streams by building dams (Machen, 2016). Pre-colonization, many floodplains in North America were anastomosing systems and wetlands developed via biogenic features, such as large wood and beaver dams (Walter & Merritts, 2008). Importantly, these biogenic features have been influencing our streams since the Carboniferous Period (~359 Ma), coinciding with the evolution of tree-like plants (Wohl, 2013b). *Castor* diverged from a semi-aquatic beaver during the Miocene epoch (~23-5 Ma) with at least 10 other species (Rybczynski et al., 2010), making the contribution of wood from beaver structures a legacy in North American streams for millions of years.

Beavers build dams to extend their foraging habitat and to create protection from predators (Naiman et al., 1988). The dams that beavers construct result in elevated water tables that can direct water around dams in both high and low flow conditions, attenuating late season water table decline (Westbrook et al., 2006). In the Canadian Rockies beaver activity has been shown to create a stable water table within a suitable elevation to sustain peat formation and increase water storage (Karran et al., 2018). Beaver ponds themselves, also provide critical water storage. *Castor fiber* was able to increase storage by holding 1000 m<sup>3</sup> of water via the creation of 13 dams in Devon,

Southwest England (Puttock et al., 2017). These dams were also shown to lower diffuse pollutant loads of nitrogen and phosphate.

Beaver dams can increase instream stage and impound water that creates a backwater effect and decreases stream velocity (Stout et al., 2017). Decreased velocity creates a depositional environment where sediment can aggrade and reconnect channel elevations to the floodplain (Pollock et al., 2007). A connected floodplain allows for creation of braided channels networks allowing for further dam development (Polvi & Wohl, 2012). These cycles occur repeatedly by raising the water table which leads to channel widening, aggradation, and ultimately the breakdown and filling of reservoirs behind dams. When beaver dams break down, channel braiding occurs and the dams are eventually reconstructed (Pollock et al., 2014).

Beaver benefits also extend to the biotic community. Beaver impacts on fish have been a contentious area of research with studies citing both beneficial (Pollock et al., 2004, Rosell et al., 2005, Johnson, 2006) and detrimental (Cunjak & Therrien, 1998, Cairns et al., 2012, Malison et al., 2016) consequences. Positive benefits include, but are not limited to, higher fish abundance and productivity, species diversity, and rearing habitat. Detrimental effects include impediment of fish migration, disconnection of floodplain habitat, and excessive water temperature and low dissolved oxygen. A meta-analysis of 108 articles regarding interactions between beaver and fish, however, concludes that benefits of beaver on fish populations outweigh negative impacts and many negative impacts may be negligible or short lived (Kemp et al., 2012).

The overall removal of beaver dams throughout the 18<sup>th</sup> and 19<sup>th</sup> century also caused significant impacts to stream systems, however, the presence of other legacy effects such as deforestation (Marsh 1864, James 2019), channelization (Shields et al 1995) and mining (Harter and Hines, 2008), make these impacts difficult to quantify (Wohl, 2021).

Science has only recently documented the ecosystem benefits provided by beaver. Unfortunately, the advances in post-colonial understanding of beaver comes more than four centuries after the beginning of their near extinction and in many cases their total extirpation from areas throughout North America (Naiman, 1988). The North American fur trade began as early as the 1500s with European fisherman casually exchanging beaver pelts in Newfoundland. These modest beginnings soon cascaded into industrial scale extraction with the creation of infamous companies such as the Hudson Bay Company and others extracting beaver through the 19<sup>th</sup> century (Goldfarb, 2018, p 41-54). The estimated beaver population declined from 60-400 million in North America to 6-12 million (Naiman et al., 1988, Ringelman, 1991).

While beaver's populations have since rebounded, the benefits they provide now occur at a much smaller scale. Just as we now understand the benefit of having beaver on the landscape, there is also a deeper knowledge of what has been lost. As beaver dams are removed by humans, the geomorphology is likely to evolve from wetland ecosystems into single thread channels lacking structural diversity that heavily impact riparian area structure (Green & Westbrook, 2009, Polvi and Wohl, 2012). This loss of woody debris and concentration of flows into a single thread channel can lower the riparian water table

through channel incision (Wohl, 2021). This leads to a more arid landscape where grasses can take hold, resulting in a simpler stream morphology that negatively impacts stream exchanges occurring in the hyporheic zone, while reducing overall retention of stream fluxes (Beschta & Ripple, 2009, Burchsted et al., 2010, Wohl, 2021).

Moving into an ever-warming climate, it is also important to mention that beaver dams act as carbon sinks. Dams capture organic carbon by entrapping sediment along with the organic matter within it. In Rocky Mountain National Park, it was estimated that beaver meadows account for between 8-23% of total carbon storage across 27 watersheds. Additionally, carbon storage decreased by more than a factor of three in areas where there were no longer beavers (Wohl, 2013a).

## 1.2 Beaver Dam Analogues

The cumulative benefits of beavers throughout low grade rivers have inspired a relatively new methodology for restoring riparian habitats. Beaver Dam Analogues (BDAs) are a restoration tool used to simulate the effects of naturally occurring beaver dams, by constructing dams in riparian habitats that have a similar morphology to natural beaver dams (Pollock et al., 2012). As a restoration tool, BDAs are considered a low-tech process-based restoration, defined as “A practice of using simple, low unit-cost, structural additions (e.g., wood and beaver dams) to riverscapes to mimic functions and promote specific processes” (Wheaton et al., 2019). These practices are used to increase the structural diversity of riparian ecosystems by forcing changes to channel hydraulics that amplify the geomorphic process (Wheaton et al., 2019), resulting in a more anastomosing



system, a complex system of webbed stream channels with vegetated islands (Cluer & Thorne, 2014).

Recently, studies have started to address if BDAs provide similar ecosystem benefits as natural beaver dams. BDAs have been shown to increase the density, survival, and production of steelhead trout in Bridge Creek, Oregon (Bouwes et al., 2016). This project consisted of two years of pre-installation data from 2007-2009 and three years of post-installation data 2010-2013. A year later, another study on Bridge Creek showed a moderation of diel temperature cycles during low flow via the increase of storage and surface/subsurface water exchange (Weber et al., 2017). A study on Red Canyon Creek had similar results regarding surface/subsurface water exchange, however, it was noted that exchange varied based on BDA structure size, with hyporheic exchanges being greater in BDAs with a greater height (Wade et al., 2020). Wade et al. (2020) also point out that ideal height of a BDA to promote exchange is likely specific to each site's hydrology and streambed sediment.

On the South Fork, a tributary to the Crooked River in Oregon, BDAs increased groundwater levels, promoted willow growth, and caused sediment aggradation (Orr et al., 2020). Groundwater levels and surface water levels also increased in Red Canyon Creek, Wyoming (Pearce et al., 2021). On Fish Creek in Colorado, BDAs also caused sediment accumulation 1-year post installation, however, there was no observed increase in the water table height (Scamardo & Wohl, 2020). Importantly, hydrologic impacts of BDAs will vary depending on structural density and water table increases will diminish with lateral distance from the stream (Munir & Westbrook, 2021). Coho salmon

(*Oncorhynchus kisutch*) and Steelhead trout (*O. mykiss*), two species that have spawned in systems with BDAs, have been shown to pass through and over BDAs at high success rates (Pollock et al., 2019, O’Keefe, 2021).

### 1.3 Miners Creek BDA Study

Success at various study locations indicate that there are aspects of BDA restoration that can be generally applied, but site-specific differences in hydrology, climate, geology, and land use practices make regionally specific studies critical (Johnson-Bice et al., 2018). Here, I present monitoring data from Miners Creek, California, a tributary stream with a 20.26 km<sup>2</sup> watershed (Figure 1). Miners Creek is a tributary to French Creek, one of the largest tributaries to the Scott River, located ~22 km southwest of Yreka, California. Miners Creek is of particular interest due to a combination of legacy effects that have impacted the region since the 1800s. These include, but are not limited to, deforestation, mining (hydraulic and dredge), industrial agriculture, beaver removal, and fire suppression (Sommarstrom et al., 1990).

My objectives in this study are 1) to present data from one of the first BDA projects in California to increase the data density required to address the function of BDAs as a stream restoration tool. This would fulfill the calls of action of better monitoring of BDAs across a range of regional influences, scale (watershed and site), and temporal dynamics (Bouwes et al., 2016, Lutz et al., 2019, Scamardo & Wohl, 2020); 2) to address the interplay between groundwater and surface water dynamics on a 500 m stream reach installed with four BDAs (one single BDA and a triple BDA configuration)

These objectives inform the following research questions: 1) How do reach-scale groundwater storage dynamics affect BDA recharge? 2) Do BDAs provide sufficient baseflow habitat that could support recruitment of juvenile Coho through baseflow conditions? 3) How much ponded habitat do BDAs store? Additionally, we provide data from field evidence that suggests that natural beaver dams can increase ponded habitat during baseflow in a critically dry year.

#### 1.4 Study Site

Miners Creek is a small creek that drains to French Creek, a large tributary to the Scott River Watershed in Northern California (Figure 1).



Figure 1. Geographical location of the Scott River watershed located within the greater Klamath watershed. (Madeline McNerthney, CPH, Miles Munding-Becker CPH). Inset map provides the location of the Scott Valley within the State of California.

The study site is a 500 m reach of Miners Creek, a 20 km<sup>2</sup> watershed (Figure 2) spanning elevations of 896 m to 2144 m. The study site is located ~175m upstream from the confluence of Miners Creek with French Creek (**Error! Reference source not found.**Figure 3). Most of the watershed (~98%) lies below an elevation where snowpack might accumulate (Streamstats V 4.7.0; USGS, 2022), therefore, the watershed receives little recharge in the form of snowmelt during critical recharge months (April-July).



Figure 2. The  $\sim 20 \text{ km}^2$  Miners Creek watershed. In the hillshade, white represents areas of higher elevation while beige represents lower lying valley floor topography. The line cutting across the southwestern corner of the watershed indicates where snow may accumulate.



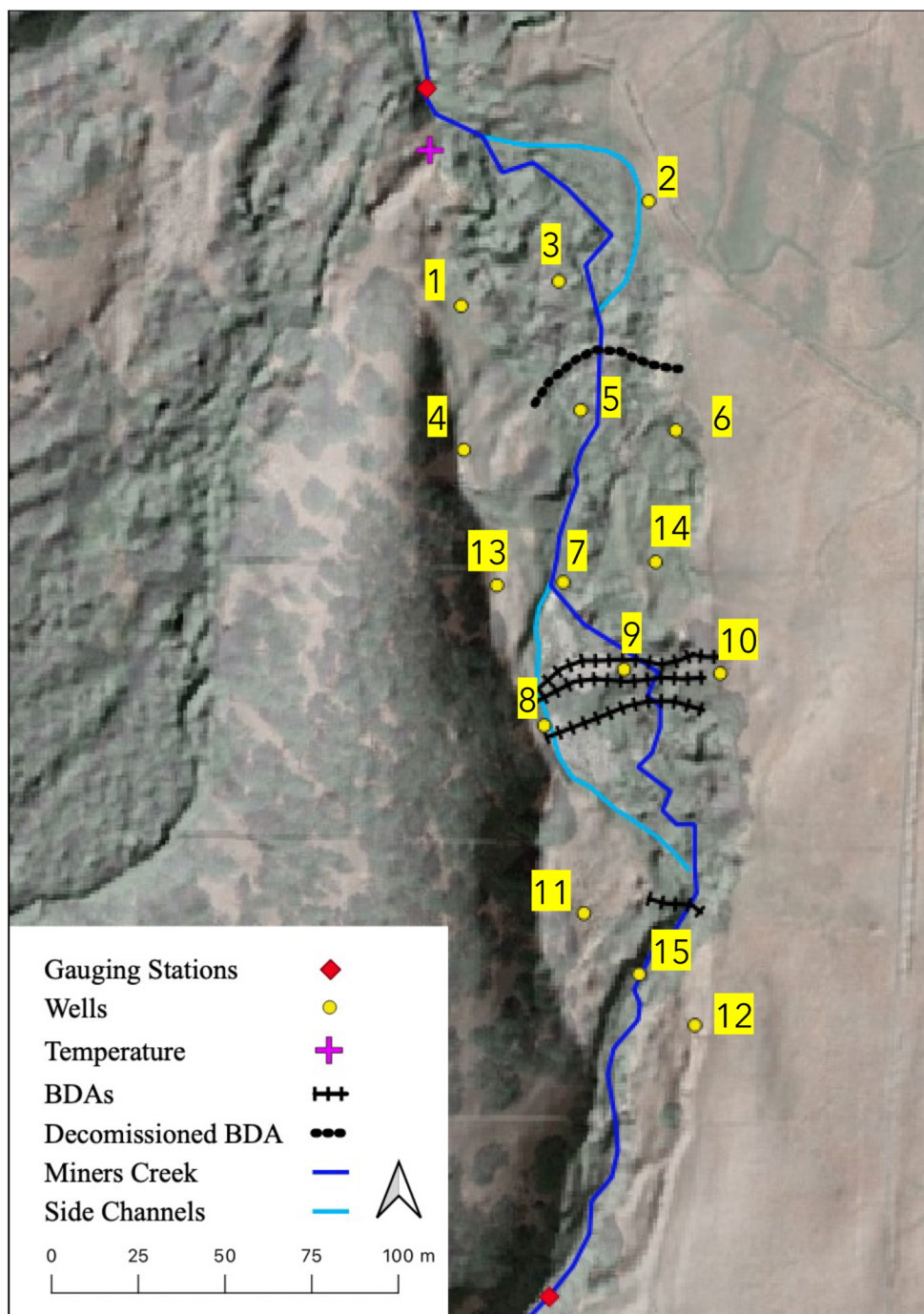
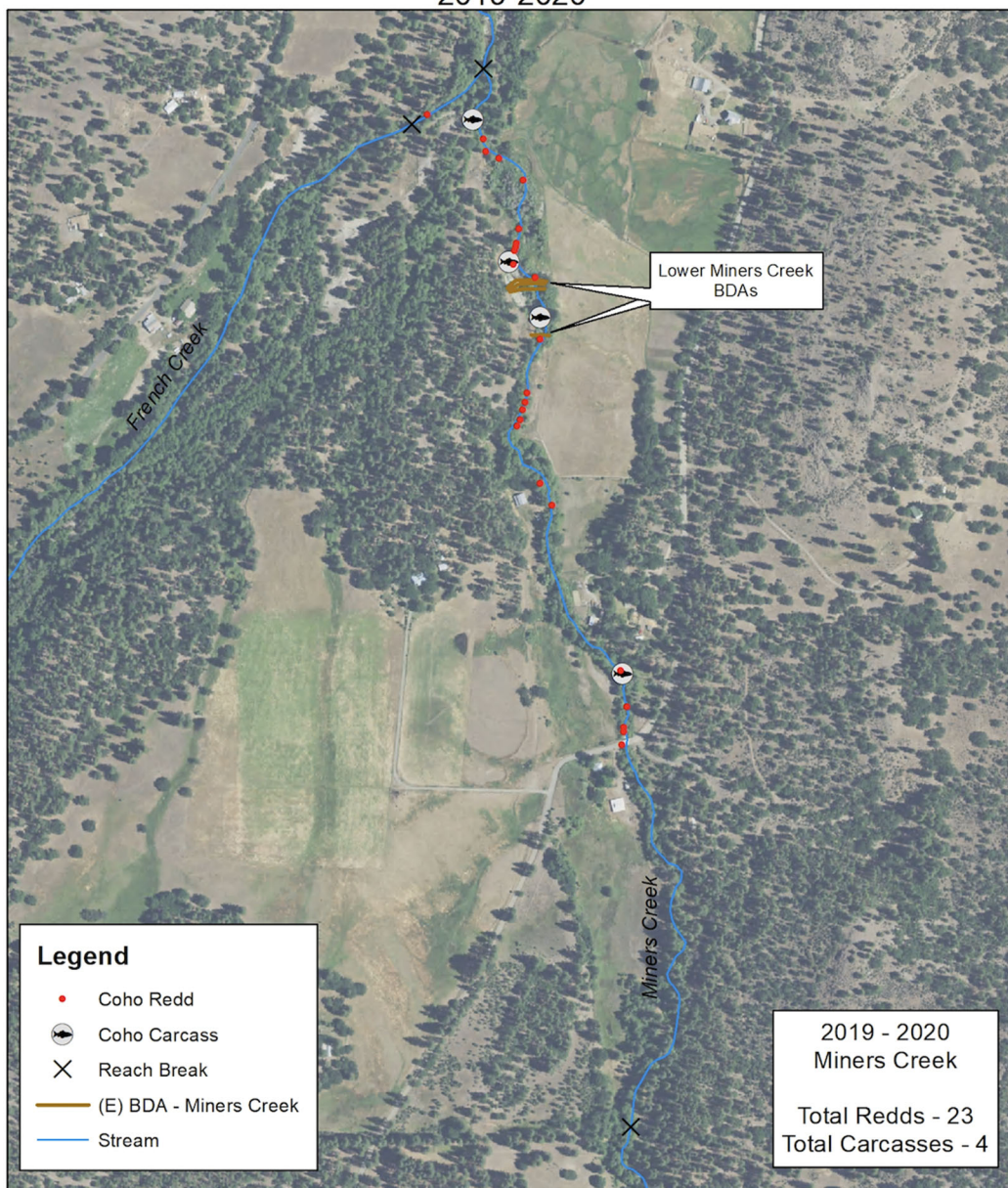


Figure 3. Miners Creek study site. Flow direction is from south to north and there are two seasonally active side channels depending on flow conditions. The upstream side channel is located west of the triple BDA configuration and the downstream side channel is west of well 2. Labels correspond to well number.

Miners Creek is highly utilized by Coho salmon (*Oncorhynchus kisutch*), hence forward referred to as “Coho”, and is considered a spawning “hotspot” (Quigley, 2006). Historical accounts suggest that the population of Coho on Miners Creek thrived. One family documented that it took only an hour to provide enough of a Coho catch to last a year (Denny, 1970). The CDFW Coho Recovery Strategy states that the population of Coho in Miners Creek needs improvement to establish a healthy population (CDFG, 2004). Miners Creek also has high Intrinsic Potential ( $IP > 0.66$ ), a metric used to identify potential spawning and rearing habitat (NMFS, 2014). This means that Miners Creek has been flagged as an important area to Coho and represents an area where they can be successful depending on stream flow. In recent years, there have been several documented accounts of Coho Redds (spawning beds) on Miners Creek in the BDA ponds and throughout the reach (Figure 4 **Error! Reference source not found.**).



Coho Salmon Redds - Lower Miners Creek  
2019-2020



SCOTT RIVER  
WATERSHED COUNCIL E. Yokel - 2/26/2020



0 250 500 1,000 Feet

Figure 4. Number of Coho Redds on lower Miners Creek during Water Year 2020. Twenty-two Redds were observed along with four carcasses. Redds and carcasses were flagged both upstream and downstream of the BDAs. (Erich Yokel, SRWC)

The prioritization of Coho motivated significant restoration efforts beginning in October of 2015 with the installation of two BDAs in the lower reaches of Miners Creek. In October 2018, three new BDAs were constructed, and one downstream BDA was removed due to fish passage concerns.

The site is instrumented with 15 shallow groundwater wells, two gauging stations, and a tipping bucket used to record precipitation. The project site is sometimes referred to as a “system” in this study. The term system refers to the contributing area between the upstream and downstream gauging stations. This contributing area is ~160,000 m<sup>2</sup>.

The BDAs considered in this study are the triple BDA configuration (BDA 1.1, 1.2, 1.3) located upstream of the decommissioned BDA. These BDAs create three ponded habitats that vary in size and shape throughout the water year depending on inputs (precipitation and discharge) (Figure 5).



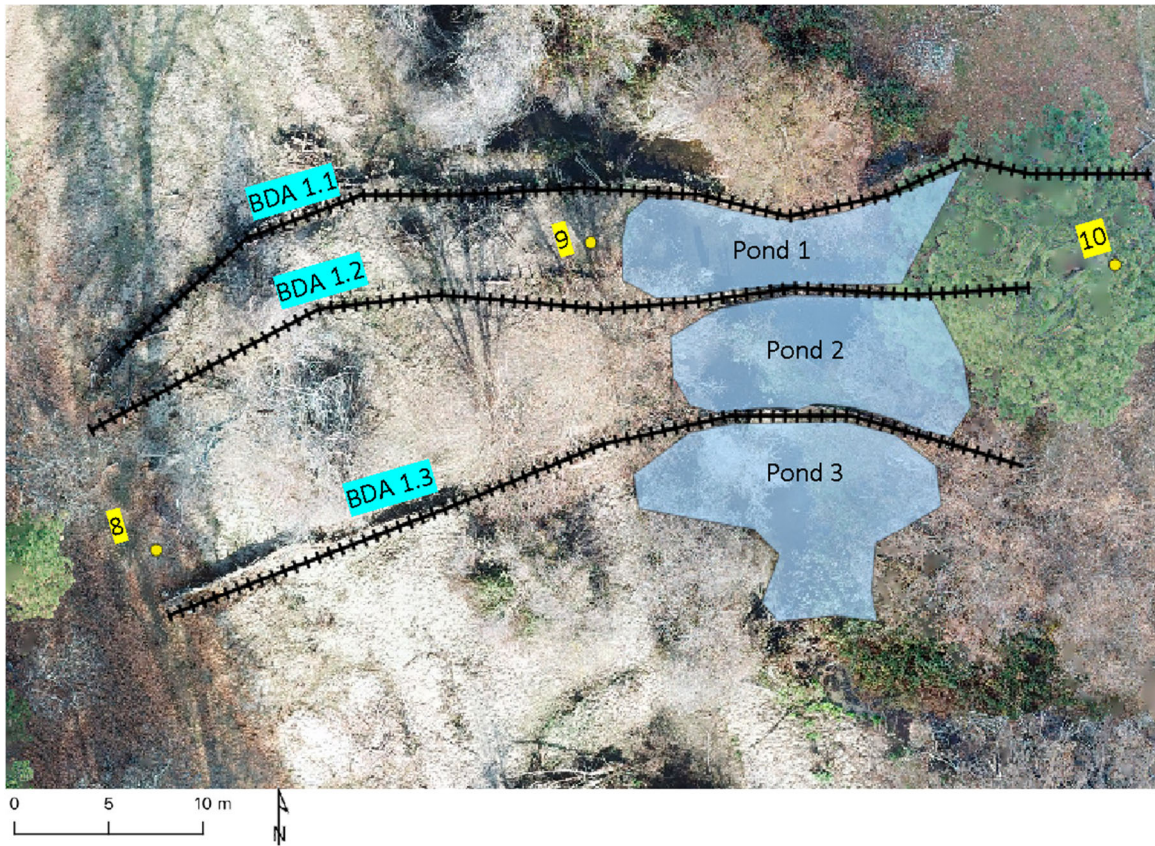


Figure 5. BDA labels and outlined ponded areas on December 18<sup>th</sup>, 2022. Image is meant for visual purposes and is not used for quantitative values.

The study reach is primarily a former floodplain with alluvial deposits derived from decomposed granite and metasedimentary rocks and is bounded by upstream and downstream in-channel bedrock of serpentinite.

The upper portion of the watershed (~47%) is the Russian Peak Pluton, consisting of Mesozoic granite and quartz monzonite. The rest of the watershed is a combination of metasedimentary rocks (i.e., slate, sandstone, shale) and ultramafic rocks (i.e., serpentine, gabbro) (Figure 6) (California Department of Conservation). Here we also note that beginning on 04/01 of each water year, flood irrigation occurs within the watershed.

Fields to the east of the restoration site are irrigated in unknown quantities. Fields upstream are also irrigated and managed by a local watermaster.

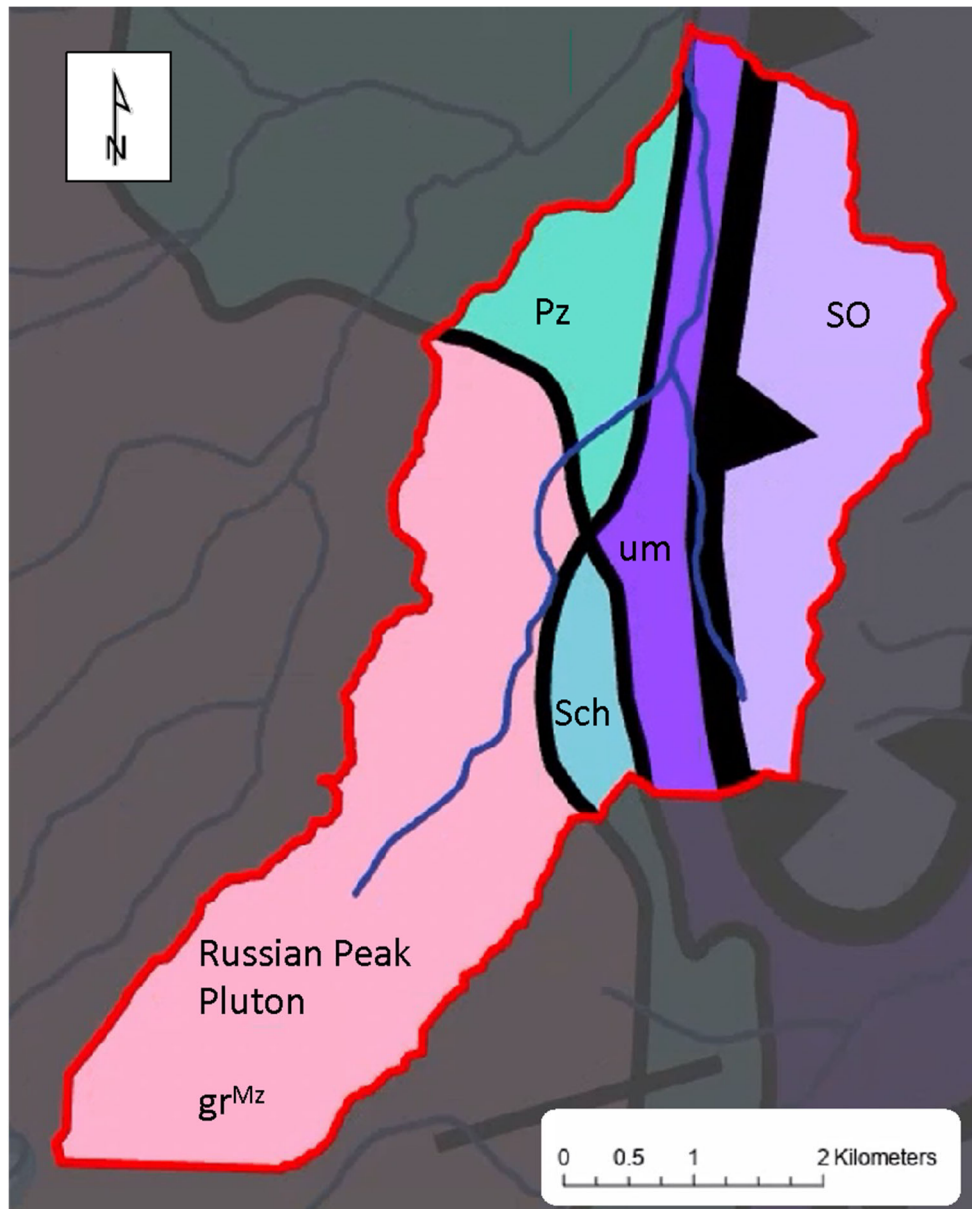


Figure 6. Underlying geology of the Miners Creek Watershed: gr<sup>Mz</sup> - Mesozoic granite, quartz monzonite, granodiorite, and quartz diorite. Sch - Schists of various types; mostly Paleozoic or Mesozoic age; some Precambrian. Pz - Undivided Paleozoic metasedimentary rocks. Includes slate, sandstone, shale, chert, conglomerate, limestone, dolomite, marble, phyllite, schist, hornfels, and quartzite. um - Ultramafic rocks, mostly serpentine. Minor peridotite, gabbro, and diabase; chiefly Mesozoic. SO - Sandstone, shale, conglomerate, chert, slate, quartzite, hornfels, marble, dolomite, phyllite; some greenstone (California Department of Conservation).

The large amount of granite in the system, coupled with evidence of hydraulic mining and logging, is the source of the high volumes of decomposed granite (DG) in the watershed. The DG is characterized by (<1mm) coarse and angular grains with a field estimated porosity of ~0.40. There is evidence of channelization, likely circa 1850s-1900s, to drain former wetlands and beaver complexes on the restoration reach and throughout the watershed.

## 2. METHODS

### 2.1 Data Collection & Processing

In this section, I discuss in detail the instruments used in this study to calculate the water table, precipitation, and discharge and the processes using these variables to estimate ponded and groundwater storage. I present the field protocols followed to ensure consistency with the data collection process. Each method also has an associated uncertainty; therefore, statements and equations are provided to estimate a range of uncertainty within the data.

#### 2.1.1 Shallow Groundwater Well Network

The shallow groundwater well network on Miners Creek consists of fifteen *HOBO* Honest Observer temperature and pressure loggers (ONSET, Bourne, MA). In water year (WY) 2016, members of the SRWC (Scott River Watershed Council) installed twelve wells (1-12) (**Error! Reference source not found.**Figure 3). On 01/21/2021, the SRWC placed three more wells to increase the density of the well network. Loggers were placed into each well and secured with metal wire to allow for the removal and monitoring of each sensor. Thirteen of the shallow groundwater wells are made of nominal 1 ½-inch NPS/SCH40/GRA 40 steel pipes with a 1 ½-inch Internal Diameter (ID). The remaining two shallow groundwater wells are stilling wells made of nominal 2-inch Polyvinyl Chloride (PVC). All wells are vented to reflect the ground water level.

Wells were monitored nine times throughout WY 2021. During each field visit, the data from each well was downloaded and loggers were inspected. Field protocol was conducted in the following order:

1. Pick up the necessary tools from the office (field laptop, data couplers, data log sheet, and well sounder).
2. In the field, remove the well cap and logger. Record time and date in Pacific Time (PT).
3. Use a well sounder to measure depth to the water table and record it in a data log sheet (check multiple times).
4. Carefully remove any dirt or build up around the sensor and use a coupler to download data.
5. Look for warnings or data corruption once data is run through HOBOWare V 3.7.22 (software used for data loggers).
6. Name file: MinersCreek\_YearMonthDate.
7. Relaunch logger, secure logger cap, and lower carefully back into well.
8. Repeat these steps for all wells.

Loggers recorded temperature and pressure at 15-minute intervals. A nearby barometric logger is used to correct the sensor depth for atmospheric pressure influence. The sensor depth is then converted into the calculated water surface elevation (cWSE) by adding the sensor depth (ft) to the surveyed sensor elevation (ft). The surveyed sensor



elevation was surveyed during well installation and the sensor depth registers the amount of accumulated water from the surveyed sensor elevation.

$$S_d + S_e = cWSE \quad \text{Equation 1}$$

Where  $S_d$  is the sensor depth and  $S_e$  is the sensor elevation. The  $cWSE$  is then compared to the measured WSE ( $mWSE$ ) provided by the field measured depth to water table relative to a surveyed in Reference Point elevation (RP). The  $mWSE$  is used to assess sensor error (Appendix A). If the  $cWSE$  deviated from the  $mWSE$  by ( $>0.1\text{ft}$ ,  $>0.3048\text{ cm}$ ) the  $cWSE$  was adjusted to match the  $mWSE$ . If data was corrupted during the study, producing spurious, unreliable datapoints, they were removed and not used in any analysis. This resulted in wells 13 and 14 being removed from analysis for water year 2021.

All data was summarized into daily WSE using a Microsoft Excel Macro and was converted into metric units (m).

### 2.1.2 Rain Gauge

A HOBO rain gauge data logger RG3 (ONSET, Bourne, MA) was used to record precipitation (mm) from 11/06/20-09/30/21 (Figure 3). Precipitation data presented in this study is limited from 11/06/20-06/20/21, to match the period when the BDAs retain water. I do, however, discuss the role of precipitation prior to this period (when BDAs are dry) to highlight dry season recharge that occurred prior to the study period. The rain gauge collects continual precipitation via an internal tipping bucket that tips at 0.01-inch

(0.254 mm) intervals. Each tip of the bucket is considered an event and is registered by the rain gauge. The data was uploaded during some field visits and converted from the event data timestamps into mm/day. Accuracy of measurements vary based on the calibration of the instrument. The calibration accuracy is  $\pm 1\%$  (ONSET, 2005-2018). Additionally, snowfall can impact the accuracy of precipitation data; however, this is assumed to just affect the intervals and intensity of precipitation and not the overall quantity.

For time periods when the onsite rain gauge was not yet installed, data from the California Data Exchange Center (CDEC) Callahan Station (CHA) was used to estimate the Miners Creek precipitation data. This was done by plotting the Miners Creek and Callahan data for Water Year 2021. A linear trendline was then used to define the relationship between precipitation at Callahan vs Miners Creek. The linear equation was then used to calculate how much it might have rained at the project site in years without direct measurements (Appendix B).

I used data from the tipping bucket to assess a Wet and Dry season precipitation quantity. I defined these periods based on trends in precipitation. Ultimately the Dry Season was characterized by small, short-lived precipitation events that occur sporadically versus more consistent rainfall at higher magnitudes during the Wet season.

### 2.1.3 Discharge Measurements

Two gauging stations were established to record continuous discharge through Water Year 2021 (10/01/2020-09/30/21) (**Error! Reference source not found.**) (Figure

7). Discharge measurements were taken with a *FlowTracker2* (SonTek, San Diego, CA). Each gauging station had an 1 ¾-inch ID PVC stilling well supported by a steel t-post with a *HOB0* Honest Observer temperature and pressure logger (ONSET, Bourne, MA). Metal wire was attached to the cap of each logger and connected to the threaded cap of the stilling well. This allowed for easy removal and stability of the logger. Staff plates in engineering feet were adhered to each well with stainless steel metal fasteners. Loggers recorded data at 15-minute intervals. The upstream flow station was installed by the Scott River Watershed Council (SRWC) during water year 2020. The downstream flow station was established 11/06/20, by SRWC and California State Polytechnic University, Humboldt (CPH). Both gauging stations are in incised channels of serpentinite bedrock. The upstream gauging station was located ~116m upstream of the most upstream BDA. The downstream gauging station was located ~87m downstream of the decommissioned BDA. These locations were selected to measure the flow in the system upstream and downstream of the BDAs.



Figure 7. Photos of the upstream and downstream gauging stations on Miners Creek.  
(Erich Yokel)

Upstream discharge was measured from 10/1/20-09/30/21 and downstream discharge was measured from 11/6/20-09/30/21. Due to extremely low flows and precipitation; however, Miners Creek reach did not have continuous flow until 11/16/20 and Miners Creek flow became discontinuous again on 06/20/21. During discontinuous conditions, flow was hyporheic; therefore, I limited the analysis of upstream and downstream discharge from 11/6/20-06/20/21 to minimize errors that occur under extremely low flows ( $>0.02 \text{ m}^3/\text{s}$ ). This also resulted in one discharge measurement being discarded when assessing uncertainty (Appendix C).

Twelve measurements were collected at each gauging station at varying flow conditions throughout WY 2021 (Max 180 L/s, Min 4 L/s). I followed the same field protocol as the other technician (Erich Yokel) to avoid any sampling biases that may have arisen from different people collecting data. The protocol is as follows:

1. Set up a transect to establish the wetted width of the channel ( $\sim 3.66 \text{ m}$  upstream,  $\sim 2.86 \text{ m}$  downstream).
2. Record initial staff plate height and record the time.
3. Measure flow at  $\sim 15 \text{ cm}$  intervals along the transect to ensure minimal uncertainty (3.08-7.2%).
4. Record the calculated flow, uncertainty, end time, and end time staff plate height.

Data was analyzed using Microsoft Excel to develop a sensor stage and discharge relationship. If there was a change between the beginning staff plate stage or the end staff

plate stage throughout the duration of the measurement the average of the start and end time height was used. Recording both the staff plate stage and sensor stage (post processing) allowed for an additional check on the field measurement. If there were no significant differences observed between the staff plate stage versus the sensor stage measurements, then the sensor stage measurements were used as the values for the rating curves. These measurements could have an expected uncertainty of  $\pm 0.1\%$  (Onset, 2014-2018).

A rating curve was developed using a Least-Squares Regression model (Rstudio, 2022). The robustness of the model used to predict discharge ( $Q$  in  $m^3/s$ ) at varying sensor depths was established by the highest  $R^2$  and a low residual standard error. Two other models considering the highest and lowest uncertainty for each flow measurement were also developed to evaluate uncertainty in the flow time series calculated using these rating curves. Uncertainty in the rating curve was calculated by comparing error between the observed and predicted flows.

$$Error = \left( \frac{\left( \frac{\sum_{i=1}^n |Q_{observed} - Q_{predicted}|}{Q_{observed}} \right)}{n} \right) \quad \text{Equation 2}$$

Where  $Q_{observed}$  is the discharge measured with the *FlowTracker2*,  $Q_{predicted}$  is the discharge predicted by the rating curve, and  $n$  is the number of flow measurements collected at each station during water year 2021.

To convert from (m<sup>3</sup>/s) to daily flow volume (m<sup>3</sup>), the mean daily flow was multiplied by the number of seconds in a day.

$$Q_d = \left( \frac{1}{n} (\sum_{i=1}^n Q_i) \right) 86400 \quad \text{Equation 3}$$

Where,  $Q_d$  is daily flow,  $n$  is the number of 15-minute measurements in a day (96), and  $Q_i$  is the 15-minute discharge determined from 15-minute stage data using the station rating curve (m<sup>3</sup>/s).

## 2.2 Water Balance

An annual water balance is used to inform how inputs (precipitation and upstream runoff) and outputs (Evapotranspiration and downstream runoff) vary over the course of the study period. While this is not used in direct analysis of BDAs, the use of a water balance informs watershed-wide hydrology. I rearrange the water balance to track the dynamic change in storage over the study period:

$$\Delta S = \sum_{t=1}^T (Q_{up} + P) - (Q_{down} + ET) \quad \text{Equation 4}$$

Where  $Q_{up}$  is the upstream runoff (mm/day)  $\left( \frac{Q_{up}}{Upstream\ Area} \right)$ ,  $P$  is the on-site precipitation measured via a tipping bucket rain gauge (mm) (ONSET, Bourne, MA),

$Q_{down}$  is the downstream runoff (mm/day)  $\left(\frac{Q_{down}}{Upstream\ Area}\right)$ , ET is evapotranspiration (mm), and  $\Delta S$  is the dynamic change in storage (mm) including both the surface water and the subsurface aquifer. To measure ET,  $E_{to}$  (reference evapotranspiration) is multiplied by a crop coefficient  $K_c$ .

$$ET = E_{to} * K_c \quad \text{Equation 5}$$

$E_{to}$  is measured locally within the Scott Valley by a CIMIS (California Irrigation Management Information Systems) weather station. An initial  $K_c$  value of 0.6 was used from February 15<sup>th</sup> to November 15<sup>th</sup> and a  $K_c$  value of 0 was used for the remainder of winter months as per appendix 2-C of the *Scott Valley Integrated Hydraulic Model* (Foglia et al., 2013). This value of 0 for  $K_c$  is used based on temperatures that occur in the valley throughout this time that result in no use by plants.

### 2.3 Reach Scale Storage Dynamics and Ground Water Storage

This section includes the methods for reach scale and ground water storage dynamics. Reach scale dynamics refers to the storage conditions of Miners Creek (surface flows) while ground water storage dynamics refers to the filling of the adjacent aquifer. These topics are addressed together because there is an exchange between these dynamics throughout the water season.



### 2.3.1 Reach Scale Dynamics

Storage on Miners Creek was divided into four different storage periods (*Initial Wet Up, Steady State, Secondary Storage, Baseflow*). To define these stages, I subtracted the downstream from the upstream discharge. This allowed calculation of an effective discharge ( $\Delta Q$ ) (Majerova et al., 2015).

$$\Delta Q = Q_{down} - Q_{up} \quad \text{Equation 6}$$

When  $\Delta Q$  is positive, the stream is gaining: water is moving from the aquifer to the stream resulting in more water registered at the downstream station than the upstream station. When  $\Delta Q$  is negative, the stream is losing: water is moving from the stream to the aquifer, therefore, less water is registered at the downstream station than the upstream station.

Equation 6 describes fluctuations of water volume ( $Q_{up} > Q_{down}$  or  $Q_{up} < Q_{down}$ ) over the duration of the water year. It is useful, however, to normalize  $\Delta Q$  by the upstream discharge to establish the magnitude of  $\Delta Q$  in the system. This allows the relationship of gaining vs losing to be expressed as a percent (Majerova et al., 2015).

$$\% \Delta Q = \frac{\Delta Q}{Q_{up}} * 100 \quad \text{Equation 7}$$

To establish the most conservative estimate of uncertainty, I take the difference between the high and low estimates of discharge. The high and low estimates occur due to error in the rating curve equations for both the upstream and downstream stations.

$$\% \Delta Q_{high} = Q_{low_{down}} - Q_{high_{up}} \quad \text{Equation 8}$$

$$\% \Delta Q_{low} = Q_{high_{down}} - Q_{low_{up}} \quad \text{Equation 9}$$

$\Delta Q_{high}$  is the upper limit of uncertainty,  $Q_{low_{down}}$  is the downstream discharge using the model considering the low *FlowTracker 2* uncertainty, and  $Q_{high_{up}}$  is the upstream discharge using the model considering the high *FlowTracker 2* uncertainty.

### 2.3.2 Ground Water Storage

Estimates of groundwater storage were developed to assess the fluctuation in the groundwater table as  $\Delta Q$  varied over the course of the study period. Groundwater storage was estimated by the average head (h) of the well network relative to the average bottom of the well network ( $GW = h * S_y * A$  Equation 10). As previously mentioned, Wells 13 and 14 were not used due to data quality issues. Well 15 was not included because it was not installed until 01/21/2021 and Well 8 was not included due to an incomplete dataset. Well 8 data was missing from 10/01/20-01/09/21 because a sensor became stuck in the well and was not able to be retrieved. The bottom of each well casing meets resistance at fractured bedrock that represents an assumed boundary layer (Zb).

Head ( $h$ ) is not representative of the true water volume stored ( $m^3$ ) because it does not account for the size of pore spaces within the substrate. It also does not consider the amount of water pore spaces hold onto as the water table fluctuates. To account for both porosity and specific retention, substrate samples were extracted to estimate a specific yield (Morris & Johnson, 1967) (Appendix D).

Last, I limit the calculation to the area defined by the well network. To aid in delineating this area I use slope and contour lines derived from LiDAR (Light Detection and Ranging). LiDAR was obtained from the National Oceanic and Atmospheric Association (NOAA) from their 3/30-3/31/2018 fly over of the Scott Valley (OCM Partners, 2022). This data was collected at a Nominal Pulse Spacing (NPS) of 0.7 m based on the U.S Geological Survey National Geospatial Program Base LiDAR specifications Version 1.2.

$$GW = h * S_y * A \quad \text{Equation 10}$$

Where,  $GW$  ( $m^3$ ) is groundwater storage,  $h$  (m) is the average head,  $S_y$  (unitless) is specific yield, and  $A$  ( $m^2$ ) is the area of the aquifer. Since the true boundary layer of the system is unknown, and the density of the well network is limited to within the riparian area, this is a minimum estimate of groundwater storage (Appendix E).

The groundwater storage estimate combined with  $\Delta Q$  allows us to compare how groundwater changes as the relationship of the reach-scale dynamics changes. The  $\Delta Q$

transitions from (+) to (-) or vice versa are used to separate the storage periods, which help evaluate how the BDAs storage changes overtime and define our storage periods.

## 2.4 Beaver Dam Analogues Storage Dynamics

Here, I describe what practices were used to evaluate the storage dynamics of the BDAs. The BDA storage is the ponded storage held behind the dam. This ponded storage is expressed relative to stage height (m) and as a volume ( $m^3$ ). These values are used to establish a total estimate of storage as well as to assess habitat availability later in the paper.

### 2.4.1 Beaver Dam Analogues Water Surface Elevation

The BDA stage was monitored from the project genesis in October of 2015 until the end of water year 2021. The BDA stage was recorded by Well 9 which represented the stage of BDA pond 1.1, located north of BDA 1.2. No stage data was available for pond 1.2 or 1.3, however, we assume the hydraulics of these ponds respond similarly to pond 1.1.

The stage was recorded and processed as outlined in Data Collection and Analysis: *Shallow Groundwater Well Network*. The BDA stage was used from water year 2017-2021. The stage data available prior to water year 2017 is representative of a different BDA configuration and was not used for the purpose of this study. BDA stage was measured relative to the pond bottom (m). This was done by subtracting WSE (m) calculated by the well 9 logger and the pond bottom elevation.

The pond bottom elevation (m), BDA crest elevations and toe elevation (m) for all BDAs were surveyed using a combination of Sokkia SET 5 total station and a Trimble R8 Model 3 GNSS RTK (Real Time Kinematic). Elevations for BDA 1.1 were used to track the location of the WSE relative to the upper and lower most sections of the BDA. Pond bottom elevation is available for the other ponds, however, WSE for the other ponds are not known due to the absence of stage data.

#### 2.4.2 Beaver Dam Analogue Poned Volume Estimates

The BDA Pond 1 storage ( $BDA_v$ ) was estimated via a simplified Volume-Area Depth (V-A-h) method (D. Karran et al., 2016, Hayashi and Van der Kamp, 2000):

$$BDA_v(h) = \int_0^h s \left(\frac{h^*}{h_0}\right)^{\frac{2}{p}} dh^* = \left(\frac{s}{1+\frac{2}{p}}\right) \left(\frac{h^{1+\frac{2}{p}}}{h_0^{\frac{2}{p}}}\right) \quad \text{Equation 11}$$

Where (h) is a given height of water above the pond bottom (m), ( $h_0$ ) is the unit height of the water surface (e.g 1m for SI units), (p) is a morphometry coefficient that represents the shape of the pond basin profile, and (s) is a scaling coefficient that represents the area of a circle ( $m^2$ ). Coefficients can be derived by measuring two pond surface areas and depth in time.

The pond morphometry coefficient and the scaling coefficient are derived by rearranging Eqn. 10 (Minke et al., 2010, Karran et al., 2016) where:

$$s = A_1 \left( \frac{h_1}{h_2} \right)^{\frac{-2}{p}} \quad \text{Equation 12}$$

and

$$p = 2 \left( \frac{\log \left( \frac{h_1}{h_2} \right)}{\log \left( \frac{A_1}{A_2} \right)} \right) \quad \text{Equation 13}$$

Here  $A_1$  and  $A_2$  ( $\text{m}^2$ ) are pond areas that correspond to depths  $h_1$  and  $h_2$ , (m) and ( $h_1 < h_2$ ). The pond areas were measured via two remotely sensed orthoimages using a DJI Phantom 4 RTK unit. Some canopy cover was present over the ponded areas; therefore, LiDAR from NOAA was used to trace the wetted contour perimeter when necessary (NCEI, 2018).

The first orthoimage was collected on 03/12/21 by Joey Howard (Cascade Stream Solutions) and Erich Yokel (SRWC). This corresponds to  $h_2$  and  $A_2$  at ~83% maximum pond fill for WY 21. The second orthoimage was taken on 11/18/21 by Madeline McNerthney (CPH). This  $h_1$  and  $A_1$  was matched to a depth during the study period corresponding to ~65% of maximum pond fill. This range of  $h_1$  and  $h_2$  relative to the  $h_{max}$  is within the range appropriate (i.e., 18-74% of  $h_{max}$  for  $h_1$  and 42-98% of  $h_{max}$  for  $h_2$ ) to produce accurate estimates of ponded water storage (Karran et al., 2016).

### 3. RESULTS

#### 3.1 Miners Creek Hydrology

Here I present the results pertinent to the general hydrology on Miners Creek. I outline analysis of the shallow groundwater wells, discharge, and precipitation, followed by the water balance. This section provides an understanding of the basic hydrologic dynamics for water year 2021. All sections build to create a water balance which provides an estimate of dynamic storage on the system level (i.e., the contributing area between the upstream and downstream gauging stations).

##### 3.1.1 Shallow Groundwater Well Network

The dynamics of WSE throughout the system varied temporally and spatially during the study (Figure 8). From 11/06/20 to 04/01/21 the rise and fall of WSE in groundwater wells on river right (Wells 12, 10, 2) and river left (Wells 11, 8, 4, 1) coincided with the rise and fall of instream wells and wells that were proximal to the stream (~IS) (Wells 15, 9, 7, 5, 3). The rise and fall of WSE at each well did not always respond in equal magnitude, notably, the WSE in Well 8 rose and fell more significantly and coincided with the activation of the river left side channel. During the onset of the irrigation season on 04/01/21 all groundwater and instream wells experienced a decline in WSE (Figure 9). This initial decline was followed by an increase in WSE driven by irrigation return flow in all river right groundwater wells. Instream wells did not recover to pre-irrigation conditions, however, Well 3 was close to pre-irrigation conditions at the

end of May before declining again. River left wells remained at or near the post decline WSE, except for Well 4. This well recharged slightly, possibly indicating some exchange of irrigated water across the aquifer located just downstream of the BDAs.

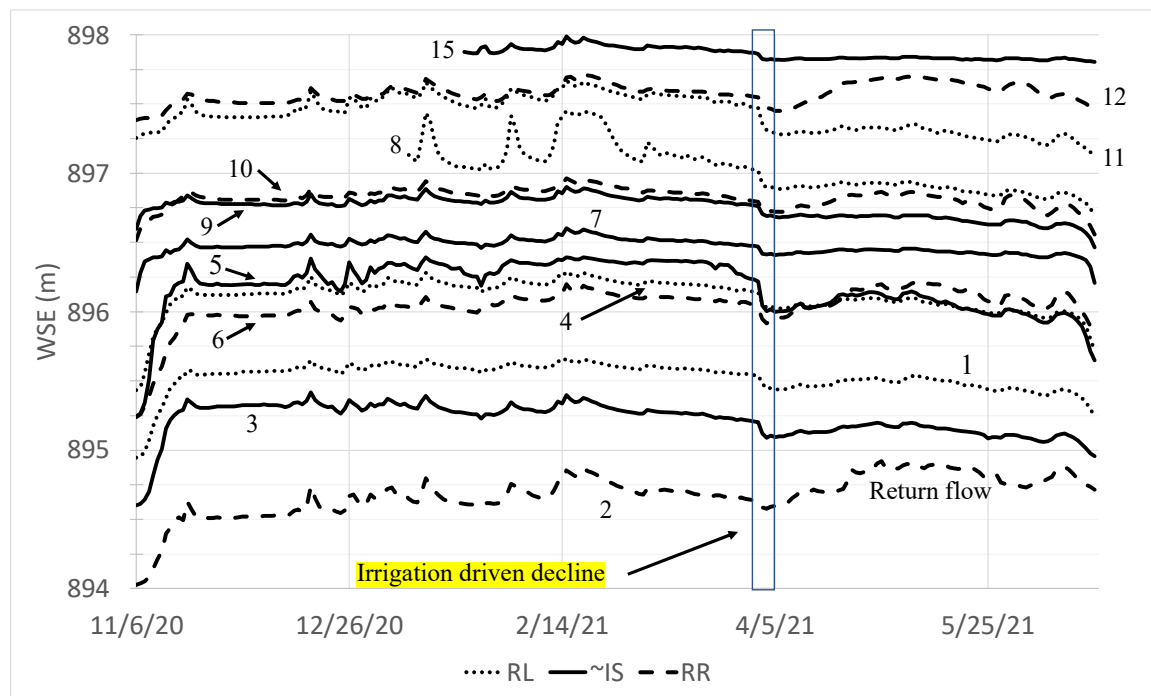


Figure 8. Graph of WSE vs time for study duration (11/06/20-06/20/21). Each line represents the WSE for a well with its corresponding number. Wells on river right (RR), river left (RL), and in-stream proximal (~IS) show that all wells decline after the onset of irrigation season shown by the red rectangle. Additionally, all RR wells receive return flow depicted by the blue ovals. For spatial representation of each well please refer to Figure 4.



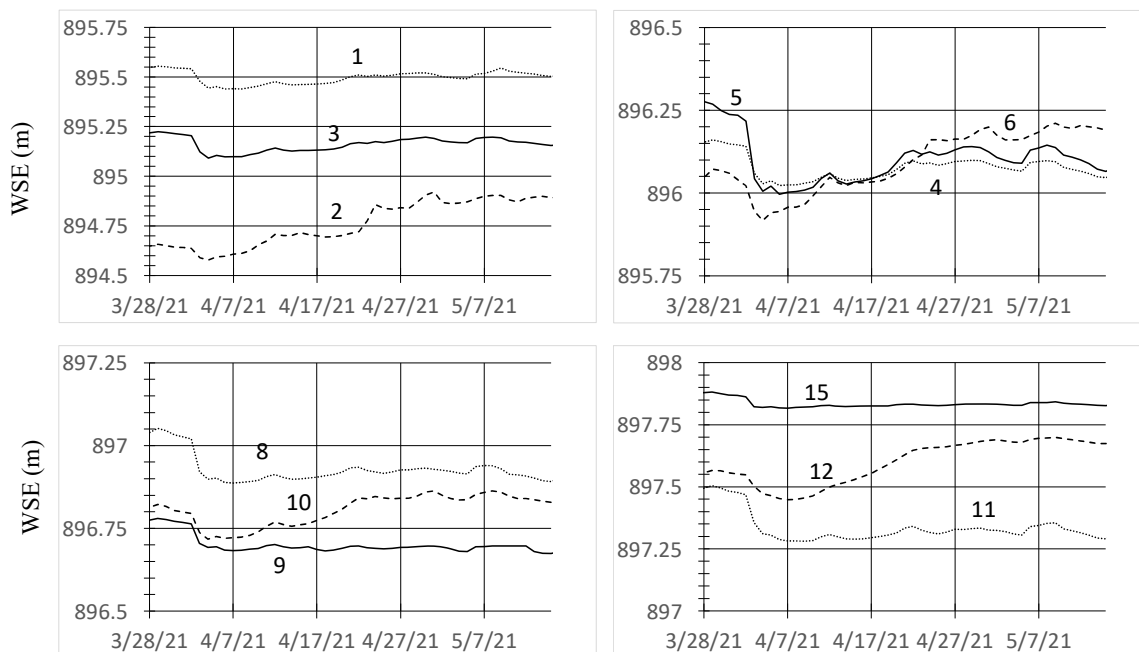


Figure 9. Graph of WSE vs. time for all wells on the same transect from 03/27/21-05/14/21. This period highlights irrigations impact on Wells. Each line is labeled to represent location (i.e., dotted = river left, solid line = instream proximal, dashed = river right). Lines are also numbered with corresponding Well number. Minor gridlines represent 0.05 m and major gridlines are 0.25 m. Wells 11 and 12 show a reverse trend compared to other wells where river left wells are higher in elevation than river right wells. This could be due to differences in hydraulic conductivity, substrate, or groundwater flow vectors.

### 3.1.2 Discharge and Precipitation

At the reach scale, variability between the upstream and downstream flow are illustrated by the daily average discharge at the two gauging stations (**Error! Reference source not found.**Figure 10). The flow on Miners Creek became continuous after the first substantial rainfall event on 11/13/20 (25.65 mm). As direct and indirect storage (storage that drives discharge generation and the storage that remains after accounting for direct storage, respectively) (Dralle et al., 2018) fill, less significant amounts of

precipitation were required to generate larger runoff events. This trend is particularly visible throughout February 2021.

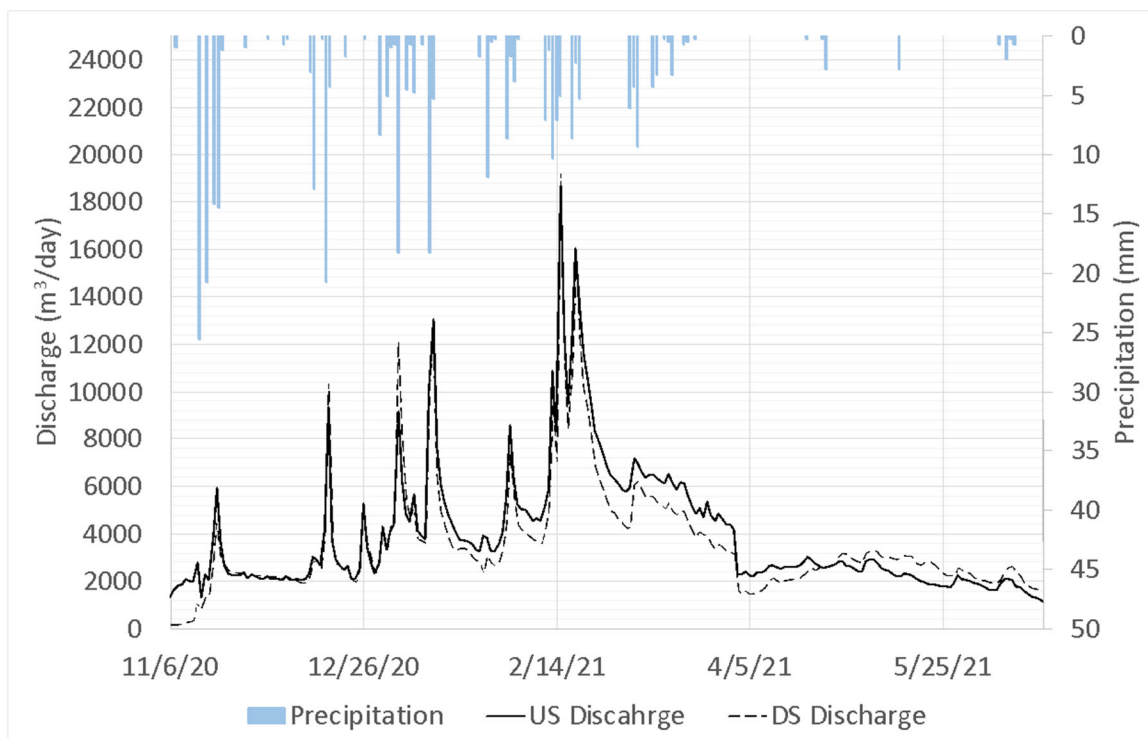


Figure 10. Graph of discharge vs. time for study duration (11/06/20-06/20/21). Lines represent variation in upstream and downstream discharge. Rectangles show precipitation (mm) by day with a secondary y-axis. The data indicated that there are notable differences in discharge between upstream and downstream gauging stations depending on the time of year.

In total, 310.39 mm of precipitation fell between 11/06/20 and 06/20/21. Water year 2021 was a drought year fluctuating between D1, D2, and D3 conditions according to NIDIS (National Integrated Drought Information System). For most of the study 55-85% of the county where Miners Creek is was experiencing D3 drought conditions classified as an extreme drought (Figure 11). An extreme drought is characterized by year-round fire conditions, inadequate water for wildlife and agriculture, and

supplemental feed necessary to support livestock, and early fruit tree budding (Fort Jones, California conditions, n.d). During water year 2020 rainfall totaled 210.75 mm and during water year 2019 it was 510.22 mm during the same period. It should be noted that the steep decline in flows on 04/01/21 are driven by the onset of the irrigation season. Irrigation occurs above the upstream gauging station in an unknown volume. Throughout water year 2021, the relationship between upstream and downstream discharge fluctuated between periods of  $Q_{up} > Q_{down}$  or  $Q_{down} < Q_{up}$  indicating transitions between gaining and losing stream conditions.

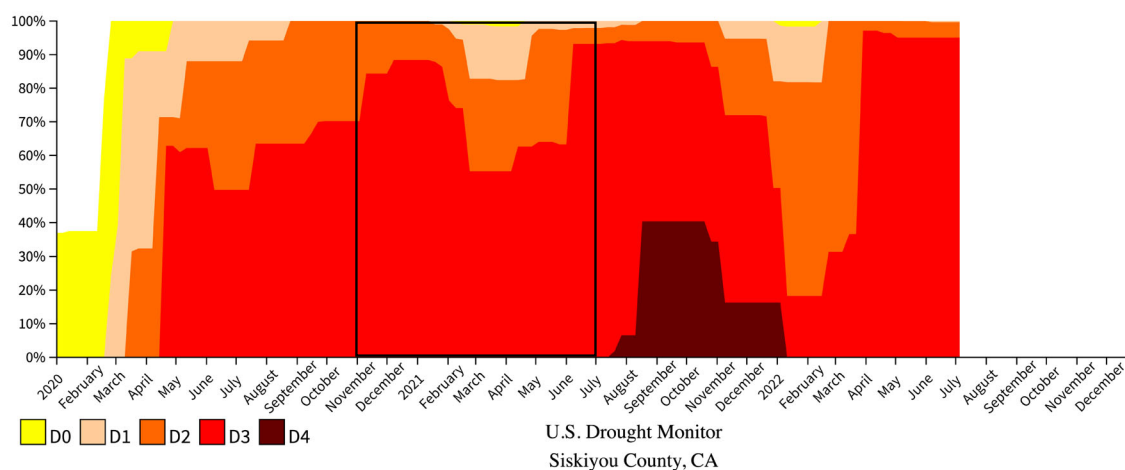


Figure 11. Graph of percent of county in drought index vs time (2020-2022). Water year 2021 is outlined by the black rectangle. (Fort Jones, California conditions, n.d)

### 3.1.3 Water Balance

The temporal changes in the water balance varied depending on the timing and magnitude of precipitation and ET (Figure 12, Figure 13). Dynamic storage closely resembled trends in precipitation until ET increased beginning (~03/06/21). As ET

increased throughout spring and summer (04/01/21-06/20/21), dynamic storage sharply declined, as there were only minor contributions of precipitation throughout the dry season 03/23/21-06/20/21 (Table 1).

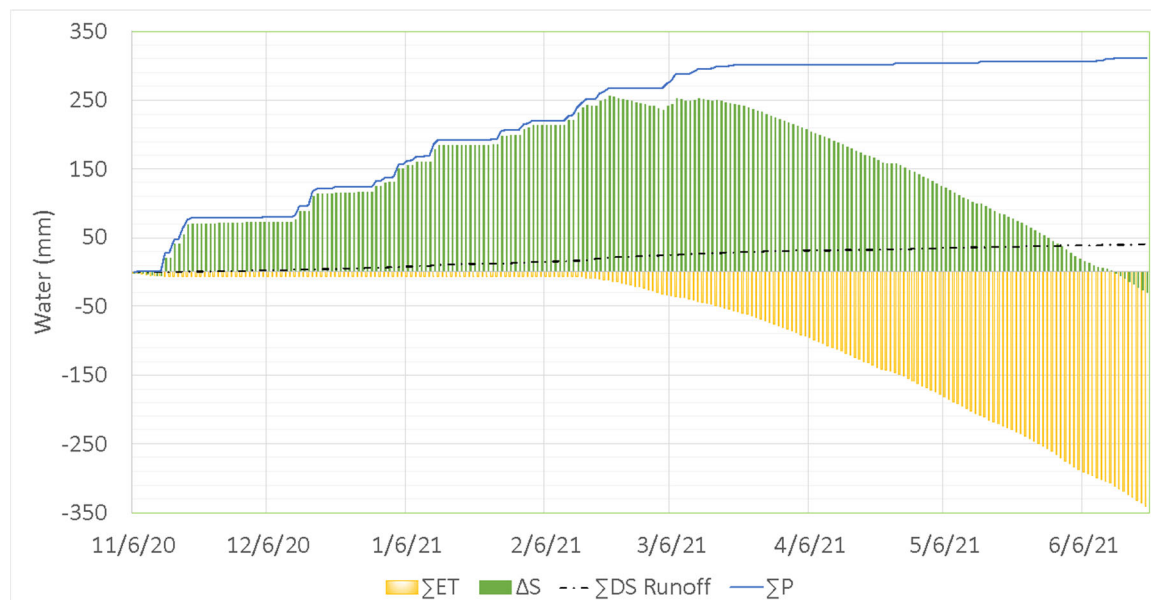


Figure 12. Graph of the temporal changes in water storage (mm) from the water balance during the study period (11/06/20-06/20/21). ET, evapotranspiration, represents water lost due to plant uptake or evaporation. P is precipitation (mm) from the onsite tipping bucket and downstream is runoff which is Q scaled by the upstream contributing area. Miners Creek maximum dynamic storage was in mid-February and the runoff ratio remained low even as dynamic storage increased by 167 mm from December 2020 to February 2021. \*Upstream runoff is accounted for in dynamic storage, it is not shown as it almost identically follows the trend of the downstream gauging station. Overall, this deficit really depicts the lack of precipitation.

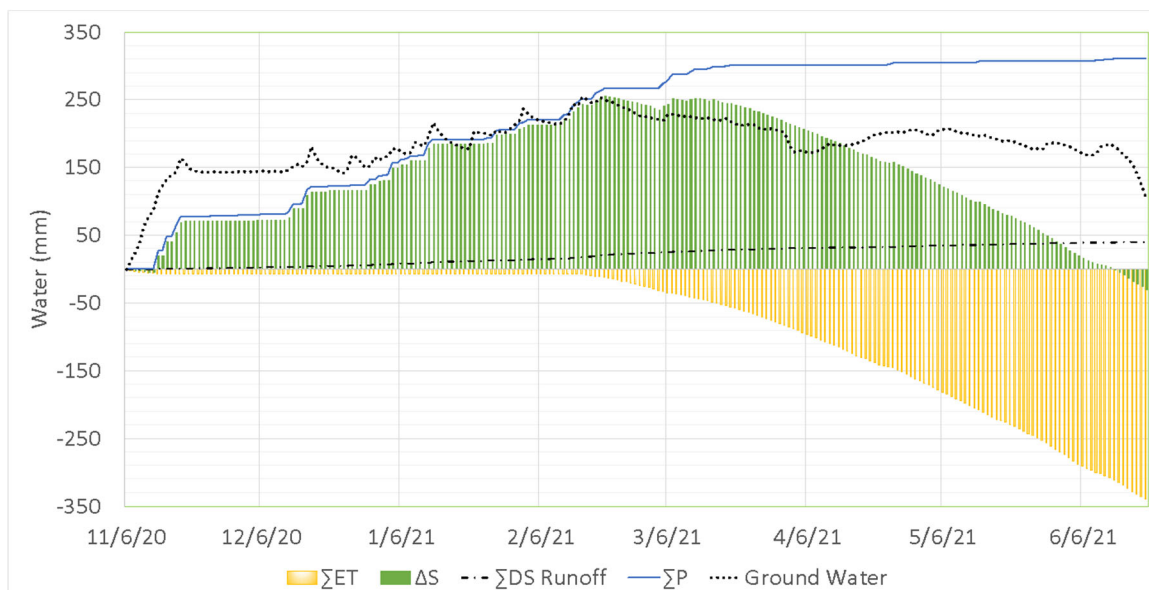


Figure 13. Graph of accumulation of water (mm) for all components of the Water Balance ( $\Sigma ET$ ,  $\Delta S$ ,  $\Sigma$ Downstream Runoff,  $\Sigma$ Precipitation) and groundwater storage from 11/06/20-06/20/21. For the purposes of this figure the sum of upstream runoff is excluded because it very closely resembles upstream runoff

Table 1. Summary statistics for WY 21 water balance on Miners Creek broken down by Wet, Dry, and Total season values. \*US = upstream \*\*DS = downstream

	US* Runof f (mm)	DS** Runof f (mm)	Precipitatio n (mm)	ET (mm)	Inputs (mm)	Output s (mm)	$\Delta$ Storag e (mm)	Runof f Ratio (Q/P)
<b>Wet Season</b> 11/06/20 - 03/22/21	33.40	29.19	300.48	60.10	333.8 8	89.29	244.59	0.10
<b>Dry Season</b> 03/23/21 - 06/20/21	11.21	11.24	9.91	280.7 2	21.12	291.96	- 270.85	1.13
<b>Total</b>	44.61	40.43	310.39	340.8 2	355.0 0	381.25	-26.25	0.13

During WY 21, 96% of precipitation fell during the wet season (11/06/20-03/22/21). Throughout this period, however, only 10% of precipitation was registered as runoff at the downstream gauging station. The runoff ratio is calculated by normalizing the sum runoff (Q) over a given period by accumulated precipitation over the same period. During the study period, outputs exceed inputs which could mean there was a higher demand for water than was provided during the wet season, however, accommodating for all plant species uptake from ET accurately is difficult. Therefore, it is more likely that the calculation of it is more PET (potential evapotranspiration) and that the error in ET could explain outputs exceeding inputs by 26.25 mm.

### 3.2 Miners Creek Storage

Storage on Miners Creek is separated into four sections: Reach Scale and Groundwater Dynamics, BDA Water Surface Elevation, BDA Poned Volume Estimates, and Storage Comparisons. The goal of these results is to breakdown storage into categories that summarize the large-scale storage mechanics, followed by storage occurring behind the BDAs. I also examine the WSE of the BDAs from water year 2019-2021, to assess how pond dynamics have varied since the installation of the triple BDA configuration in October of 2018. I then compare how changes in storage and flow state affect BDA poned storage during water year 2021.

### 3.2.1 Reach Scale and Ground Water Dynamics

During the system *Initial Wet-Up* (11/06/20-11/19/20), Miners Creek flow became continuous on ~11/16/20 (Figure 14.) This resulted in a steep decline in  $\Delta Q$  as the upstream and downstream discharge stations equilibrated. A total of 47.5 mm of precipitation fell between 11/06/20-11/16/20. Most of this precipitation fell in two events on 11/13/20 and 11/15/20, with 25.65 mm and 20.82 mm of rain, respectively. The sum of precipitation over this time provides an estimate of the magnitude of precipitation needed to meet the soil moisture deficit that satisfies stream connectivity. It is important to note, however, that some of this deficit is satisfied prior to the study period, under xeric conditions from 10/01/20-11/06/20, where minor changes in precipitation and discharge result in significant gains in well head (Figure 15).

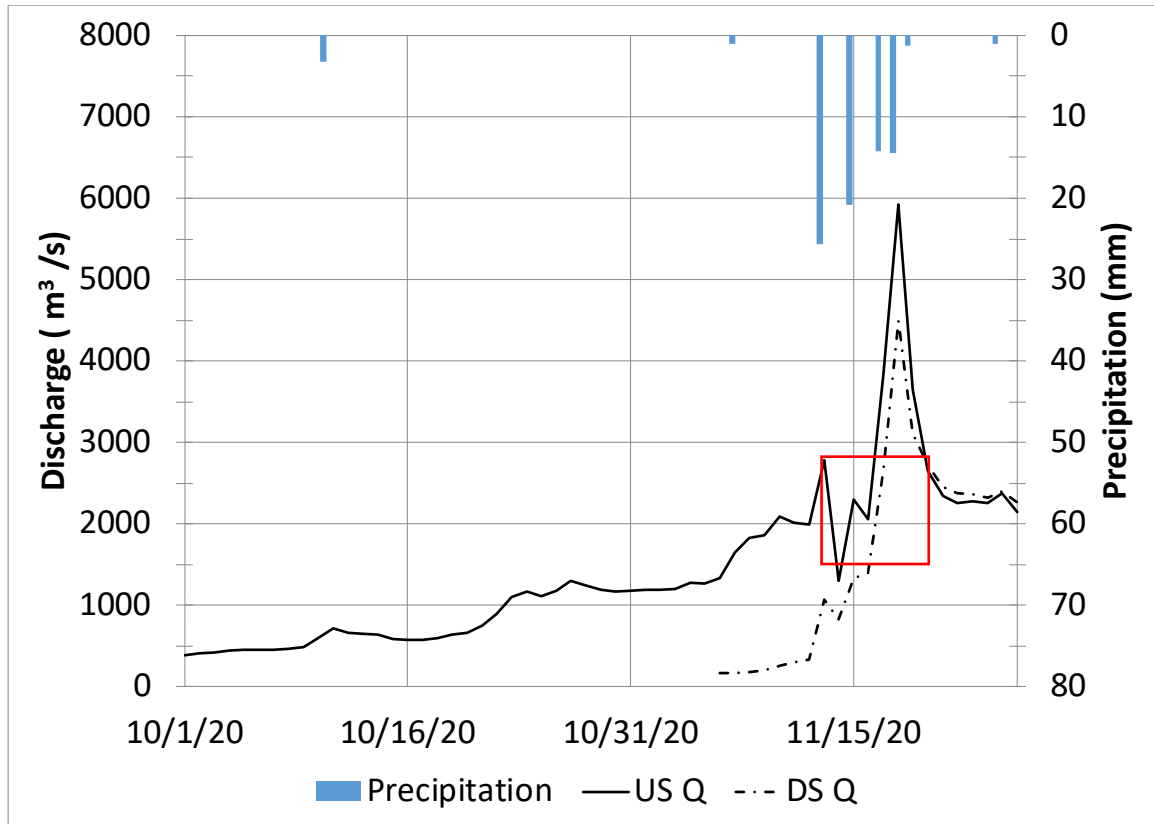


Figure 14. Graph of discharge (Q) vs time from 10/01/20-11/26/20. Precipitation (mm) is on the secondary y-axis. Upstream discharge is shown prior to the study period to provide a sense of the antecedent conditions. The red square highlights the window where flow became continuous.



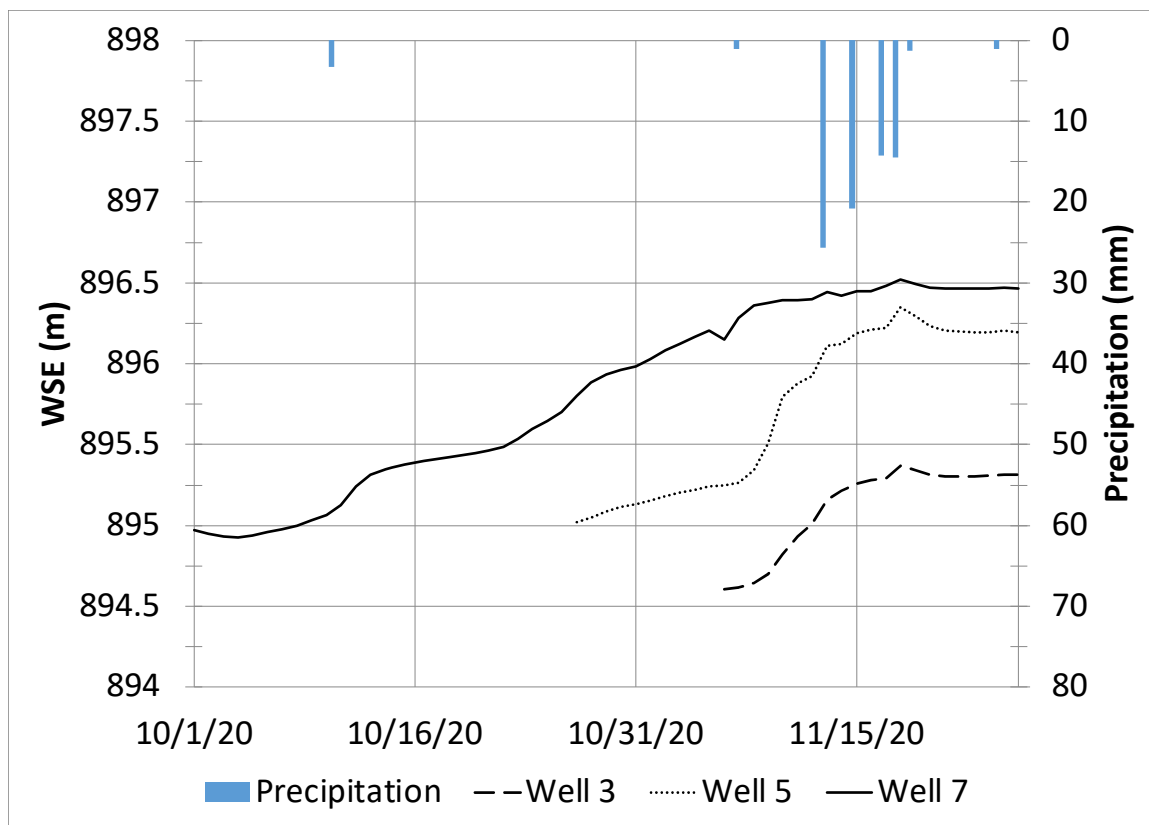


Figure 15. Graph of WSE vs time from 10/01/20-11/26/20. Precipitation (mm) is on the secondary y-axis. Well 3 is instream proximal, with Wells 5 and 7 directly instream. Even under xeric conditions, there is dry season recharge (over 1 m at Well 7).

The groundwater storage increased rapidly over a short duration from 11/06/20-11/19/20 and is described as the *Initial Wet Up* which occurred under losing stream conditions. From 11/20/20-01/03/21 inputs and outputs were roughly equal (*Steady State*) and groundwater storage was stable at  $\sim 6990 \text{ m}^3$  (Figure 16). Beginning around 01/04/21 the stream reach shifted to a prolonged losing state where groundwater storage gradually increased. Peak groundwater storage occurred on 02/15/21 at  $9048 \text{ m}^3$  and then gradually receded until 04/09/21 when it increased again after the onset of the irrigation season

(04/01/21). This *Secondary Storage* period ended on 04/27/21 and transitioned into *Baseflow*, a period where  $Q_{\text{down}} > Q_{\text{up}}$ , characterized as gaining conditions (04/28/21-06/20/21). During baseflow, water from the aquifer flowed to the stream and resulted in an increase in flow at the downstream gauging station relative to the upstream gauging station.

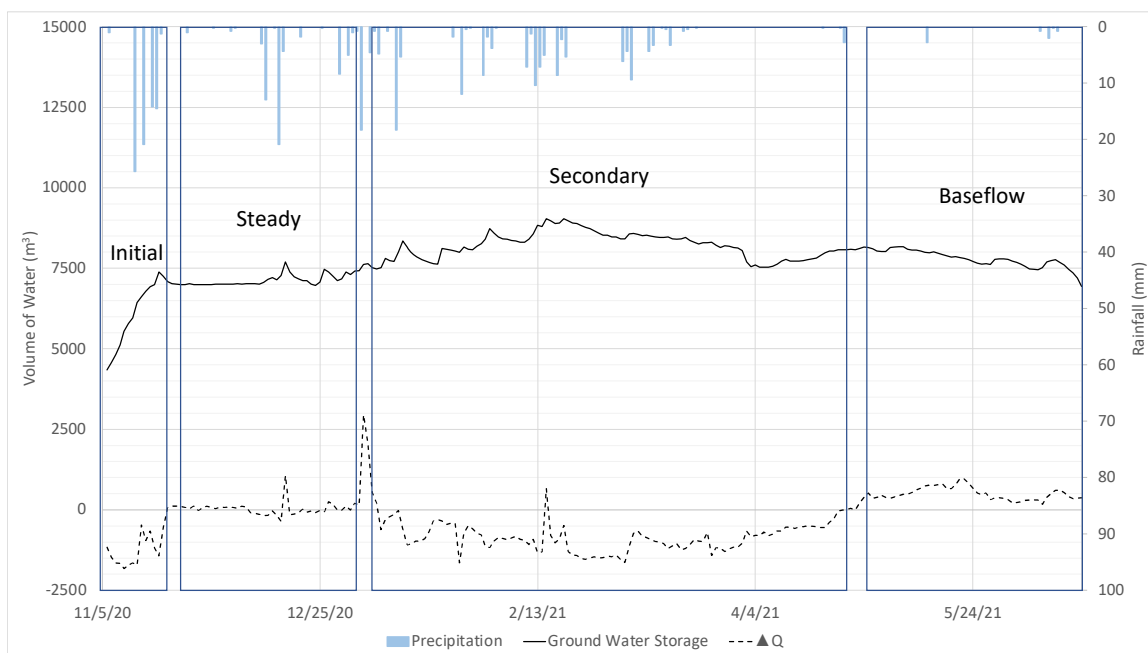


Figure 16. Groundwater storage, Precipitation, and  $\Delta Q$  over the course of the study (11/6/20-06/20/21). Storage stages are broken into four categories: Initial=Initial Storage, Steady=Steady State, Secondary=Secondary Storage, Baseflow.

Losing versus gaining stream conditions are evaluated by the  $\% \Delta Q$  ( $\% \Delta Q =$

$$\frac{\Delta Q}{Q_{up}} * 100 \quad \text{Equation 7). The magnitude difference of } \% \Delta Q \text{ was most drastic during}$$

the *Initial Wet Up*. This indicated that most of the incoming discharge went into deep

groundwater storage as it is not expressed at the downstream station. During *Steady State*, conditions were slightly gaining or losing. During *Secondary Storage*, storage conditions were mostly losing with a few exceptions. Throughout *Baseflow*, conditions were gaining. Reach scale conditions during *Secondary Storage* and *Baseflow* are confirmed by the upper and lower estimates of uncertainty (Figure 17). It is important, however, to acknowledge that reach scale dynamics vary spatially (Appendix F).

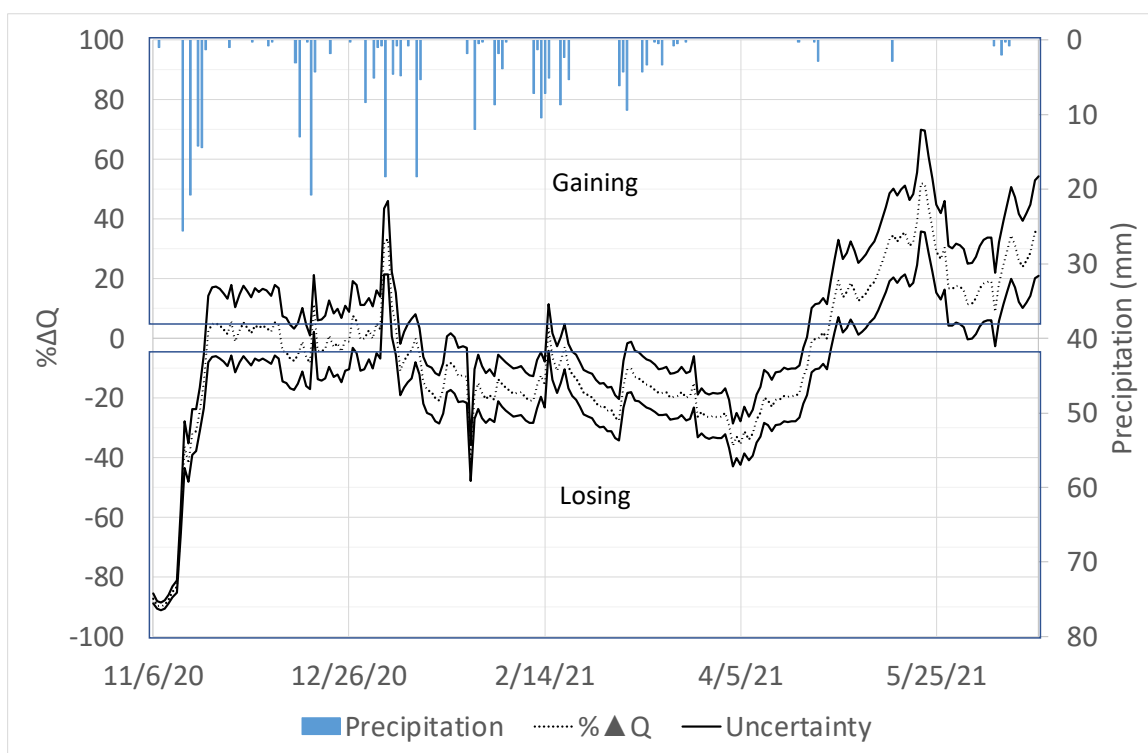


Figure 17. Gaining and losing stream reach conditions between upstream and downstream gauging stations for water year 2021. Gaining stream conditions are shown in red with positive values. Losing conditions are represented by blue with negative values. The bounds of uncertainty provide support for the characterization of reach scale storage dynamics. The gaining period in mid-April can either represent contributions from groundwater storage to the stream or return flow during irrigation.

### 3.2.2 BDA Water Surface Elevation

During water year 2019, BDA 1.1 (Figure 4) WSE remained high relative to its crest elevation from 11/19/18-4/01/19 (Figure 18). During this time the BDA was between 80%-100% full (average ~87% full). From 04/01/19-07/23/19 the BDA WSE declined and on average was ~55% full. During water year 2020, at its maximum, BDA 1.1 WSE was 68% full, a significant decline from water year 2019. The BDA stage remained low relative to the crest elevation in water year 2021 and at its maximum was 60% full. More rainfall in water year 2021 compared to water year 2020, 310.39 mm compared to 210.75 mm did not result in higher stage.

Therefore, since 2019 there has been an inability of the BDAs to impound and maintain water due to initial and subsequent degradation of their porosity over the years. Even in the wettest year (2019), the BDAs dried out in mid-July (~07/15/19) only three weeks later than water year 2021 (06/20/21). This indicates that even in wet years, there is not suitable habitat for fish during the dry summer months.

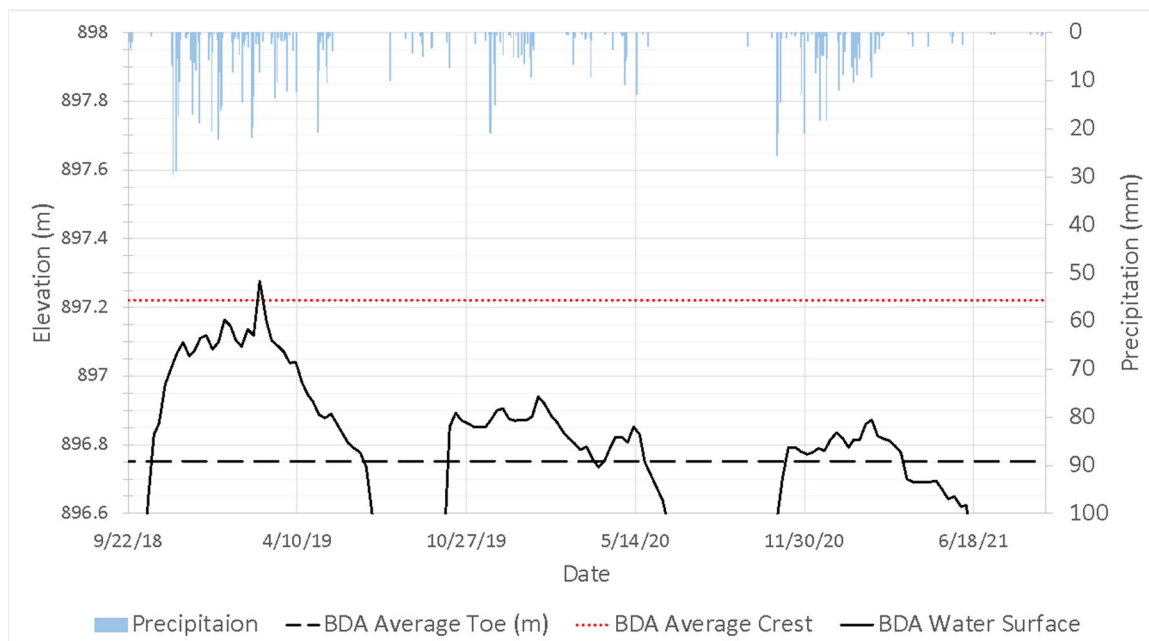


Figure 18. Weekly WSE (m) from Well 9 vs time (water year 2019-2021). Secondary y-axis shows daily precipitation (mm) during the same period. Pond bottom was only surveyed in water year 2021, therefore WSE (m) is used relative to masl (meters above sea level) instead of ponded depth. This is because pond morphometry can vary by year depending on the movement of sediment.

### 3.2.3 BDA Ponded Water Volume Estimates

The BDA ponded water volume remained low relative to the average crest elevation throughout water year 2021. The wet season average volume of BDA Pond 1.1 was  $\sim 10.19 \text{ m}^3$ . The maximum pond storage reached was  $\sim 12.14 \text{ m}^3$ . The dry season average storage was just  $\sim 5.21 \text{ m}^3$ , just 34% full relative to the average crest elevation. This volume is located below the toe elevation of the BDA, meaning that on average, water was not in direct contact with the BDA during the dry season (Figure 19).

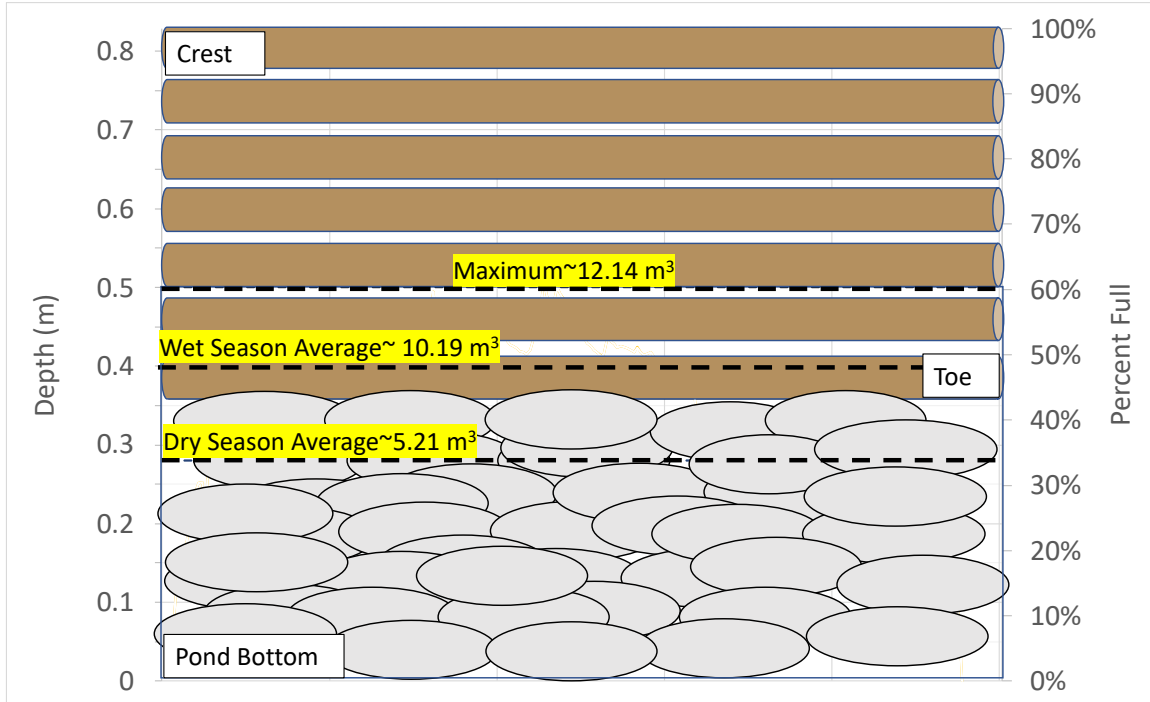


Figure 19. Conceptual model of ponded volume relative to BDA average crest elevation (left y-axis) and percent full (right y-axis). Volumes are separated into maximum, wet season average, and dry season average volumes with dashed lines. The brown horizontal cylinders represent the horizontal willow weaves that make the BDA structure. Bottom spheres represent cobbles that support the base of the BDA structure leading down to the pond bottom. These cobbles support the upstream section of each BDA.

I cannot assess the exact pond volume of the other BDA ponds as previously discussed due to absence of stage data. BDA Pond 1.1 is the second largest pond when it comes to area and maximum depth. BDA Pond 1.2 is the smallest pond in terms of area, but largest in depth. BDA Pond 1.3 is the largest pond in area but the shallowest in depth. Additionally, these sizes can vary depending on flows. To approximate total pond storage, we can assume that all BDAs store similar amounts of water. Using the

maximum volume from BDA 1.1 of  $\sim 12.14 \text{ m}^3$ , a total storage of  $36.42 \text{ m}^3$  is a reasonable estimate given the available data.

### 3.2.4 Storage Comparisons

Scatterplots were used to show the relationship between BDA storage, discharge, and groundwater storage. In each scatterplot, BDA storage estimates are on the y-axis with discharge and groundwater storage on the x-axis, respectively (Figure 20)(Figure 21). These relationships are labeled based on storage states (i.e., *Initial Wet Up*, *Steady State*, *Secondary Storage*, *Baseflow*). These plots help establish how system wide storage dynamics affect BDA storage increase and decline over water year 2021.

During the *Initial Wet-Up*, small changes in upstream discharge resulted in rapid changes in BDA ponded volume (Figure 20). Throughout the *Steady State* period, upstream discharge was mostly consistent at  $\sim 2000 \text{ m}^3/\text{day}$  and there was little change in BDA ponded volume, except for a few runoff events (12/17/20, 12/26/20, 12/31/20). In the *Secondary Storage* state, BDA storage gradually increased until the highest upstream flow event  $\sim 18640 \text{ m}^3/\text{day}$  on 02/15/21. The relationship between BDA storage and upstream discharge shifted after this maximum threshold, and similar upstream discharge resulted in lower BDA ponded volume estimates, perhaps due to slowly increasing ET. A large shift occurred at the onset of the irrigation season (irrigation runs from 04/01/21-

10/01/21<sup>1</sup>). Upstream irrigation diversions dropped the BDA storage from ~8.4 m<sup>3</sup> to an average of 5.7 m<sup>3</sup> in the following days, equating to a 32% drop in pond volume. During *Baseflow*, similar inputs in the form of upstream discharge during *Initial Wet-Up* do not result in equal BDA ponded volume estimates. Instead, there is a decline in ponded volume estimates as the downstream discharge station registers more discharge than the upstream station, indicating that groundwater is yielding from the aquifer to the stream.

---

<sup>1</sup> *Irrigation season is subject to change based on water mastering. Data is not publicly available to assess the exact duration of the irrigation season. Additionally, there is always the possibility of illegal diversions within the watershed.*



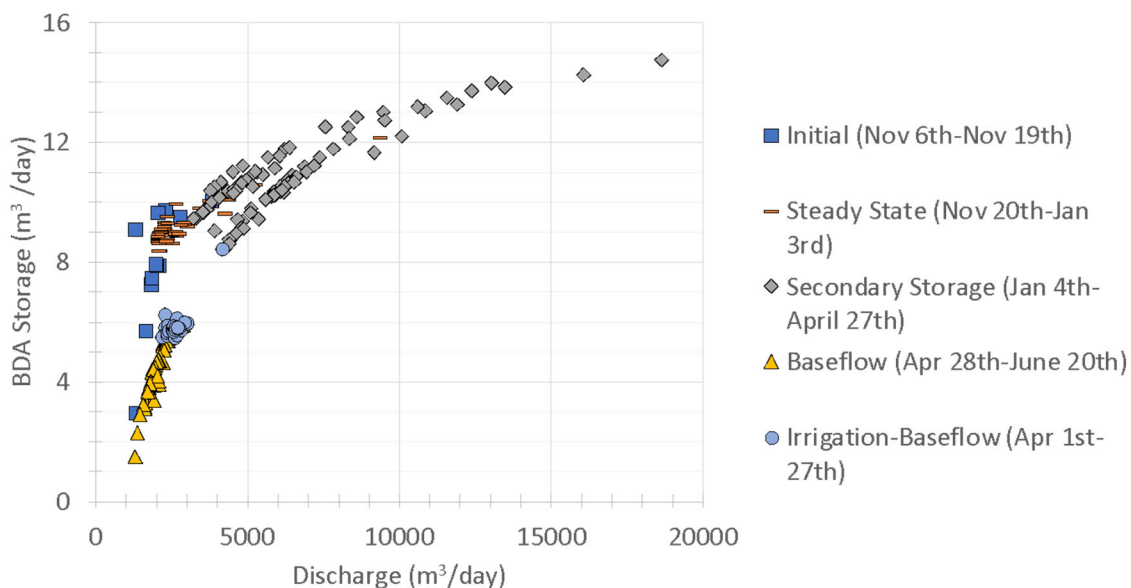


Figure 20. The relationship between BDA storage vs upstream discharge. Each data point represents a daily time step separated by storage stages. Blue circles show a shift in BDA storage and upstream discharge at the onset of irrigation which overlap partially with *Secondary Storage* into *Baseflow* conditions. The drop in both BDA storage and upstream flow indicates how changes in water use effect Miners Creek.

Under low groundwater storage estimates, during *Initial Wet Up*, BDA storage increased rapidly (Figure 21). As groundwater storage increased through the *Steady State* and *Secondary Storage* phases, BDA storage increased gradually. This remained true even after the maximum groundwater storage value was reached on 2/15/21 (9048 m<sup>3</sup>). Gradual shifts up and down in groundwater result in minor increases or decreases in BDA storage. A shift was observed after the onset of irrigation season where groundwater storage decreased by a maximum of 500 m<sup>3</sup> before recovering at the end of April. During

*Baseflow*, groundwater storage remained above estimates for *Initial Wet up* and *Steady State*, while BDA ponded volume storage decreased.

It is notable that the BDAs are dry when groundwater storage is still relatively high on 6/20/21 (~7000 m<sup>3</sup>) at the end of baseflow, whereas the BDAs began to fill at relatively low groundwater storage values (>5000 m<sup>3</sup>) during the initial wet-up.

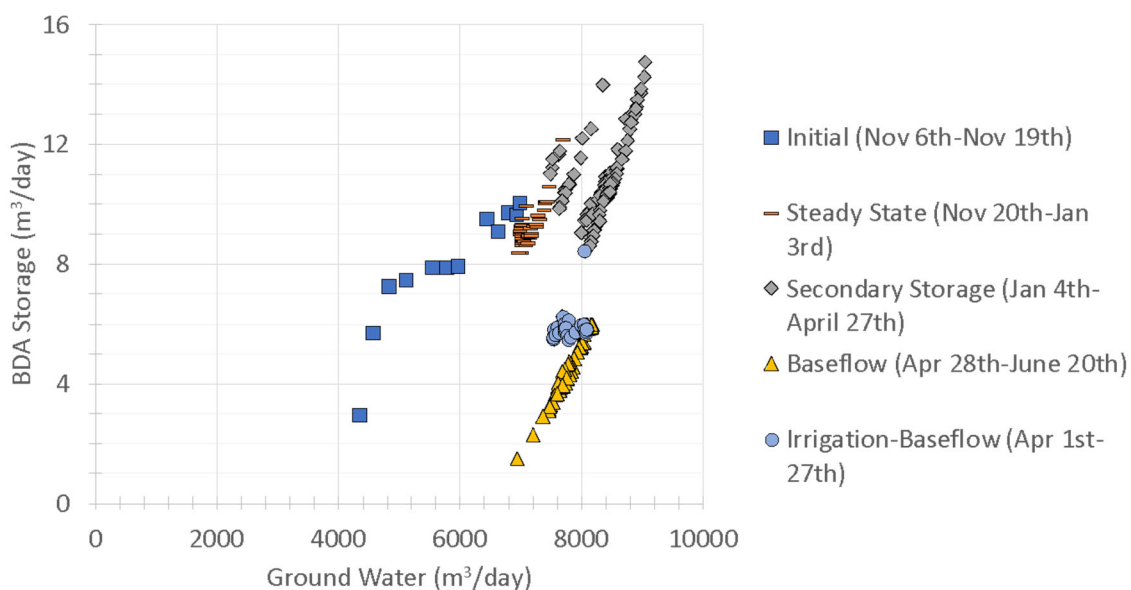


Figure 21. The relationship between BDA storage vs GW Storage. Each data point represents a daily time step separated by storage stages. Blue circles show a shift in BDA storage and GW Storage at the onset of irrigation which overlap partially with *Secondary Storage* into *Baseflow* conditions. There is large decline in BDA storage during the onset of irrigation, but only minor changes in groundwater storage, which highlight BDAs dependency on surface flows.

## 4. DISCUSSION

### 4.1 Shallow Groundwater Well Network

The dynamics of the well network during water year 2021 suggests a highly connected surface water and groundwater system proximal to the stream (within ~35 m). This is evidenced by the rise and fall of each well, and the lack of idiosyncratic dynamics of individual wells prior to irrigation (i.e., the rise in one well but not another). There is, however, discrepancies in transect dynamics (Figure 9). Without additional wells, spaced further into the adjacent aquifer, I cannot quantify the true connectivity of the aquifer moving east through the system. Based on the gravelly sandy loam of the adjacent agricultural fields (Web Soil Survey), however, I can still assume a high degree of interconnectivity. This is due to the high conductivity of alluvial soils, in addition to irrigation return flows from the agricultural fields to the stream.

The rise and fall of water in the study wells tended to coincide with the rise and fall of peak discharge events at the upstream and downstream gauging stations (Figure 22). Notably, each peak event regardless of magnitude seems to cause an almost equal response rise in head at each well, except for Well 8. Well 8 has higher peaks relative to other wells due to the activation of an ephemeral side channel river left of the triple BDA configuration. Well 8 also had a week (02/15-02/23/21) where there was active flooding or stream flow directly over the well indicated by the lack of rise or fall in head the week

following 02/15/21. This side channel activity was also confirmed during field visits on 02/16/21 and 02/19/21.

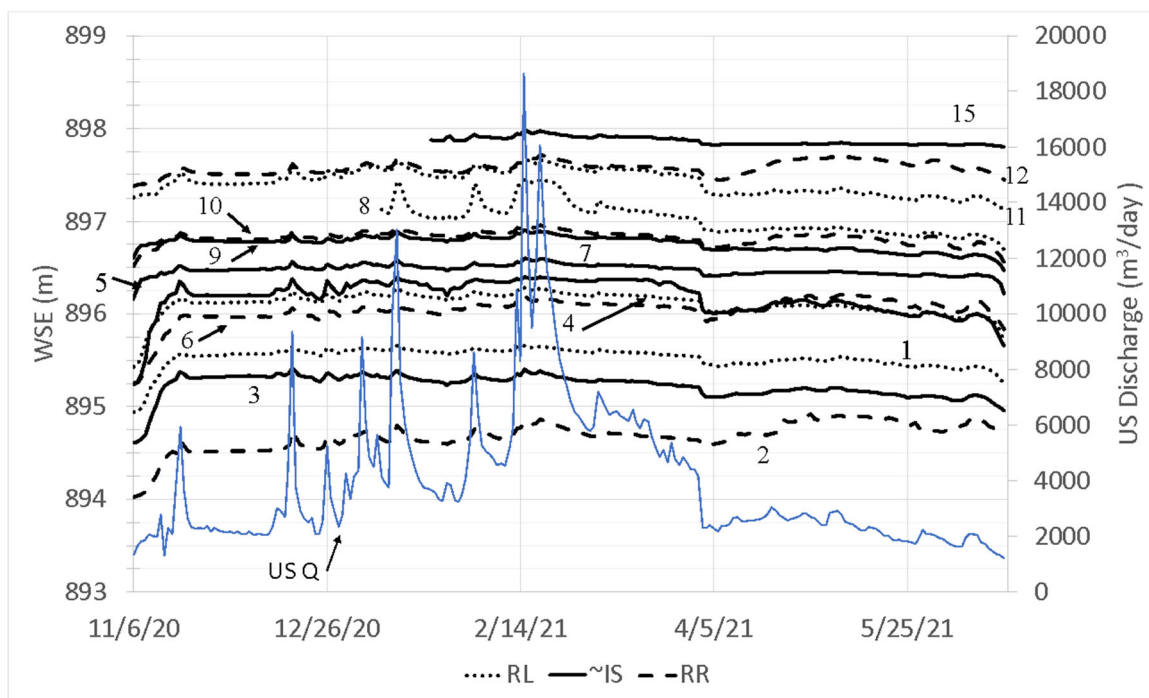


Figure 22. Well WSE (m) rise (primary y-axis) upstream discharge (secondary y-axis) over water year 2021. Numbers on the graph indicate Well number while change in line pattern indicates whether the well is instream proximal (~IS), river right (RR) or river left (RL). Peak discharge events, regardless of magnitude, generally produce a similar rise in head throughout the shallow groundwater well network.

The similarity in well head rise under successive increasing runoff events (12/11/21-02/19/21) may indicate that hydrologic controls in the system (such as BDAs, large wood, pools, riffles, and channel geometry) reached a maximum threshold. The ability for these hydraulic controls to create a rise in head as discharge increased, diminished after the initial rise of each well ended on ~11/26/20. Therefore, higher runoff events would be required to drive an increase in groundwater storage or stream stage.

These types of limitations are observable in much of the well network, however, I use Wells 3 and 11 to highlight this relationship because they highlight the threshold effectively (Figure 23).

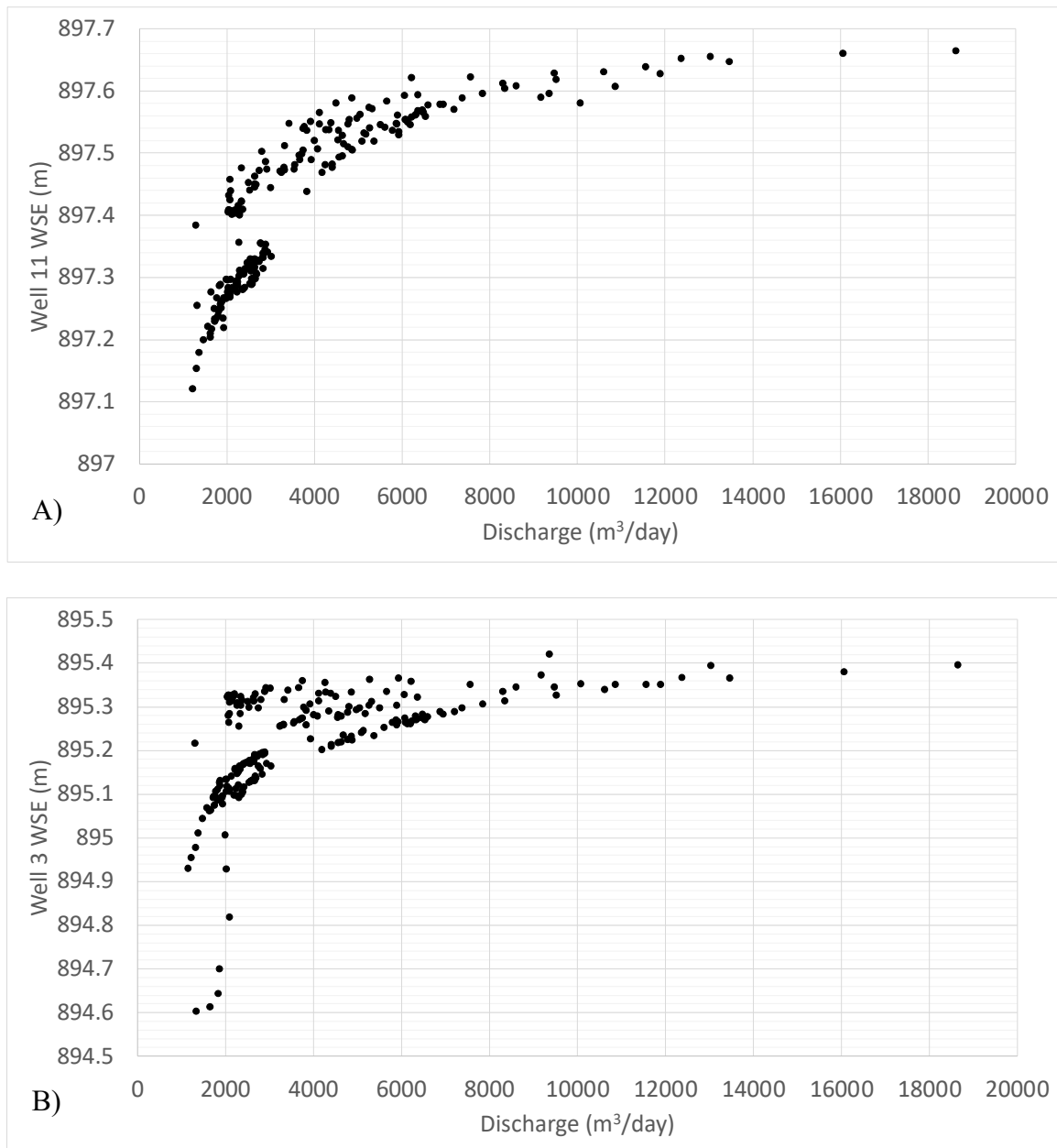


Figure 23. Well WSE and upstream discharge throughout the study. As discharge increased in an instream proximal well (Well 3) and a groundwater well (Well 11), increases in WSE became less significant as upstream discharge increased. In A), increases in upstream discharge resulted in an increase in WSE until  $\sim 8000$   $\text{m}^3/\text{day}$ , after which there was no significant rise in WSE. In B), WSE increased rapidly under low discharge and maximum WSE occurred at  $\sim 2000$   $\text{m}^3/\text{day}$ . Larger increases in discharge did not result in a greater WSE.

Although the primary goal of this study was not to comment on the impacts of irrigation on the study reach, results from the well network indicated that irrigation influenced the well network. Therefore, it became necessary to address. Irrigation was shown to decrease BDA pond volumes, temporarily decrease groundwater storage, and cause significant declines in discharge at both upstream and downstream gauging stations (Figure 10, Figure 20, and Figure 21). Decline in discharge was detected as a  $\sim 1988$   $\text{m}^3/\text{day}$  drop in discharge at the upstream station and  $\sim 1686$   $\text{m}^3/\text{day}$  drop at the downstream station one day after the onset of irrigation on 04/01/21. While groundwater storage recovered, BDA ponded volumes and discharge did not return to pre-irrigation levels.

Irrigation return flows (Figure 8) caused significant increase, 25-30 cm in well head in all river right wells (Figure 9). All river right wells exhibited an increase in head above the pre-irrigation conditions, however, all other wells declined and did not recover to pre-irrigation conditions. Post-irrigation wells sustained a relatively constant head before sharply declining leading up the drying of the entire reach on 06/20/21.

These results suggest an interconnected groundwater and surface water system where changes in the usage of water result in depletion of both surface and groundwater as suggested in the executive summary of the Scott Valley Groundwater Sustainability Plan (Siskiyou County Flood Control and Water District Groundwater Sustainability Agency, 2021). The issue on Miners Creek is that the demand for water in dry years puts pressure on an already runoff dependent environment that cannot sustain continuous

flows. Additionally, beneficial users identified in section 1.4.3.2 of the Scott Valley Groundwater Sustainability Plan, such as surface water users, agricultural users, and well users are in direct conflict with environmental users, such as Coho, and other aquatic dependent species. This is because the extraction of water,  $\sim 1988 \text{ m}^3/\text{day}$  (or 23 L/s) following irrigation makes a significant difference in small sub-catchments.

## 4.2 Water Balance

My water balance is meant to provide a framework in which to understand the underlying mechanisms of  $\Delta S$  within the contributing watershed between the upstream and downstream gauging stations. I overlap the  $\Delta S$  with the estimated groundwater storage to assess how the observed fluctuations in groundwater compare to the Water Balance.

There are some discrepancies between  $\Delta S$  and change in groundwater storage. In the beginning of the study the rise in groundwater storage exceeds values of the  $\Delta S$  by 87 mm by the end of the *Initial* storage phase on 11/19/21. This suggests that inputs are unaccounted for in the simplified water balance. These inputs could have occurred from deep groundwater discharge or recharge contributions, or trans boundary groundwater flux (Nash et al. 2018; Sayama et al. 2011). Similarly, there is a discrepancy of 85 mm between the  $\Delta S$  and groundwater storage after the rebound of irrigation return flows on 05/06/21. Irrigation itself could have caused issues with the water balance since we do not know how much water left then re-entered the system from flood irrigation. Additionally, there is the possibility that the  $ET_o$  (reference evapotranspiration) provided



through the CIMIS, combined with the natural vegetation crop coefficient of 0.6, represents an overestimate of ET. The true value of ET for the system on Miners Creek would be difficult to accurately represent as the vegetation community extracts water from both saturated and unsaturated sources in varying amounts throughout the water year. The complexity of where vegetation accesses water and to what degree could be better understood through direct measurements of ET, sap flow measurements (conifers), and stable isotopes (e.g. Oshun et al., 2015; Link et al., 2014).

The simplified water balance, however, is still useful to quantify maximum storage for water year 2021 which matches the groundwater storage at  $\sim 255.4$  mm for  $\Delta S$  and  $\sim 254.4$  mm for the groundwater storage. The interplay between cumulative runoff and  $\Delta S$  provides information about the larger watershed's capacity to store water. In some watersheds  $\Delta S$  plateaus at low values even as precipitation increases to high values ( $>2000$  mm). This means that an increase in precipitation does not always translate into an increase in dynamic storage. Once  $\Delta S$  remains stable, the runoff ratio rises since the watershed's capacity to store water is fulfilled, meaning more water becomes runoff and does not contribute to storage. In other watersheds,  $\Delta S$  continues to increase as cumulative precipitation increases. One of the controlling factors in how much a watershed can store is the thickness of the underlying critical zone structure (the distance from the lower subsurface boundary of the watershed to the overlying canopy) (e.g. Sayama et al. 2011; Dralle et al., 2018; Hahm et al. 2019).

In this study, I am not able to fully address the maximum thresholds for dynamic storage on Miners Creek due to the low precipitation for water year 2021. Overall runoff

values remain low throughout the wet season indicating that most of the precipitation is not translated into runoff, but rather stored in off channel aquifers. When comparing runoff and  $\Delta S$  runoff begins to increase once storage values between ~225-260 mm are reached (Figure 24). Overall, however, runoff remained low throughout water year 2021.

Utilizing a simple water balance during a wet year may provide further information on how the Miners Creek watershed stores water and to identify a threshold of dynamic storage above which will produce runoff to rapidly increase. There are limits to how much dynamic storage can increase in a watershed. Once a maximum threshold is exceeded, a higher ratio of inputs is translated into runoff instead of causing increased storage. These methods are useful for management decisions as well as understand how the environment might respond to more frequent dry conditions.

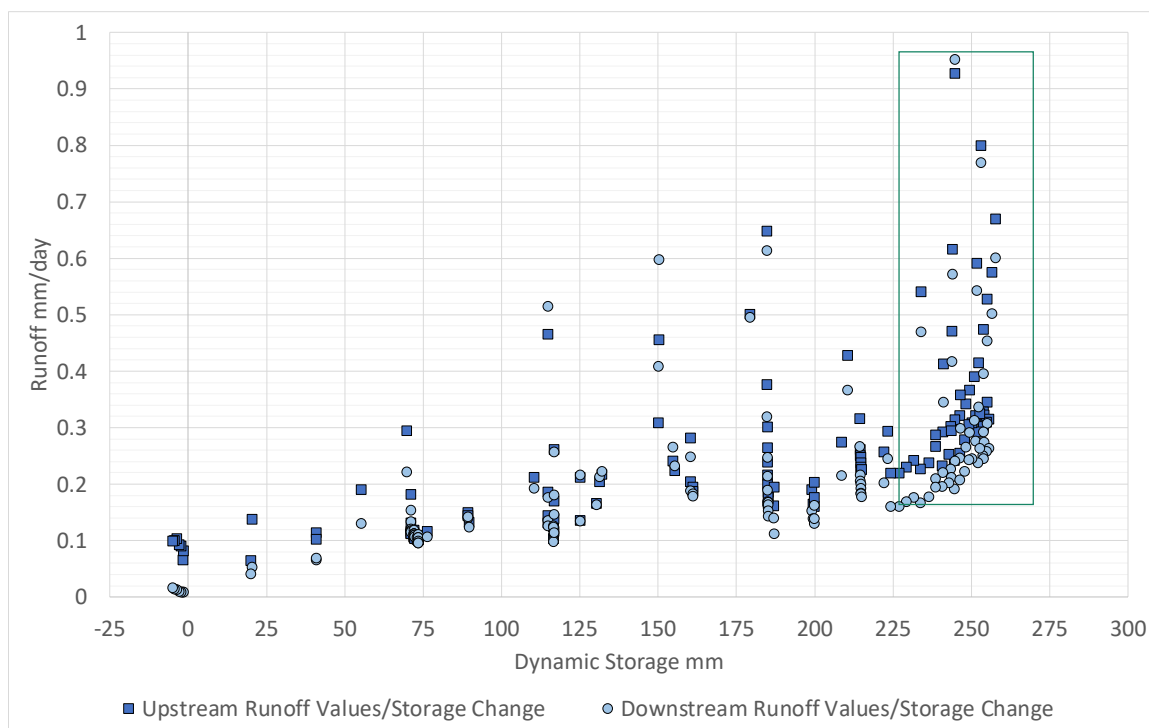


Figure 24. The relationship between total dynamic storage (x-axis) and runoff at the upstream and downstream gauging stations (y-axis). Generally, runoff only begins to increase once total storage exceeds 225 mm. However, this is unlikely to represent a maximum change in storage threshold. More precipitation would be needed to further establish this relationship.

### 4.3 Reach Scale and Ground Water Storage Dynamics

#### 4.3.1 Reach Scale Storage

At the reach scale, while there are significant transitions between gaining and losing states with regards to  $\% \Delta Q$ , overall, Miners Creek tends to be characterized as a slightly losing reach (Figure 17). During baseflow, there is a gaining trend, however, its contribution to stream recharge remains minimal.

The losing nature of Miners Creek is not surprising for a connected alluvial aquifer where stream stage closely resembles that of adjacent river right and river left wells. What is curious is the change in losing to gaining conditions 28 days into the irrigation season (04/28/21). The increasing head in river right wells relative to instream proximal wells may indicate that the change in conditions is attributed to flood irrigation of adjacent agricultural fields (Figure 25). This could cause more water to be registered at the downstream gauging station overtime as irrigation percolates from the unsaturated zone into the saturated water table, eventually flowing from river right to the stream.

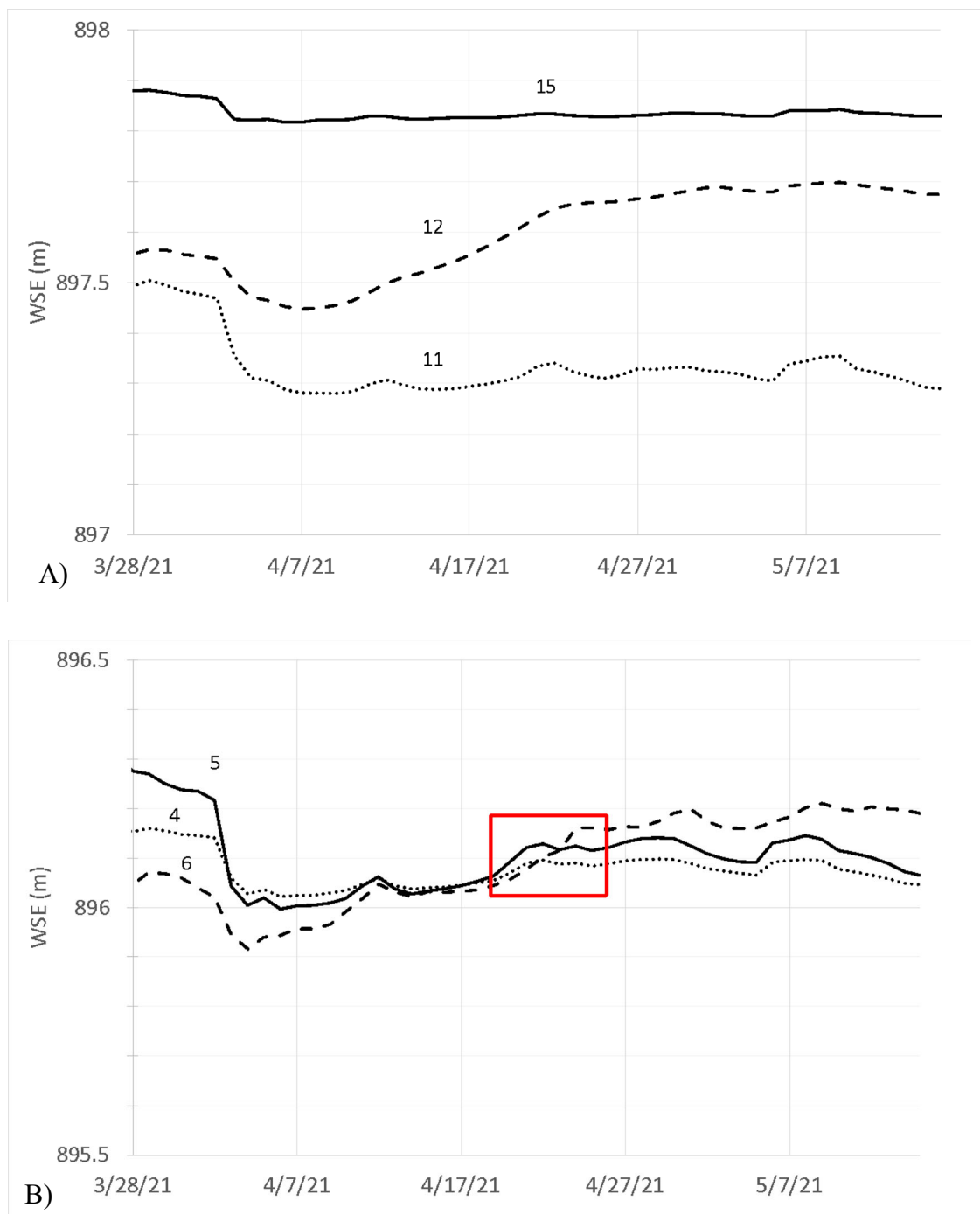


Figure 25. Graph of WSE (m) vs time (03/28/21-5/15/21). A) Shows the increase in head at well 12 (river right) and B) shift from losing to gaining conditions along well 4, 5, and 6 transect. This change in conditions coincide with the shift from *Secondary Storage* to *Baseflow* conditions.

Extreme fluctuations in  $\% \Delta Q$  can be attributed to side channel activation ~1/4/21 or exceeding maximum storage thresholds ~2/15/21 (Figure 16, Figure 17). These events may have triggered significantly more water to quickly register at the downstream gauging station in comparison to the upstream gauging station.

#### 4.3.2 Groundwater Storage

From the groundwater storage calculations, we can estimate the groundwater contribution from the aquifer to the stream during baseflow. During baseflow, groundwater storage declines  $1839 \text{ m}^3$ . During this period, we know that water is being yielded from the aquifer to the downstream gauging station. Therefore, at its maximum there is an  $1839 \text{ m}^3$  contribution from the aquifer to the downstream station.

This baseflow recharge, however, does not recharge the shallow groundwater network, but rather provides ephemeral stability to the surface water flow before the creek goes completely dry (Figure 26).

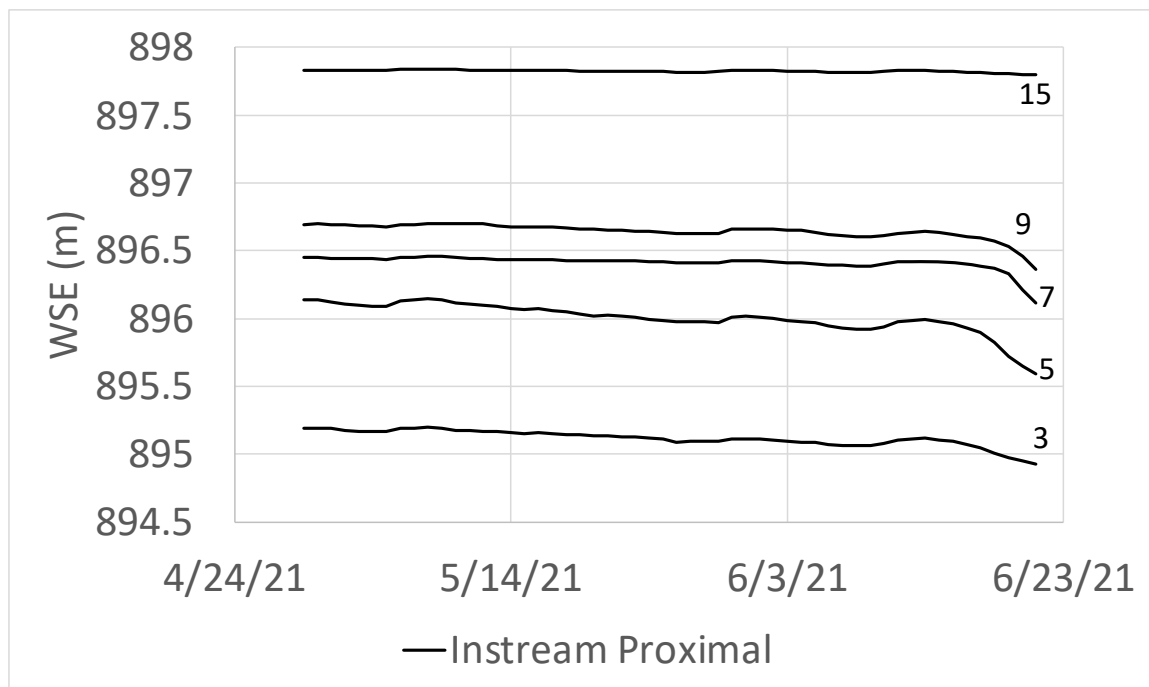


Figure 26. Change in WSE during *Baseflow* conditions. Overall, there is head stability, however, no recharge from groundwater sources or elsewhere. Meaning that none of these instream wells received gains throughout baseflow.

#### 4.4 BDA Storage Dynamics

##### 4.4.1 BDA Structure

A possible reason for diminished BDA water surface elevation over the study time could be due to changes in BDA structural integrity. After the reconfiguration of the BDA positions in water year 19, BDAs had high structural integrity (Figure 27). BDA 1.1 was reinforced with cobbles, hay, and new weaves where needed, BDAs 1.2 and 1.3 were newly constructed. BDAs were packed with fine materials such as hay and supported with cobbles. Since then, structural integrity of BDAs has diminished. Specifically, finer material that was used to pack the BDAs such as hay and larger

support in the form of weaved branches has been eroded from the structure (Figure 28). Loss of these packed materials and loss of wood created a highly porous structure which made water retention difficult (Figure 29).

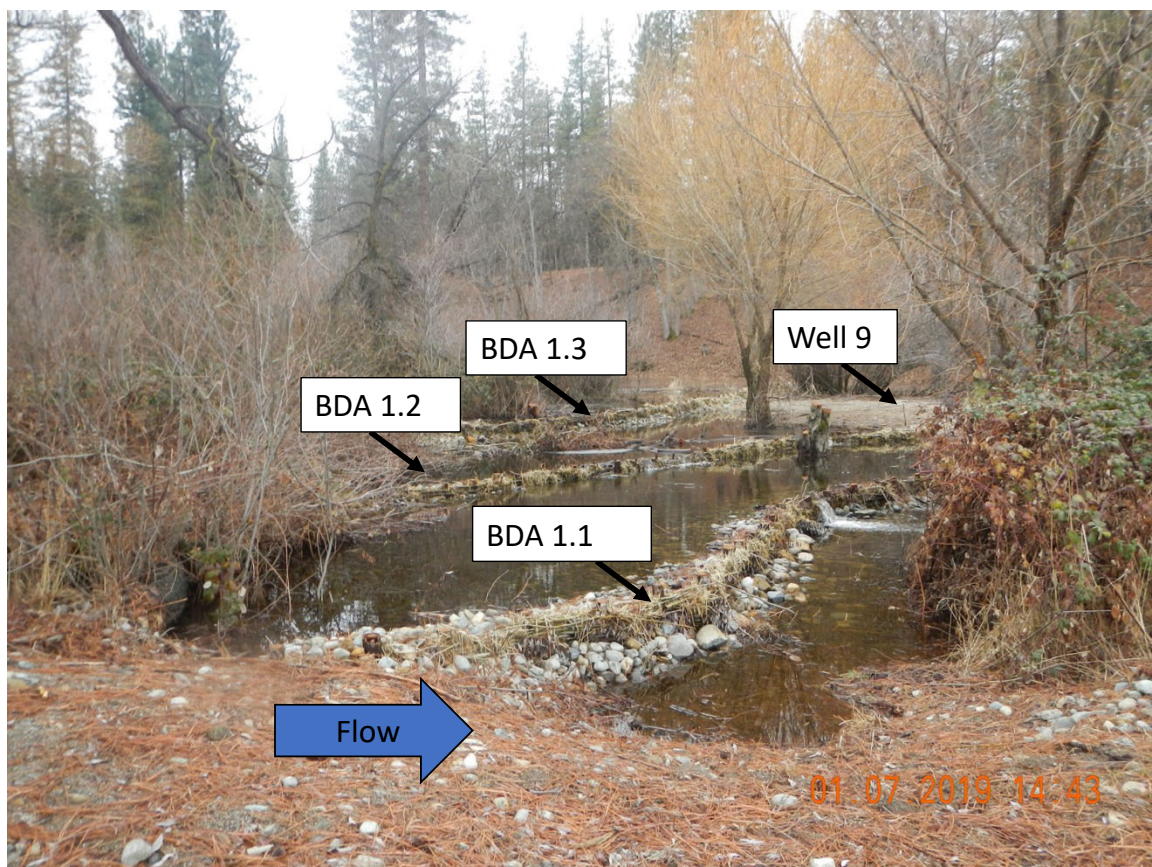


Figure 27. Survey photo of BDAs on Miners Creek 01/07/2019. Photo is looking Southwest towards well 9, slightly downstream of BDA 1.1. (Photo by Erich Yokel)



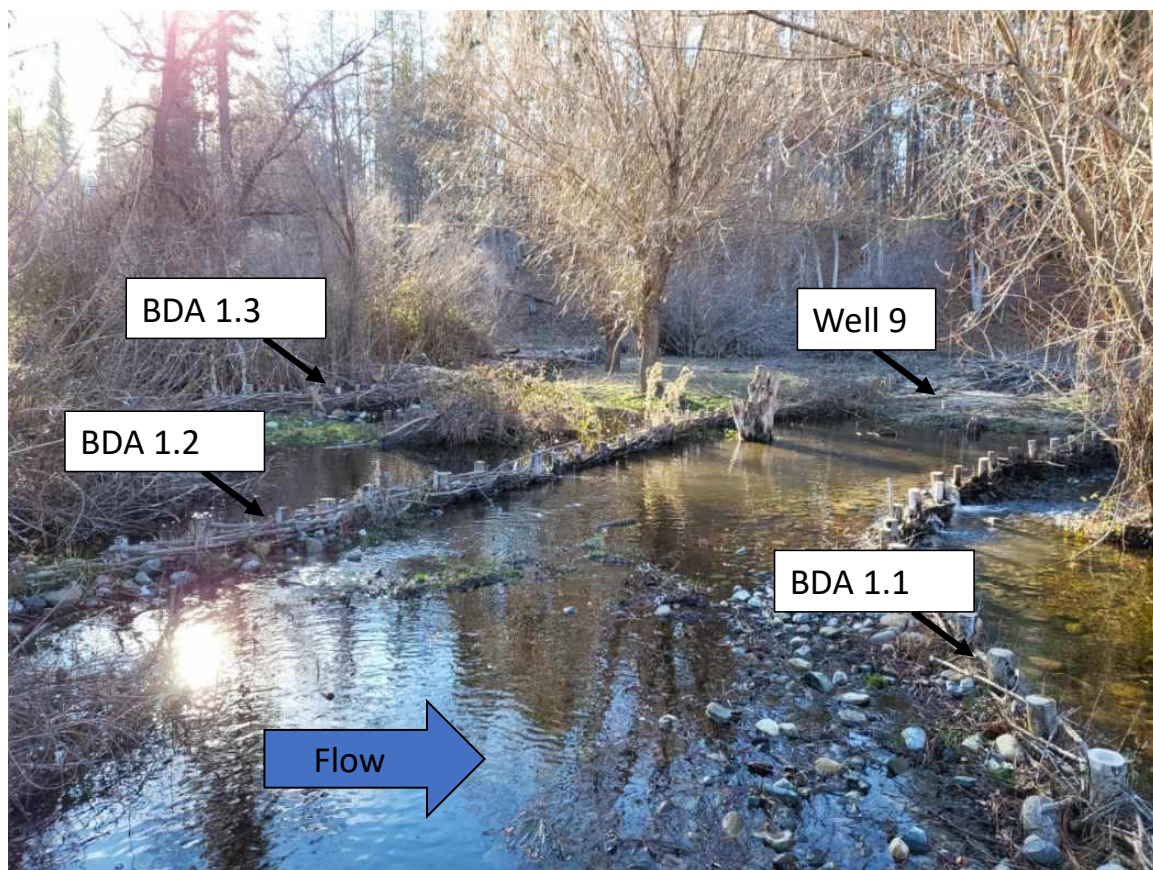


Figure 28. Photo of BDA taken 01/12/2022. This photo does not overlap with the study period and is used to provide perspective on changes overtime. Photo is from almost the same perspective as Figure 27. This photo is taken slightly above BDA 1.1 still facing Southwest. (Photo by Dominic Schenone)



Figure 29. Image of portion of BDA 1.1 that is always in direct wetted contact as stream stage fluctuates. All the BDA fill material has been washed out with the addition of several willow weaves.

#### 4.4.2 Sediment Aggradation

High volumes of decomposed granite (1-2mm) were deposited around large sections of each BDA (Figure 30). Aggradation of sediment varied from 32 cm-65cm around instream wells (Figure 31). This sediment deposition effectively reduces the area available for ponded habitat as sediment aggradation increases overtime. Spaces filled by sediment may cause a rise in the water table, however, it will also occupy space that may be otherwise filled by ponded water.



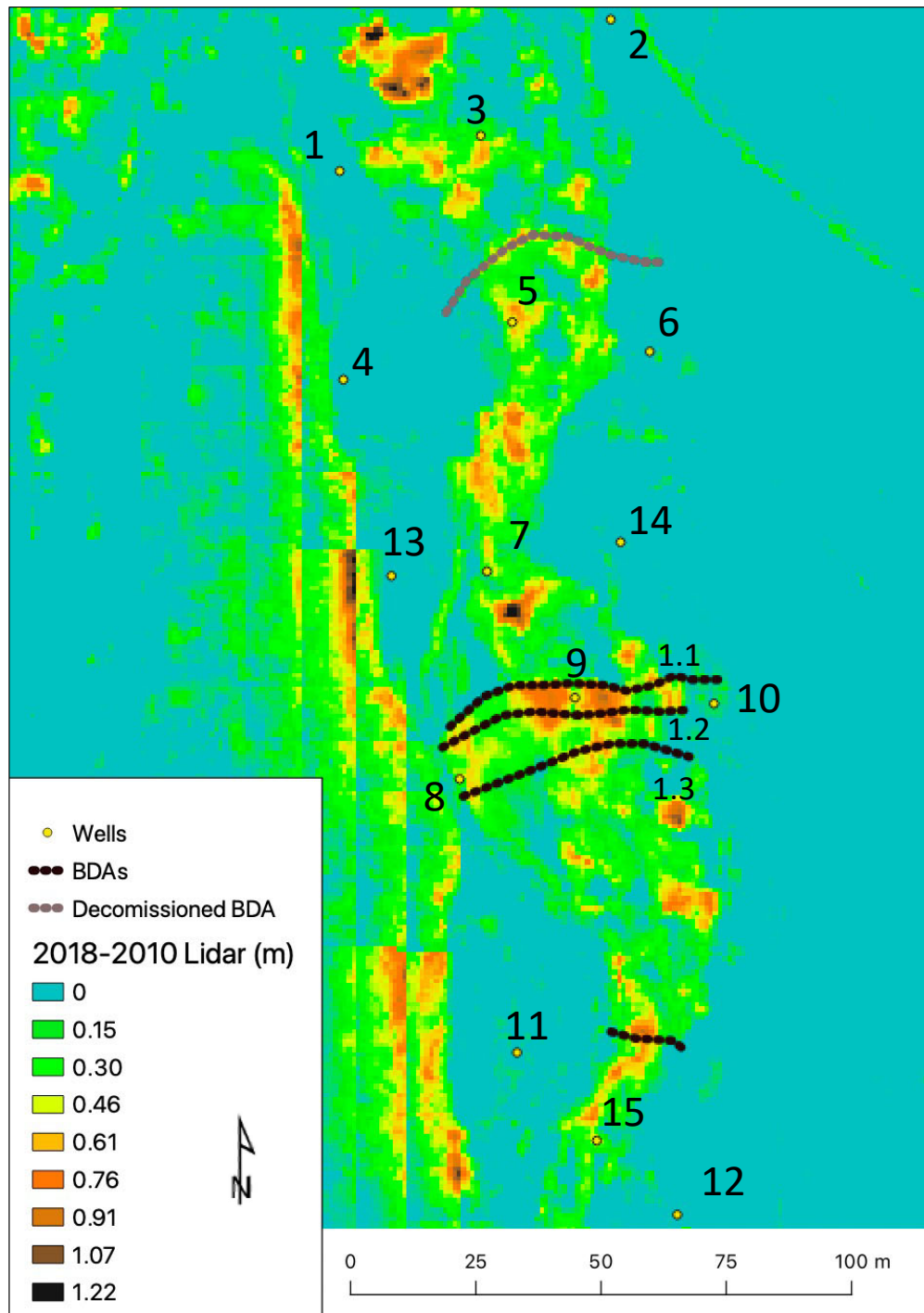


Figure 30. Lidar data showing the difference between 2018 and 2010 imagery (2018 – 2010). This data only captures aggradation of sediment up until the reconfiguration of the BDAs in water year 2019. The aggradation shown west of river left Wells (1,4,13,8,11) is likely due to cattle grazing the adjacent hillside.

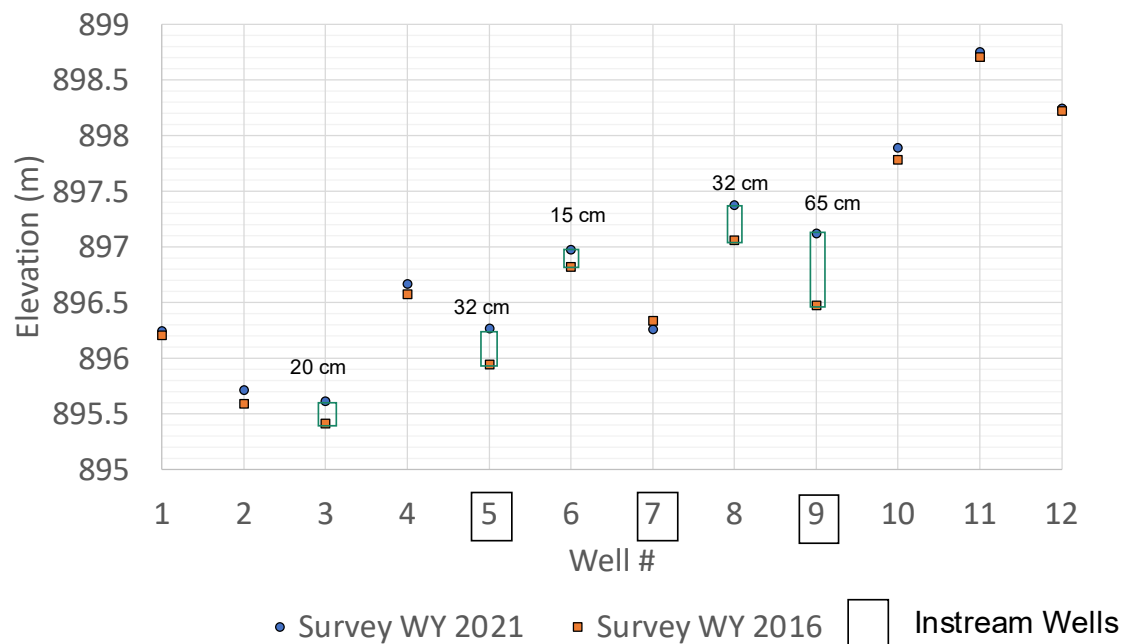


Figure 31. Elevation of surveyed well ground surface elevations from water year 2016 and water year 2021. Significant aggradation by wells is highlight by rectangles between survey points. Most instream wells, highlighted by blue squares, had significant aggradation. Aggradation around Wells 3 and 6 is most likely due to external factors such as cattle grazing and is not associated with stream deposition.

#### 4.4.3 Hydraulic Conductivity

I attempted to quantify hydraulic conductivity in the field via falling head tests, however, piping (when water continually funnels through the well indefinitely without causing head rise) was a common occurrence and representative values were not obtainable for most wells. Instead, I rely on values provided by Domenico and Schwarz (1990) for unconsolidated coarse sand that measured hydraulic conductivity that varied from  $9 \times 10^{-7}$  and  $6 \times 10^{-3}$  (m/s). Two tests using the Bouwer method to calculate

hydraulic conductivity at wells 2 and 8 produced results within the bounds from Domenico and Schwarz (1990) at  $3.87 \times 10^{-6}$  m/s and  $5.02 \times 10^{-6}$  m/s, respectively.

After the BDA ponds dry out at the end of June, there is a substantial subsequent decline in the water table (Figure 32). This decline is mainly observed in the mid-section of the reach upstream and downstream of the BDAs where there are large amounts of decomposed granite. At the upstream and downstream gauging stations, flow is extremely low; however, water is still present and does not dry out. This is because the gauging stations are bound by serpentinite bedrock. At these bedrock boundaries the hydraulic conductivity is very low and not much water would percolate at these locations.

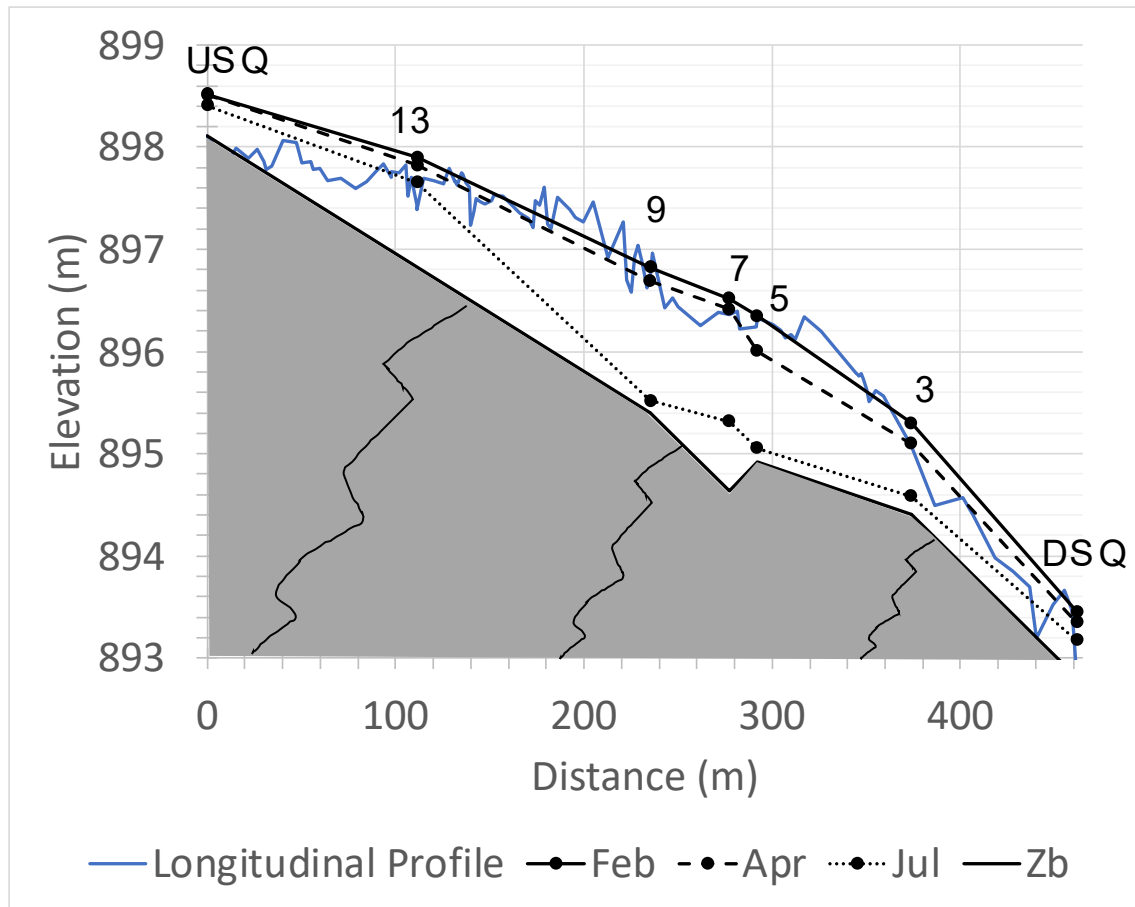


Figure 32. Longitudinal profile of stream channel on Miners Creek on 7/1/21 in comparison to other times of the year. Below the bedrock boundary (Zb), shown by the solid black line, the material is assumed to match the fractured Serpentinite at the upstream (US) and downstream (DS) gauging stations. Between the Zb and the channel elevation in yellow with a light blue solid line, is the fill of decomposed granite. This figure makes assumptions on connectivity of Zb material based on where instream proximal wells reached a resisting layer. Here we see that groundwater quickly declines after the BDA pond dries out

While the average reach slope is just 1.1%, there is a drastic increase in slope the last 500 m of the reach. From Well 3 to the downstream gauging station the slope increases to 2.5%. This increase in slope is likely due to channel incision near the downstream gauging station. While a small increase, a change in slope drives a steeper

head gradient that could result in the quick draining of the water table in July after the BDAs and other portions of the reach become discontinuous.

Since the mid-section of the reach on Miners Creek is largely decomposed granite, it is advisable for future studies to install BDAs near the upstream and downstream gauging stations where surface water is present year-round. This would provide the added benefit of causing aggradation on the two most incised sections of the reach and centralize the restoration effort.

Other projects such as the Sanctuary Forest's String of Pearl recharge ponds have attempted to control groundwater recharge using Bentonite clay (Wyeth Wunderlich, *Personal Communication*). Thus far, the method has slowed the rate that water leaves the recharge ponds, although its effectiveness and impact vary depending on timing and magnitude of precipitation events. A similar approach could be used to set a target hydraulic conductivity of the BDAs subsurface.

#### 4.4.4 Precipitation

Changes in seasonal precipitation from wet years (e.g., water year 2019) and dry years (e.g., water years 2020 and 2021) also clearly influence the BDAs ability to sustain ponded WSE elevation. Water year 2019 had the highest BDA WSE while water year 2020 and water year 2021 exhibited much lower pond levels (Figure 20). Even in dry years, however, side channels were activated, and runoff events occurred that increased pond storage. I, therefore, argue that structural degradation in combination with aggradation of sediment are the main culprits in reducing BDA water storage.

#### 4.4.5 BDA Poned Volume Estimates

Providing surface volume estimates in addition to depth provides a spatial extent to ponded habitat that might be utilized by Coho. While spawning maps show Coho actively use the BDA reach in winter, site observations indicated that juvenile Coho become dispersed and segmented to pools located near the upstream and downstream gauging stations in late spring through early summer. From there juveniles are likely to die as days of disconnection continue and result in water quality and increasing water temperature (Obedzinski et al., 2018).

The maximum ponded depth for BDA 1.1 was 50 cm which corresponded to 12.14 m<sup>3</sup> of water. This depth also happens to be just above the 48 cm threshold for the ideal ponded depth for June recruitment and optimal summer survival of Coho (Woelfle-Erskine et al., 2017) . The average June value, however, is just 21 cm, which corresponds to 3.31m<sup>3</sup> ponded volume. These values characterize BDA pond 1.1 as a small pond (<4.05 m<sup>3</sup>, <0.3 m), unlikely to offer over summer survival (Woelfle-Erskine et al., 2017).

During the dry season, BDA Pond 1.1 offered suitable habitat based on volume from 3/23/21-05/24/21 and from 3/23/21-5/11/21 in terms of depth (Figure 19). BDA Pond 1.2 had the deepest maximum depth but had a smaller surface area than Pond 1.1 and 1.3. BDA Pond 1.3 was the shallowest pond but had the largest surface area. I only assess BDA Pond 1.1 because it is the only pond with stage data available. Overall, I assume that the dynamics of BDA Ponds 1.2 and 1.3 act similarly to BDA Pond 1.1 and likely offer similar abiotic habitat parameters throughout the year.



I also acknowledge that there are many other abiotic and biotic factors that influence summer habitat for Coho (e.g., temperature, dissolved oxygen, water quality, grain size). I only suggest that in terms of pond depth and area that there is not sufficient habitat to sustain Coho for the summer survival.

From a positive perspective, estimates of ponded volumes, and knowledge of minimum ponded depth to maximize summer survival could act as target parameters to establish effective BDA ponds designed for baseflow on Miners Creek.

## 5. NATURAL BEAVER DAMS CASE STUDY

In the beginning of September water year 2021, a group of beaver constructed a dam ~1.6 km downstream of Miners Creek on French Creek (Figure 33). During this time flow on Miners Creek was discontinuous and flow on French Creek, based on previous flows available from the DWR gauge (Department of Water Resources), was  $<0.028$   $\text{m}^3/\text{s}$ . Dam building began ~9/11/21. Over an eight-day period, WSE behind the dam location increased 42cm from 9/11/21-9/18/21. There was an additional 14 cm increase in WSE from 9/18/21-10/04/21, when the WSE reached the crest elevation of the newly constructed dams (Figure 34). This created a ponded depth of 77 cm and a 56 cm total rise associated with the dam.

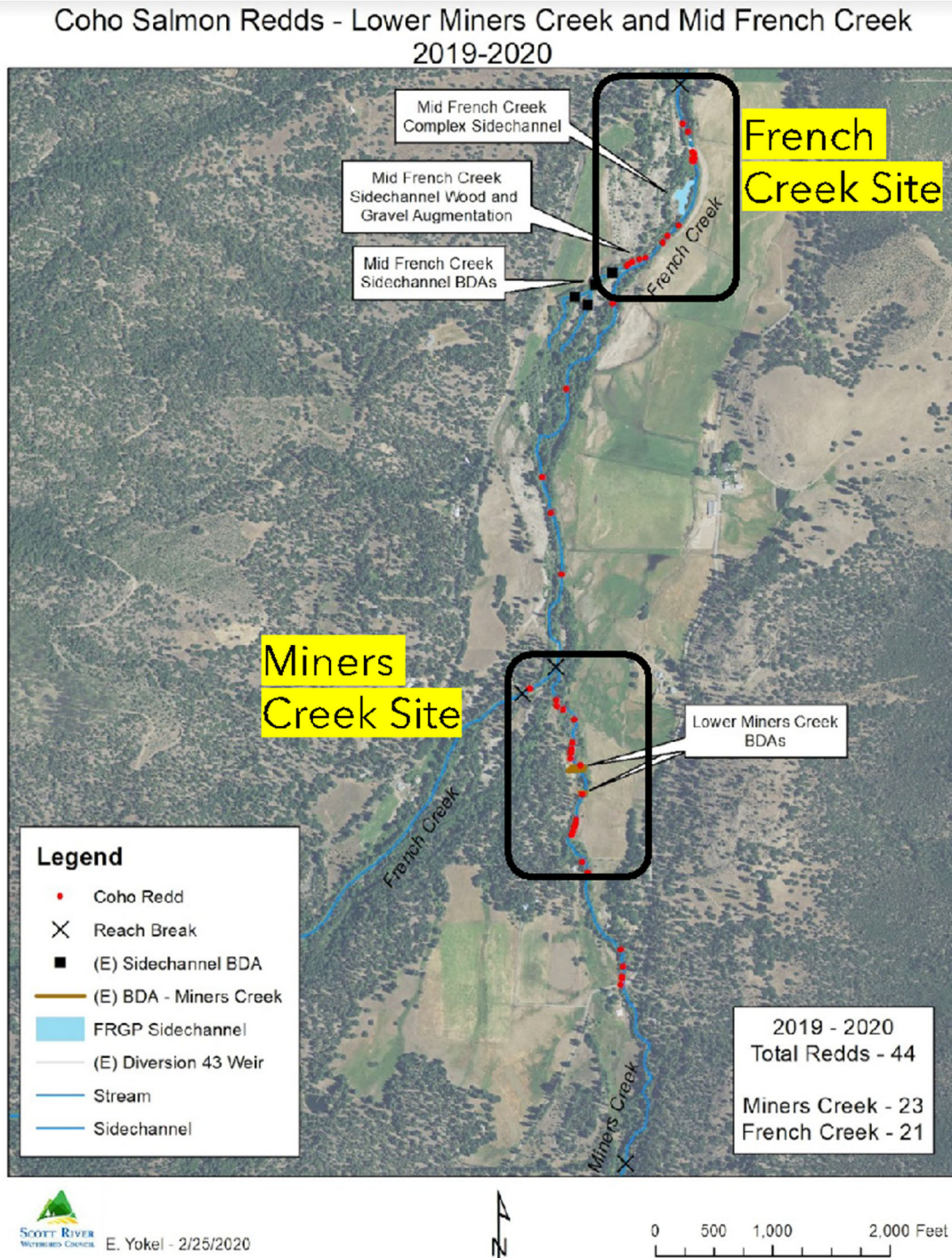


Figure 33. Satellite imagery of Miners Creek and French Creek restoration sites, delineated by black rectangles. Red circles indicate the observed total Redds (spawning beds) during water year 2019 as surveyed by Erich Yokel (SRWC).

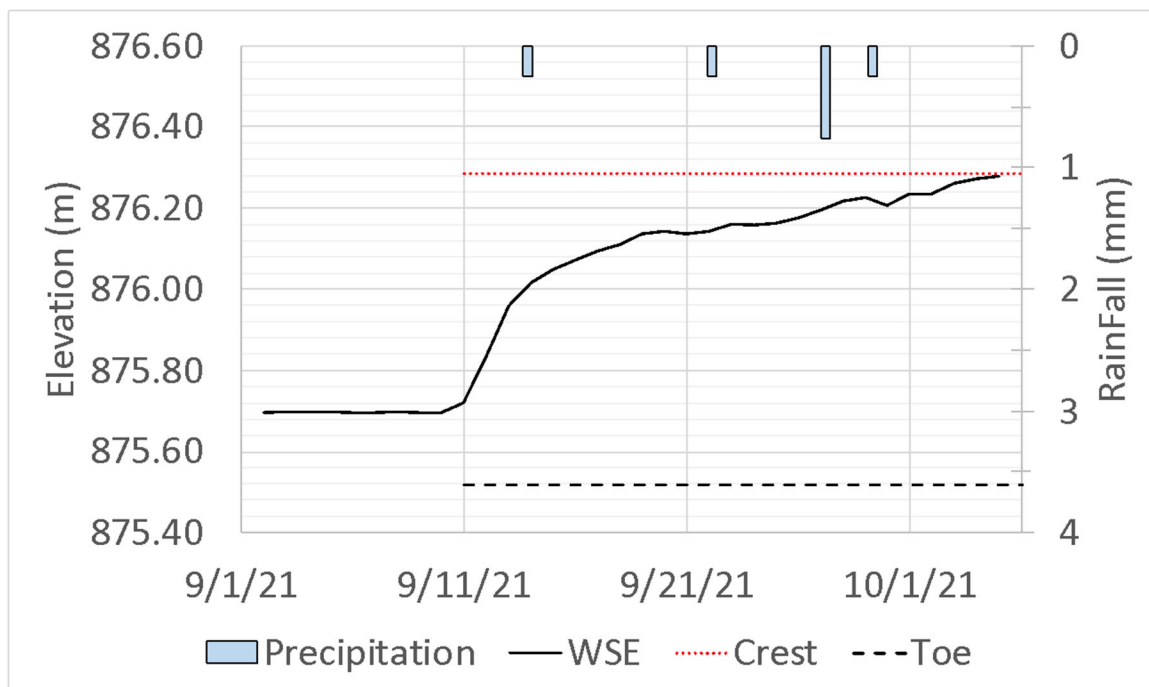


Figure 34. Rise in WSE at French Creek beaver dam from 09/01/21-10/04/21.

To check if this rise in WSE was due to regional influences, I compared the rise in WSE on the French Creek site to the WSE in all wells on Miners Creek. There was only a small amount of precipitation during this time (1.52 mm) and a rise in head in four of the thirteen active wells upstream on Miners Creek (Figure 35). The increases in head in wells (2,7,11, and 12) are all ground water fluxes as there is no expressed surface water at these wells. The rise in these wells, but the lack in rise in all other wells on Miners Creek indicates no regional pulse in the watershed significant enough to cause a rise in WSE on French Creek. It does remain interesting, however, that there are spatial and temporal fluxes in well head without significant input of precipitation.

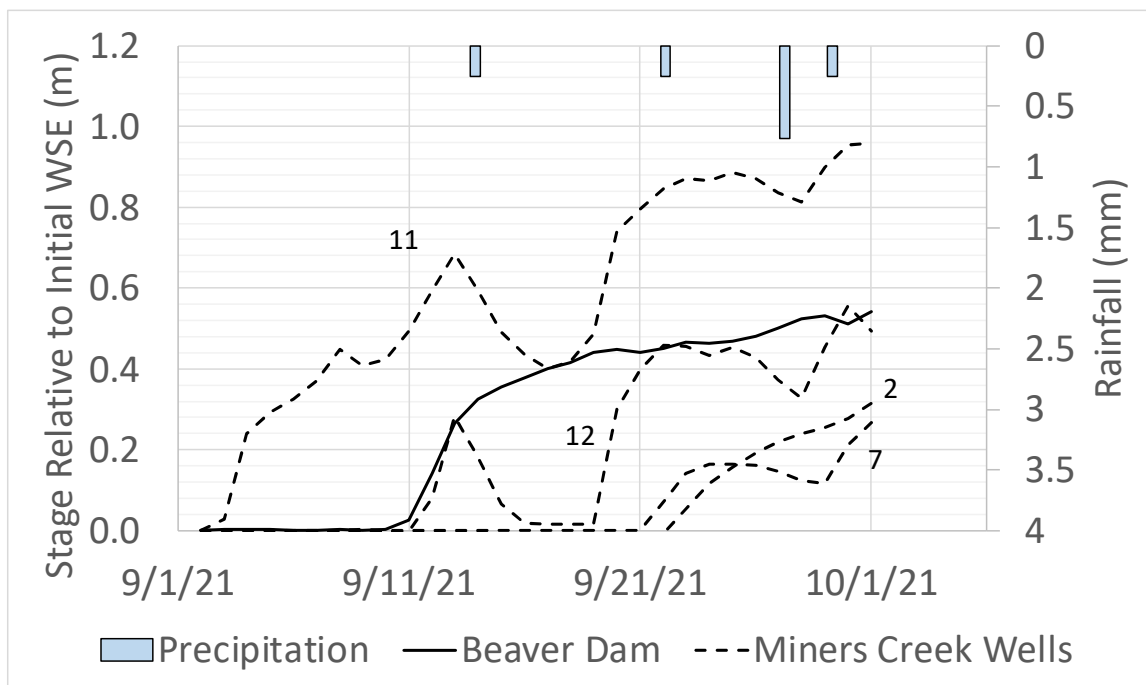


Figure 35. Rise in WSE relative to initial values on 09/01/21- 10/01/21. Here we see an increase in WSE on Miners Creek in Wells 11,12,7, and 2. The increases in WSE in individual wells but not the system suggests that there was no regional pulse that may have caused an increase in stream stage on French Creek during the construction of the Beaver Dam.

The Miners Creek watershed is characteristically different from French Creek, however, baseflow conditions in both basins are subject to extremely low flows. I suggest that due to the extremely low flows, data between sites are comparable. The data presented suggest that the new structurally sound, natural beaver dam can sustain ponding at or near its crest elevation during baseflow conditions. The three-year-old, porous BDA configuration on Miners Creek, however, does not sustain ponding near its crest even during flow events that exceed the magnitude of baseflow on French Creek.

This also suggests that the benefit of having an active beaver colony to maintain dams overtime may be a better long-term solution to having standalone BDA structures that do not receive consistent maintenance. While a hands-off approach is appropriate in systems with adequate flow, maintenance may be particularly important in systems like Miners Creek where small changes in ponded volume is critical for the survival of aquatic species. This natural dam also created a substantial increase in WSE during baseflow conditions from a ponded depth of 17 cm to 61 cm, which in terms of summer survival would bring the depth from a less suitable to more suitable habitat for Coho (Obedzinski et al., 2018) (Figure 36).



Figure 36. Game camera photo of Beaver Dam construction on French Creek. There is a pair of Coho (bottom left) and a beaver (upper right).

## 6. RECOMMENDATIONS

The Miners Creek watershed, like many watersheds in California, has a critical recharge problem. During the wet season, even under drought conditions, inputs are sufficient to drive continual flow, side channel flooding, and provide suitable spawning habitat for Coho at the restoration site. Much of the water that enters the restoration reach as discharge, however, exits as discharge. This indicates that only a small percentage of flow is translated into storage behind the BDAs or groundwater storage. Additionally, the runoff ratio within the system remains low indicating that subsurface storage pathways do not fill enough to drive higher runoff ratios. In spring, there is not sufficient recharge from snowpack to sustain baseflow or suitable rearing habitat into the following wet season. Instead, Miners Creek solely relies on its groundwater reservoirs to sustain surface flow during the dry season. Therefore, restoration on Miners Creek needs to be focused on recharge and holding water on the landscape in the form of meadows or ponded habitats (BDAs or recharge ponds) as there is essentially no recharge in the form of snowpack.

At the headwaters of the Miners Creek watershed there is a ~158,000 m<sup>2</sup> meadow, Paradise Hollow. Miners Creek flows through the meadow and has caused ~3-4 m of incision. This meadow, if restored to its ground surface elevation, could store large sums of groundwater that could recharge Miners Creek and provide water for riparian vegetation during successive drought years (Hunsaker et al. 2015).

While BDAs have their place in restoration within the Scott Valley, they are more suitable to be used in areas where *Castor canadensis* has a population that could potentially maintain them (Bouwes et. al 2016). Without proper maintenance by restoration practitioners, landowners, or beaver; BDAs will ultimately degrade and become porous making it difficult to sustain sufficient ponded habitat.

If maintained, BDAs could potentially provide ponded habitat further into baseflow if installed at a high density towards the upstream and downstream gauging stations where surface water is constantly expressed due to the exposed bedrock. Additionally, it is suggested that restoring anthropogenic related channel incision (upstream and downstream) of the BDAs would foster overbank flooding and may promote continuous flow longer into baseflow, unless there is an increase in ET due higher water availability for plant use and evaporation. It is, however, pointed out by Paul Powers (personal communication, US Forest Service) that these efforts are most effective if the geomorphic control of the watershed is identified and restored to match the relative elevation of the adjacent floodplains.

It is also important to consider the role of high volumes of decomposed granite in Miners Creek. Historic hydraulic mining and logging have increased the rate that granite would naturally weather. The deposition of this decomposed granite is not an ideal substrate for beaver to work with to promote ponding as it has a high hydraulic conductivity compared to substrates such as silt or clay (Domenico and Schwarz, 1990). This legacy effect would be difficult to ameliorate, however, attempts to set target conductivity of ponds as suggested in section 4.4.3 may be of interests.



## 7. CONCLUSIONS

This study is an analysis of the system scale storage dynamics (*Initial Wet Up, Steady State, Secondary Storage, Baseflow*) established by gaining and losing stream conditions. I also assess the impact of ground water storage and discharge on surface water retention and recharge of BDAs ponds. Additionally, I analyze whether BDAs provided ponded habitat through baseflow conditions and quantified how much ponded habitat increased.

I demonstrated that Miners Creek is a runoff dependent system that is sensitive to changes in discharge. The main indicators of this sensitivity to runoff is the 32% drop in pond volume in BDA Pond 1.1 as irrigation began and upstream discharge declined by  $\sim 1870 \text{ m}^3$  and conversely a rapid increase in BDA storage during the onset of the wet season under losing stream conditions with relatively low discharge and groundwater storage values compared to seasonal highs for water year 2021. Additionally, BDA Pond 1.1 dries under relatively high groundwater storage values indicating that the proportion of drainable water from the aquifer to the stream is not sufficient to support ponding or stream connectivity. This suggests that in dry years, under baseflow conditions, precipitation will be the main driver of connectivity and that ground water is not a significant contributor to BDA recharge. The exception, however, would be if groundwater aquifers could be filled well above the stream channel boundary elevation, ensuring that maximum amount of drainable storage returns to the stream under baseflow conditions.

Secondly, I showed a shift in the relationship between upstream discharge and BDA volume post maximum storage. After the occurrence of the highest groundwater storage and discharge values, there is a shift in the relationship of how BDA storage dynamics respond. Post maximum groundwater storage and discharge, similar values of groundwater storage and discharge yield lower BDA ponded storage. The trend of decreasing BDA pond volumes overlaps with both losing and gaining conditions from the latter portion of *Secondary Storage* into *Baseflow*. The decreases in BDA pond volume even under losing stream conditions could be driven by increases in transpiration by plants accessing water from saturated and unsaturated zones and evaporation that would decrease BDA storage under conditions that would usually result in an increase in storage.

During *Baseflow*, under gaining stream conditions, there is no significant recharge of the BDAs. There is a period of sustained pond volume, however, the contributions from groundwater storage are not significant enough to sustain perennial baseflow. The system becomes discontinuous in late July after the BDA ponds go dry. Groundwater storage values remain high until the BDAs dry out. This indicates that while groundwater storage is high much of it is not expressed at the BDAs or along the restoration reach and drains downstream.

Miners Creek failed to provide recharge that supports ponded habitat for Coho during critical dry months (June-August). Groundwater sustained flows on Miners Creek throughout *Baseflow* (04/28/21-06/20/21). The groundwater aquifer was actively filling throughout *Initial Wet-Up* (11/06/21-11/19/21) and during *Secondary Storage* (01/04/21-

04/27/21) until the maximum groundwater storage value was reached on 2/15/21. This means that during water year 2021 the aquifer was actively filling 57 days and it took 125 days to deplete the aquifer completely. The study period was 227 days, therefore 25% of the time the aquifer was filling, 55% of the time the aquifer was losing water to ET with 43% of that time there being a combination of ET and contributions from the aquifer to the stream. During *Steady State*, the remaining 20% of the time, the aquifer was stable. Sustained flows from the groundwater to the stream occurred 24% of the study period.

While BDA recharge was not significant and did not provide ponded habitat during the summer months, the ponds did increase ponded habitat on Miners Creek by  $\sim 36.42 \text{ m}^3$ . This does not consider the effect of the farthest upstream BDA or the decommissioned BDA.

Based on a natural beaver dam on French Creek, 1.6 km downstream from the study site, data show that *Castor canadensis* can create dams that increase ponded habitat under baseflow conditions when BDAs on Miners Creek failed to do so.

## REFERENCES

- Beschta, R. L., & Ripple, W. J. (2009). Large predators and trophic cascades in terrestrial ecosystems of the western United States. *Biological Conservation*, *142*(11), 2401–2414.
- Bouwes, N., Weber, N., Jordan, C. E., Saunders, W. C., Tattam, I. A., Volk, C., Wheaton, J. M., & Pollock, M. M. (2016). Ecosystem experiment reveals benefits of natural and simulated beaver dams to a threatened population of steelhead (*Oncorhynchus mykiss*). *Scientific Reports*, *6*(1), 28581.
- Burchsted, D., Daniels, M., Thorson, R., & Vokoun, J. (2010). The River Discontinuum: Applying Beaver Modifications to Baseline Conditions for Restoration of Forested Headwaters. *BioScience*, *60*(11), 908–922.
- Denny, J. (1970). *The Death of a Lady*.
- Cairns, D.K., MacFarlane, R.E., Guignion, D.L., and Dupuis, T. (2012). The status of Atlantic salmon (*Salmo salar*) on Prince Edward Island (SFA 17) in 2011. DFO Can. Sci. Advis. Sec. Res. Doc. 2012/090. iv + 33 p.
- California Department of Conservation. Geological Survey. Geological Map of California. <https://maps.conservation.ca.gov/cgs/gmc/>
- California Department of Fish and Game. (2004). Recovery strategy for California coho salmon. Report to the California Fish and Game Commission. 594 pp.
- O'Keefe, Christopher G., (2021) "Do beaver dam analogues act as passage barriers to juvenile coho salmon and juvenile steelhead trout?". *Cal Poly Humboldt theses and projects*. 508
- Cluer, B., & Thorne, C. (2014). A Stream Evolution Model Integrating Habitat and Ecosystem Benefits. *River Research and Applications*, *30*(2), 135–154.
- Cunjak, R. A., & Therrien, J. (1998). Inter-stage survival of wild juvenile Atlantic salmon, *Salmo salar* L. *Fisheries Management and Ecology*, *5*(3), 209–223.
- Dralle, D. N., Hahm, W. J., Rempe, D. M., Karst, N. J., Thompson, S. E., & Dietrich, W. E. (2018). Quantification of the seasonal hillslope water storage that does not drive streamflow: Catchment storage that does not drive streamflow. *Hydrological Processes*, *32*(13), 1978–1992.

- Domenico, P.A. and F.W. Schwartz, (1990). *Physical and Chemical Hydrogeology*, John Wiley & Sons, New York, 824 p.
- Foglia, L., A. McNally, C. Hall, L. Ledesma, R. J. Hines, and T. Harter, (2013). Scott Valley Integrated Hydrologic Model: Data Collection, Analysis, and Water Budget, Final Report. University of California, Davis, <http://groundwater.ucdavis.edu>, April 2013. 101 p.
- Fort Jones, California conditions*. Drought.gov. (n.d.). Retrieved December 6, 2022, from <https://www.drought.gov/location/Fort%20Jones%2C%20California>
- Goldfarb, B., (2018). *Eager The Surprising Secret Life of Beavers and Why They Matter*, Chelsea Green Publishing
- Green, K., & Westbrook, C. (2009). Changes in riparian area structure, channel hydraulics, and sediment yield following loss of beaver dams. *BC J. Ecosyst. Manage.*, 10.
- Hahm, W. J., Rempe, D. M., Dralle, D. N., Dawson, T. E., Lovill, S. M., Bryk, A. B., Bish, D. L., Schieber, J., & Dietrich, W. E. (2019). Lithologically Controlled Subsurface Critical Zone Thickness and Water Storage Capacity Determine Regional Plant Community Composition. *Water Resources Research*, 55(4)
- Harter, T., & Hines, R. (2008). *SCOTT VALLEY COMMUNITY GROUNDWATER STUDY PLAN*. 98.
- Hayashi, M., Van der Kamp, G. (2000). Simple equations to represent the volume–area depth relations of shallow wetlands in small topographic depressions, *Journal of Hydrology*, Volume 237, Issues 1–2, Pages 74-85,
- Hunsaker, C., Swanson, S., Viers, R., Hill, B. (2015). *Effects on Meadow Erosion and Restoration on Groundwater Storage and Baseflow in National Forest in the Sierra Nevada, California*. USDA Forest Service Pacific Southwest Region, National Fish and Wildlife Services, and the California Department of Water Resources.
- James, L. A., (2019) Impacts of pre- vs. postcolonial land use on floodplain sedimentation in temperate North America *Geomorphology* 331 59–77
- Johnson, J. (n.d.). *Catalog of waters important for spawning, rearing, or migration of anadromous fishes—Southwestern region, effective September 15, 2006*. 289.

- Johnson-Bice, S. M., Renik, K. M., Windels, S. K., & Hafs, A. W. (2018). A Review of Beaver-Salmonid Relationships and History of Management Actions in the Western Great Lakes (USA) Region. *North American Journal of Fisheries Management*, 38(6), 1203–1225.
- Johnson, J. and E. Weiss. (2006). Catalog of waters important for spawning, rearing, or migration of anadromous fishes – Southwestern Region, Effective September 15, 2006. Alaska Department of Fish and Game, Special Publication No. 06-18, Anchorage.
- Karran, D. J., Westbrook, C. J., & Bedard-Haughn, A. (2018). Beaver-mediated water table dynamics in a Rocky Mountain fen. *Ecohydrology*, 11(2), e1923.
- Karran, D., Westbrook, C., Wheaton, J., Johnston, C., & Bedard-Haughn, A. (2016). Rapid surface water volume estimations in beaver ponds. *Hydrology and Earth System Sciences Discussions*.
- Kemp, P. S., Worthington, T. A., Langford, T. E. L., Tree, A. R. J., & Gaywood, M. J. (2012). Qualitative and quantitative effects of reintroduced beavers on stream fish. *Fish and Fisheries*, 13(2), 158–181
- Lautz, L., Kelleher, C., Vidon, P., Coffman, J., Riginos, C., & Copeland, H. (2019). Restoring stream ecosystem function with beaver dam analogues: Let's not make the same mistake twice. *Hydrological Processes*, 33(1), 174–177
- Machen, Florence Consolati,. (2016) "The Role of a Beaver in Shaping Stream Channel Complexity and Thermal Heterogeneity in a Central Oregon Stream". All Graduate Plan B and other Reports. 765
- Malison, R., Kuzishchin, K., & Stanford, J. (2016). Do beaver dams reduce habitat connectivity and salmon productivity in expansive river floodplains? *PeerJ*, 4.
- Marsh, G. P., (1864) *Man and Nature: Or, Physical Geography as Modified by Human Action* (NY: Scribner)
- Minke, A., Westbrook, C., & van der Kamp, G. (2010). Simplified Volume-Area-Depth Method for Estimating Water Storage of Prairie Potholes. *Wetlands*, 30, 541–551.
- Morris, D.A. and A.I. Johnson, (1967). Summary of hydrologic and physical properties of rock and soil materials as analyzed by the Hydrologic Laboratory of the U.S. Geological Survey, U.S. Geological Survey Water-Supply Paper 1839-D, 42p.

- Munir, T. M., & Westbrook, C. J. (2021). Beaver dam analogue configurations influence stream and riparian water table dynamics of a degraded spring-fed creek in the Canadian Rockies. *River Research and Applications*, 37(3), 330–342.
- Naiman, R., Johnston, C., & Kelley, J. (1988). Alteration of North American Streams by Beaver. *Bioscience*, 38.
- Nash, C. S., Selker, J. S., Grant, G. E., Lewis, S. L., & Noël, P. (2018). A physical framework for evaluating net effects of wet meadow restoration on late-summer streamflow. *Ecohydrology*, 11(5), e1953.
- National Marine Fisheries Service. (2014). Final Recovery Plan for the Southern Oregon/Northern California Coast Evolutionarily Significant Unit of Coho Salmon (*Oncorhynchus kisutch*). National Marine Fisheries Service. Arcata, CA.
- Obedzinski, M., Nossaman Pierce, S., Deitch, M., (2018). Effects of Flow-Related Variables on Oversummer Survival of Juvenile Coho Salmon in Intermittent Streams. *Transactions of the American Fisheries Society* 147(3):588-605
- OCM Partners, 2022: 2018 FEMA LiDAR: Region 9, CA. NOAA National Centers for Environmental Information, received from URL: <https://www.fisheries.noaa.gov/inport/item/64466>.
- Onset Computer Corporation (2005-2018). *HOB0 Data Logging Rain Gauge (RG3 and RG3-M) Manual* from URL
- Onset Computer Corporation (2014-2018). *U20L Water Level Logger (U20L-0X) Manual* received from URL: [https://www.onsetcomp.com/files/manual\\_pdfs/17153-G%20U20L%20Manual.pdf](https://www.onsetcomp.com/files/manual_pdfs/17153-G%20U20L%20Manual.pdf)
- Orr, M., Weber, N., Noone, W., Mooney, M., Oakes, T., & Broughton, H. (2020). Short-Term Stream and Riparian Responses to Beaver Dam Analogs on a Low-Gradient Channel Lacking Woody Riparian Vegetation. *Northwest Science*, 93, 171.
- Pearce, C., Vidon, P., Lutz, L., Kelleher, C., & Davis, J. (2021). Impact of beaver dam analogues on hydrology in a SEMI-ARID floodplain. *Hydrological Processes*, 35(7).
- Pollock, M. M., Beechie, T. J., & Jordan, C. E. (2007). Geomorphic changes upstream of beaver dams in Bridge Creek, an incised stream channel in the interior Columbia River basin, eastern Oregon. *Earth Surface Processes and Landforms*, 32(8), 1174–1185.

- Pollock, M. M., Beechie, T. J., Wheaton, J. M., Jordan, C. E., Bouwes, N., Weber, N., & Volk, C. (2014). Using Beaver Dams to Restore Incised Stream Ecosystems. *BioScience*, 64(4), 279–290.
- Pollock, M., Pess, G., Beechie, T., & Montgomery, D. (2004). The Importance of Beaver Ponds to Coho Salmon Production in the Stillaguamish River Basin, Washington, USA. *North American Journal of Fisheries Management*, 24, 749–760.
- Pollock, M. M., Witmore, S., & Yokel, E. (2019). A field experiment to assess passage of juvenile salmonids across beaver dams during low flow conditions in a tributary to the Klamath River, California, USA. *BioRxiv*, 856252.
- Pollock, M., Wheaton, J., Bouwes, N., Volk, C., Weber, N., & Jordan, C. (2012). Working with Beaver to Restore Salmon Habitat in the Bridge Creek Intensively Monitored Watershed-Design Rationale and Hypotheses. *NOAA Technical Memorandum, NMFS-NWFSC-120*, 1–47.
- Polvi L E and Wohl E (2012) The beaver meadow complex revisited—the role of beavers in post-glacial floodplain development *Earth Surf. Process. Landf.* 37 332–46
- Puttock, A., Graham, H. A., Cunliffe, A. M., Elliott, M., & Brazier, R. E. (2017). Eurasian beaver activity increases water storage, attenuates flow and mitigates diffuse pollution from intensively-managed grasslands. *Science of The Total Environment*, 576, 430–443.
- Quigley, Danielle. (2006). Final Report Scott River Adult Coho Spawning Ground Surveys November 2005 – January 2006. Prepared by the Siskiyou Resource Conservation 3825 District for the United States Fish and Wildlife Service
- RStudio Team* (2022). *RStudio: Integrated Development for R*. RStudio, PBC, Boston, MA URL <http://www.rstudio.com/>.
- Ringelman, J. K. (1991). 13.4.7. *Managing Beaver to Benefit Waterfowl*. 8.
- Rosell, F., Bozser, O., Collen, P., & Parker, H. (2005). Ecological impact of beavers *Castor fiber* and *Castor canadensis* and their ability to modify ecosystems. *Mammal Review*, 35.
- Rybczynski, N., Ross, E. M., Samuels, J. X., & Korth, W. W. (2010). Re-Evaluation of *Sinocastor* (Rodentia: Castoridae) with Implications on the Origin of Modern Beavers. *PLoS ONE*, 5(11), e13990.



- Scamardo, J., & Wohl, E. (2020). Sediment storage and shallow groundwater response to beaver dam analogues in the Colorado Front Range, USA. *River Research and Applications*, 36(3), 398–409.
- Shields, F. D., Knight, S. S., and Cooper, C. M., (1995) Rehabilitation of watersheds with incising channels *Water Res. Bull.* 31 971–82
- Sommarstrom, S., Kellog, E., Kellog J. (1990). Scott River Basin Granitic Sediment Study. Siskiyou Resource Conservation District.
- Siskiyou County Flood Control and Water District Groundwater Sustainability Agency, Scott River Valley Groundwater Sustainability Plan (Public Draft), August (2021). <https://www.co.siskiyou.ca.us/naturalresources/page/sustainable-groundwatermanagement-act-sigma>
- Stout, T. L., Majerova, M., & Neilson, B. T. (2017). Impacts of beaver dams on channel hydraulics and substrate characteristics in a mountain stream. *Ecohydrology*, 10(1), e1767.
- USGS. (2022). Streamstats v4.7.0. US Department of the Interior. received from URL: <https://streamstats.usgs.gov/ss/>
- Wade, J., Lautz, L., Kelleher, C., Vidon, P., Davis, J., Beltran, J., & Pearce, C. (2020). Beaver dam analogues drive heterogeneous groundwater–surface water interactions. *Hydrological Processes*, 34(26), 5340–5353.
- Walter, R., & Merritts, D. (2008). Natural Streams and the Legacy of Water-Powered Mills. *Science (New York, N.Y.)*, 319, 299–304.
- Web Soil Survey*. (n.d.). Retrieved April 19, 2021  
from <https://websoilsurvey.sc.egov.usda.gov/App/WebSoilSurvey.aspx>
- Weber, N., Bouwes, N., Pollock, M., Volk, C., Wheaton, J., Wathen, G., Wirtz, J., & Jordan, C. (2017). Alteration of stream temperature by natural and artificial beaver dams. *PLoS ONE*, 12.
- Westbrook, C. J., Cooper, D. J., & Baker, B. W. (2006). Beaver dams and overbank floods influence groundwater–surface water interactions of a Rocky Mountain riparian area. *Water Resources Research*, 42(6).
- Wheaton, J., Bennett, S., Bouwes, N., Maestas, J., & Shahverdian, S. (2019). *Low-Tech Process-Based Restoration of Riverscapes: Design Manual. Version 1.0.*

- Wohl, E. (2013a). Landscape-scale carbon storage associated with beaver dams. *Geophysical Research Letters*, *40*, 3631–3636.
- Wohl, E. (2013b). Floodplains and wood. *Earth-Science Reviews*, *123*, 194–212.
- Wohl, E. (2021). Legacy effects of loss of beavers in the continental United States. *Environmental Research Letters*, *16*(2), 025010.

## APPENDICES

## Appendix A: Water Surface Elevation

Example of field data sheet for measuring field estimated WSE (

Table 2). The mWSE was then compared to the cWSE. In instances where cWSE was off by more than 3.048 cm, the calculations were adjusted to match the field mWSE. All values measured in the imperial system were converted to the metric system.

Table 2. Data sheet for Well 4 used to compare field WSE to WSE calculated by data loggers.

Date + Time	Well #	Distance to wse from RP (m)	Distance to wse from RP (ft)	Notes	RP Elevation (ft)	mWSE (ft)
1/7/21 12:58	MW4	1.13	3.71	Download	2944.11	2940.40
3/2/21 15:01	MW4	1.14	3.74		2944.11	2940.37
3/26/21 8:42	MW4	1.18	3.87	Changed from PDT to PST	2944.11	2940.23
4/16/21 8:34	MW4	1.31	4.28	Changed from PDT to PST	2944.11	2939.82
5/7/21 12:41	MW4	1.24	4.07	download Changed from PDT to PST	2944.11	2940.04
5/7/21 13:05	MW4	1.24	4.07	hydraulic conductivity download Changed from PDT to PST	2944.11	2940.04
5/19/21 11:53	MW4	1.33	4.36	Now right time	2944.11	2939.74
5/25/21 10:41	MW4	1.36	4.46		2944.11	2939.64
6/12/21 10:31	MW4	1.35	4.43		2944.11	2939.68

### Appendix B: Precipitation

This section presents how precipitation varied between the Miners Creek gauge and the Callahan gauge. There are instances when precipitation in Callahan varied, and other times precipitation was equal (Figure 37. Precipitation at both Callahan and Miners Creek stations from (11/06/20-9/31/21).

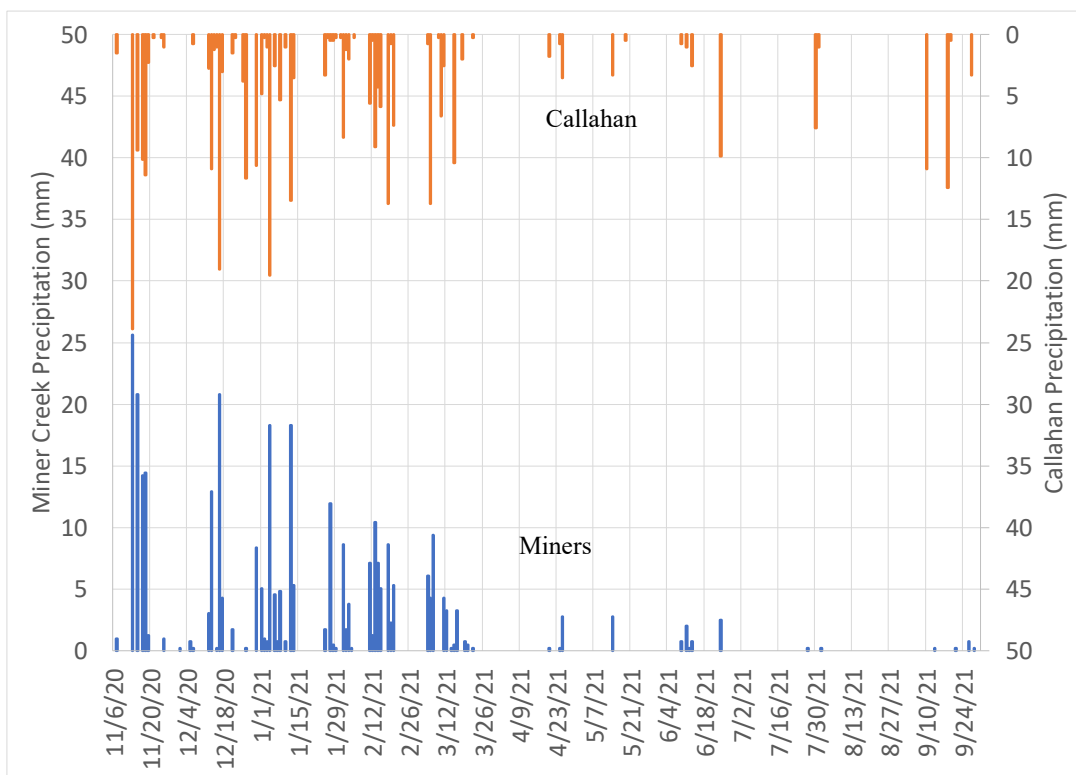


Figure 37. Precipitation at both Callahan and Miners Creek stations from (11/06/20-9/31/21).

A linear model was also used to predict precipitation on Miners Creek for years where there was no precipitation station on Miners Creek (Figure 38.)

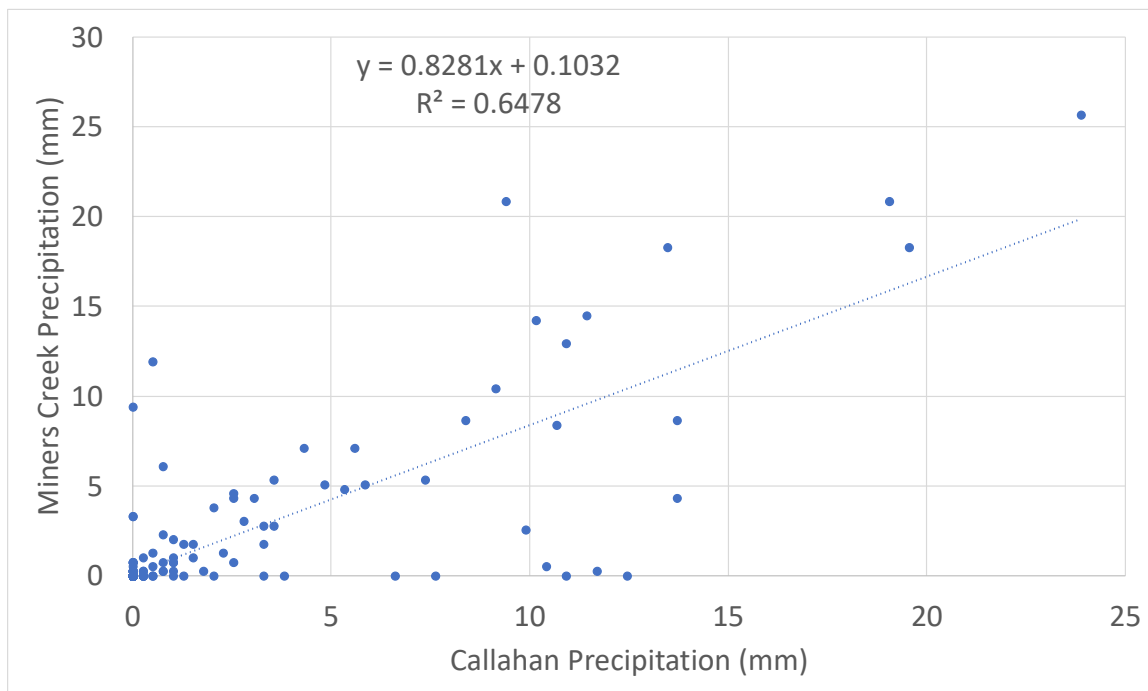


Figure 38. Miners Creek precipitation vs Callahan precipitation. The equation used to estimate precipitation is shown on the graph as well as the  $R^2$  value.

### Appendix C: Discharge

The rating curve predicted 99.4% of the variation in the upstream discharge data and 99.2% in at the downstream station (Figure 39). The residual standard error of model was 0.0061 US and 0.0068 (m<sup>3</sup>/s). These values indicated that the model was a good fit and that the residuals were close the field measured discharges. The difference in each model considering uncertainty in the FlowTracker2 indicates upper and lower limits of error did not greatly affect discharge (Figure 40, Figure 41).



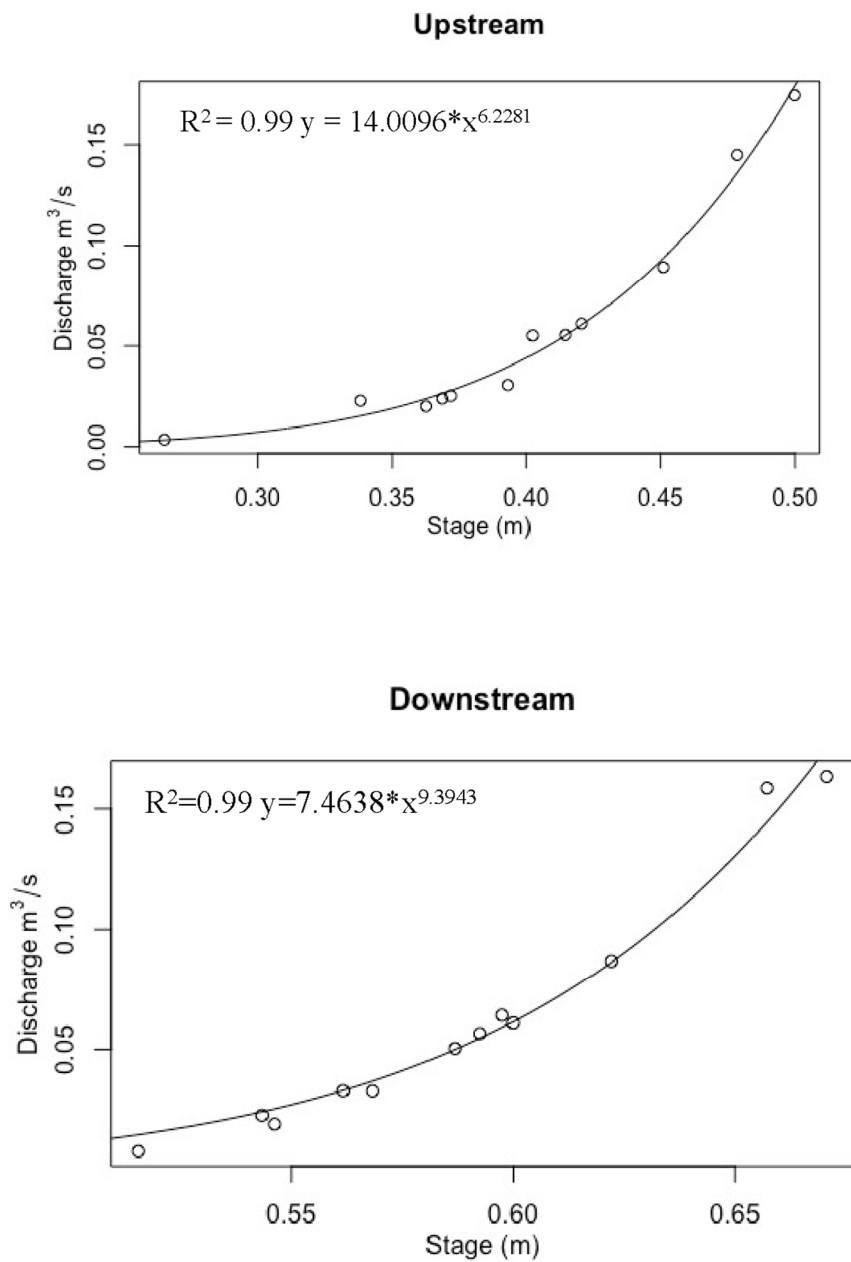


Figure 39. Upstream and Downstream rating curves, associated  $R^2$ , and equation

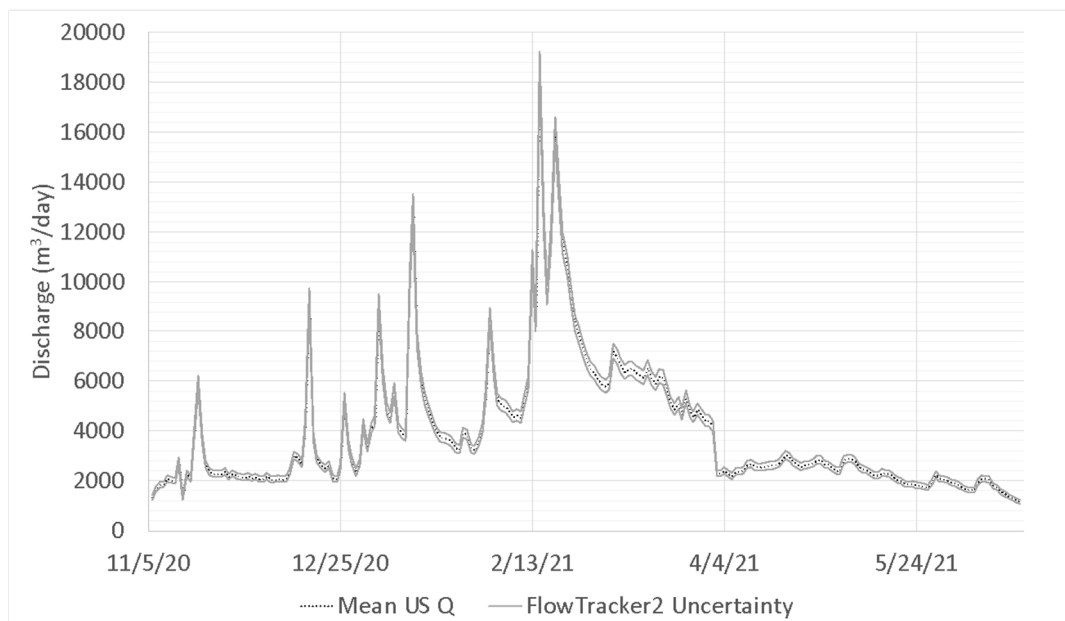


Figure 40. Upstream discharge (dashed line) and *Flowtracker2* Uncertainty (solid lines). The upper and lower estimates are estimated by making rating curves that are  $\pm$  the estimated uncertainty produced by the *Flowtracker2* ()

Table 3).

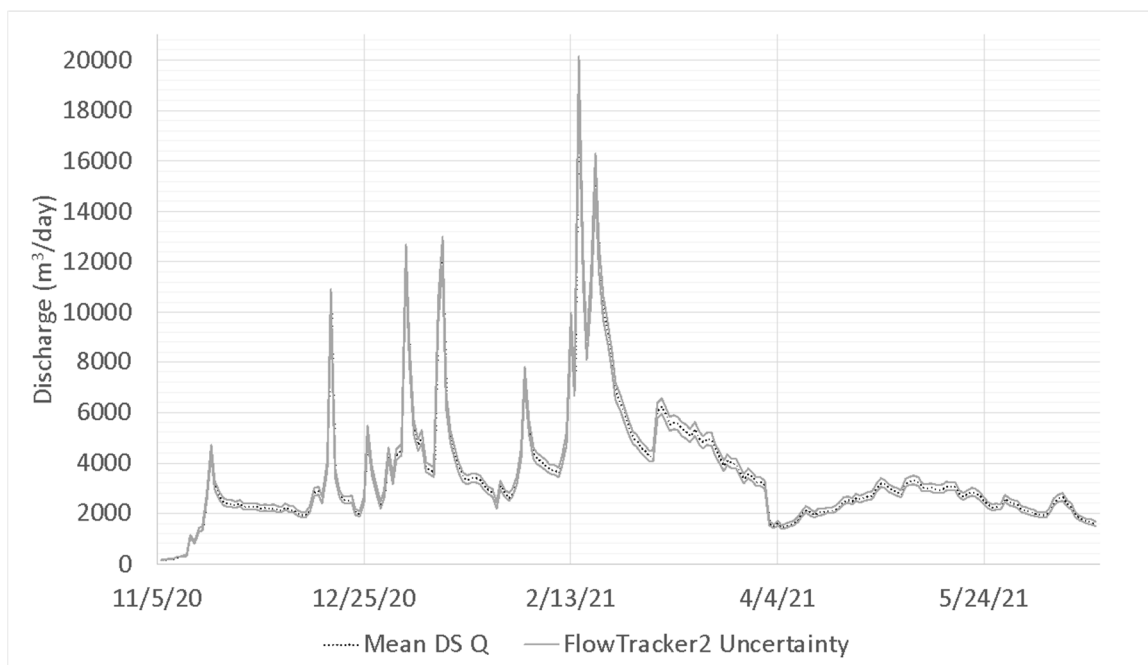


Figure 41. Downstream discharge (dashed line) and *Flowtracker2* Uncertainty (solid lines). The upper and lower estimates are estimated by making rating curves that are  $\pm$  the estimated uncertainty produced by the *Flowtracker2* (

Table 4).

Uncertainty in terms of the FlowTracker2 and in terms of the predicted vs. measured discharge varied from measurement to measurement (Table 3,

Table 4). Flows at low stage heights resulted in higher error, however, the percent errors at lower flows result in a lower magnitude of error in terms of volume of water. The upstream error (Observed vs. Predicted) was 11.07% and downstream error was 7.81%. Measurements were taken at regular intervals at a variety of flow conditions (Figure 42)

Table 3. Summary results for developing Sensor Stage vs Discharge relationship and associated uncertainties at upstream station.

Date	Discharge (m <sup>3</sup> /s)	Sensor Elevation (m)	Discharge Predicted (m <sup>3</sup> /s)	Error (Measured vs. Predicted)	Uncertainty (FlowTracker2)
10/1/20	0.0038	0.2652	0.0036	4.67%	6.70%
5/17/21	0.0214	0.3627	0.0252	-17.85%	6.31%
11/17/20	0.0240	0.3383	0.0164	31.66%	4.65%
4/16/21	0.0253	0.3688	0.0280	-10.67%	5.68%
4/28/21	0.0269	0.3718	0.0295	-9.36%	6.42%
11/19/20	0.0327	0.3932	0.0417	-27.26%	6.60%
1/7/21	0.0572	0.4023	0.0481	16.02%	3.70%
3/24/21	0.0581	0.4145	0.0579	0.38%	4.63%
2/12/21	0.0637	0.4206	0.0634	0.59%	4.30%
2/2/21	0.0933	0.4511	0.0978	-4.92%	4.32%
2/16/21	0.1513	0.4785	0.1412	6.69%	4.21%
2/19/21	0.1801	0.4998	0.1851	-2.80%	3.08%

Table 4. Summary results for developing Stage vs Discharge relationship and associated uncertainties at downstream station.

Date	Discharge (m <sup>3</sup> /s)	Sensor Elevation (m)	Discharge Predicted (m <sup>3</sup> /s)	Error (Measured vs. Predicted)	Uncertainty (FlowTracker2)
6/25/21	0.0074	0.5155	0.0140	-87.95%*	6.9%
6/4/21	0.0181	0.5462	0.0241	-32.93%	5.6%
4/16/21	0.0215	0.5434	0.0230	-6.85%	5.8%
5/17/21	0.0307	0.5683	0.0351	-14.31%	7.2%
4/28/21	0.0308	0.5617	0.0314	-1.88%	6.9%
3/24/21	0.0481	0.5869	0.0475	1.27%	4.7%
2/12/21	0.0542	0.5925	0.0520	4.02%	4.5%
3/19/21	0.0583	0.6000	0.0585	-0.36%	4.7%
3/6/21	0.0612	0.5975	0.0563	8.01%	4.9%
2/2/21	0.0833	0.6221	0.0823	1.20%	4.2%
2/16/21	0.1506	0.6571	0.1381	8.34%	5.3%
2/19/21	0.1569	0.6707	0.1674	-6.74%	4.2%

\*Measurement removed from error calculation

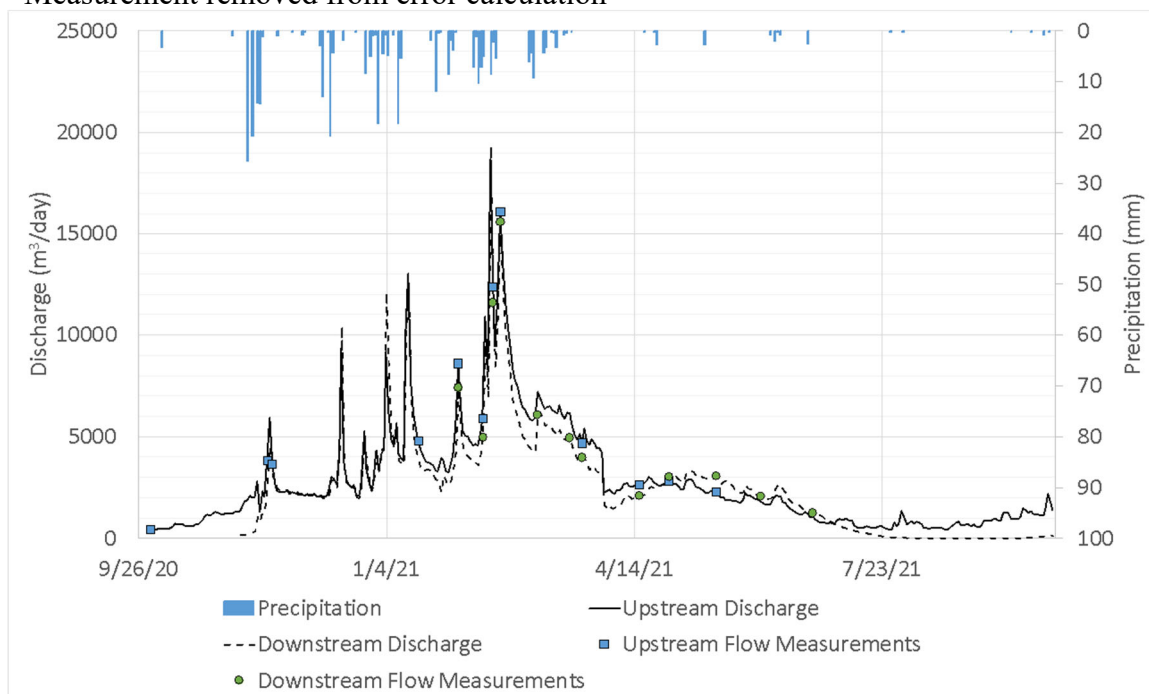


Figure 42. Each discharge measurement used to develop upstream and downstream rating curves plotted on their respective daily discharge value.



#### Appendix D: Substrate Sampling

Five wells were sampled (8,13,9,5,14) with a hand auger. Holes were dug to a resisting layer (fractured bedrock) which occurred between 0.75-1.33m depending on the well. Samples were carefully taken at various intervals above and below the static water table by inserting 5 ml vials carefully into the substrate column. These samples were brought into the lab, weighed wet, dried, and weighed again to estimate the Volumetric Moisture Content (VMC). The VMC below the static water table provides an estimate of porosity. A bulk sample of substrate was also examined to classify the substrate so that a representative estimate of specific yield could be used in the GW calculations.

### Appendix E: Ground Water Storage

Here I note that using an average head for the Well network does not pick up on the changes in head between wells. Methods such as Inverse Distance Weighting (IDW) or Kriging can be used to interpolate between wells. These methods were used in this project in other papers; however, it was decided that coming up with a system wide average was more representative to the data (Figure 43).

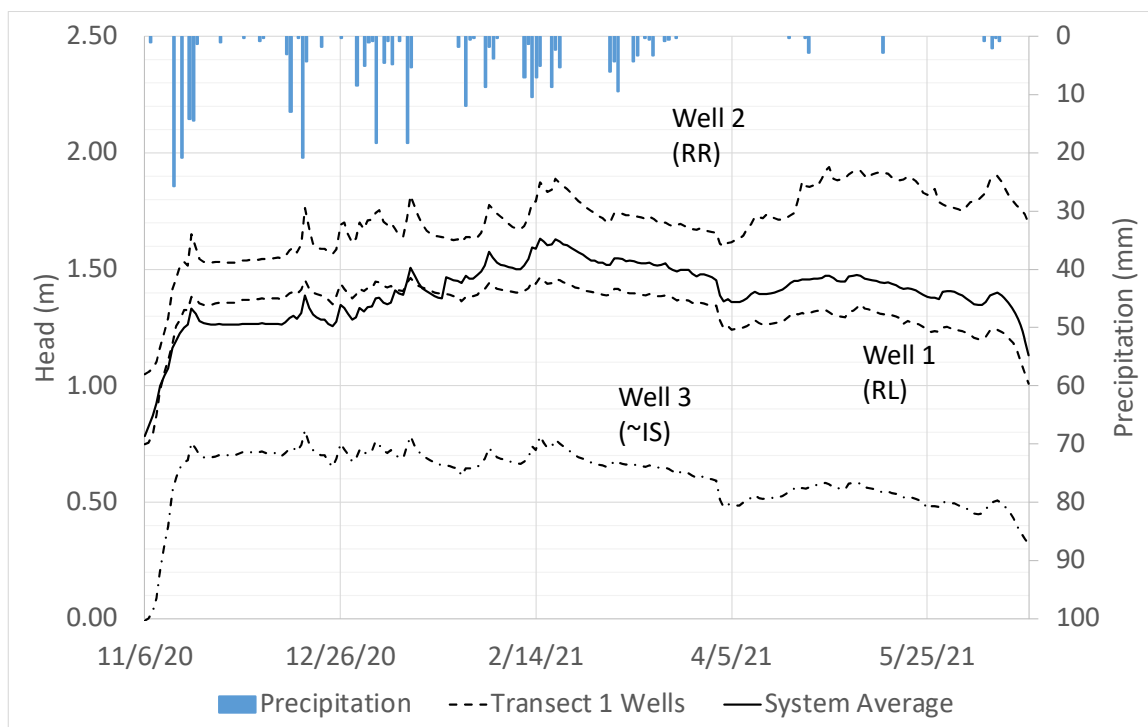


Figure 43. Well head for the furthest downstream transect (transect 1) throughout the study period and the system wide average. Precipitation is on the secondary y-axis. This shows that the system average will vary from individual well head.

## Appendix F: Reach Scale Storage

Transect data of wells showed that gaining and losing conditions varied temporally (Figures 20-23). Here we present data from three periods overlapping with Steady State, Secondary Storage, and Baseflow. During Secondary Storage and Baseflow, reach scale dynamics do not always overlap with well transect data. Transect 1 showed gaining conditions from well 1 to well 3 and losing conditions from well 3 to well 2 (Figure 44). This occurred during each storage stage. Transect 2 mirrored reach scale storage dynamics during Secondary Storage and Baseflow (Figure 45). Transect 3, where BDAs 1.1-1.3 are located was the only transect that was gaining through all storage states (Figure 46). Transect 4 was losing under all storage conditions (Figure 47). This shift in gaining or losing conditions on sub reach scales vs reach scale dynamics also discussed in Majerova et al. (2015) when considering smaller spatial scales. In their study, sub-reach variability was proposed to occur via different mechanisms in and around beaver dams put forth by Lautz and Segal (2006) and Janzen and Westbrook (2011), such as groundwater surface water exchanges.

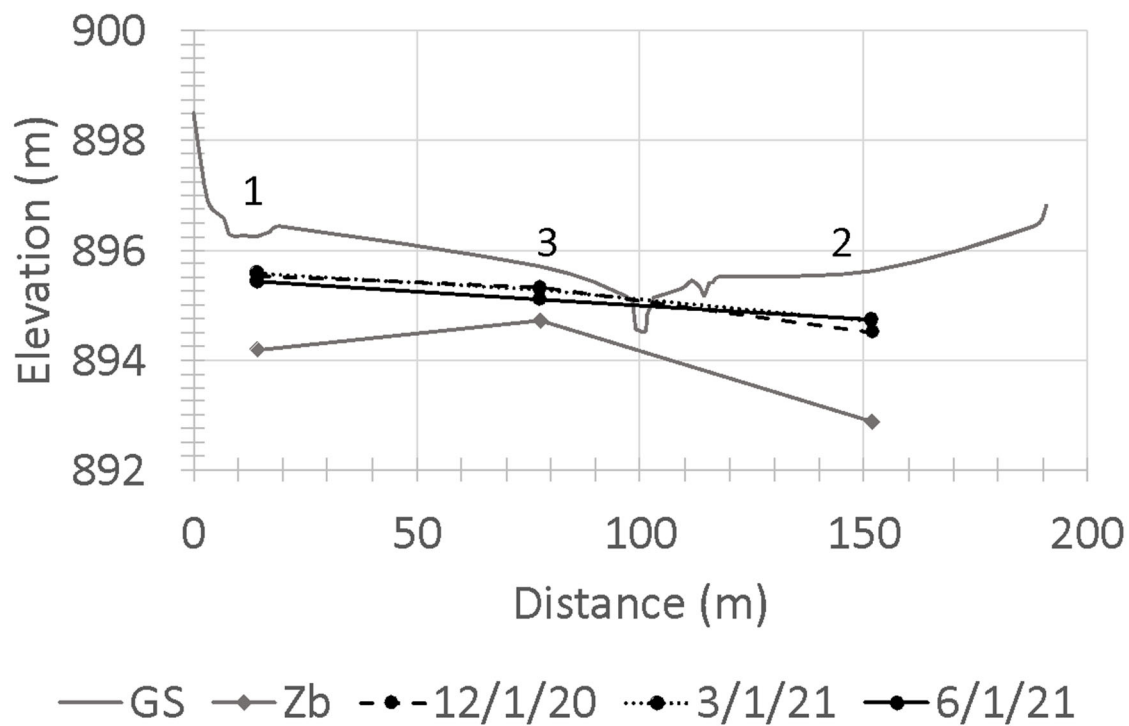


Figure 44. Cross section of Transect 1 water surface elevation at each well (1,3,2), ground surface (GS) and boundary layer Zb. Flow would be going into the page and the overall cross-sectional gradient is from river left to river right Wells. Well 3 is an instream proximal Well.

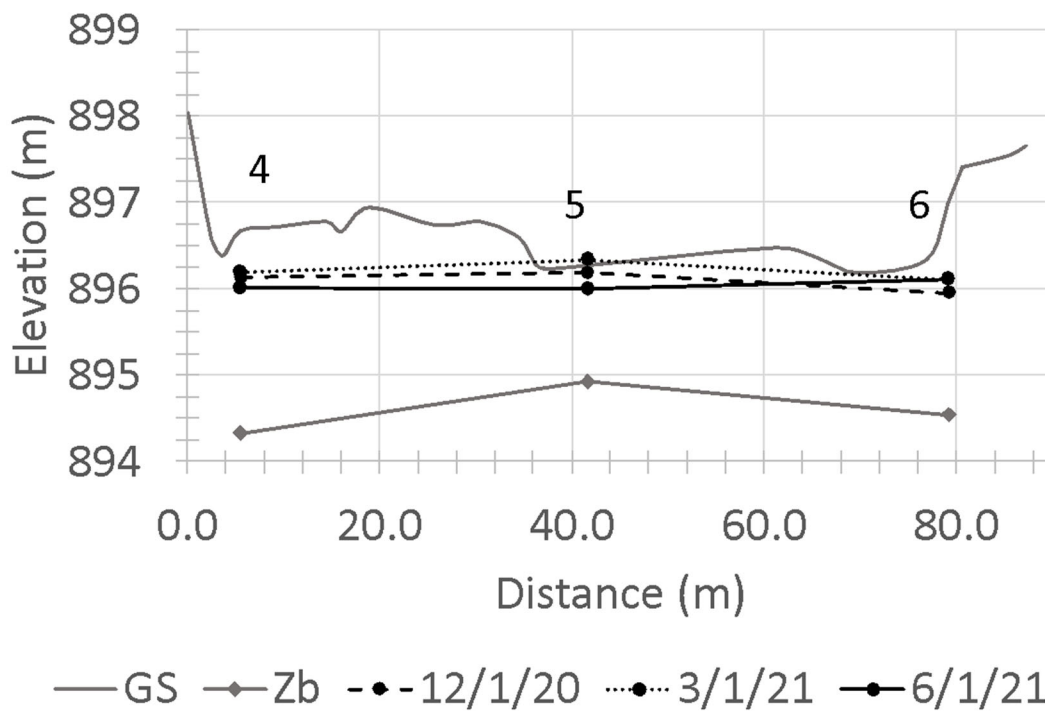


Figure 45. Cross section of Transect 2 water surface elevation at each well (4,5,6), ground surface (GS) and boundary layer Zb. Flow would be going into the page and the overall cross-sectional gradient is from the stream to RL and RR wells until baseflow conditions. Well 5 is an instream much of the year, however, becomes proximal sometime in spring as conditions dry out.

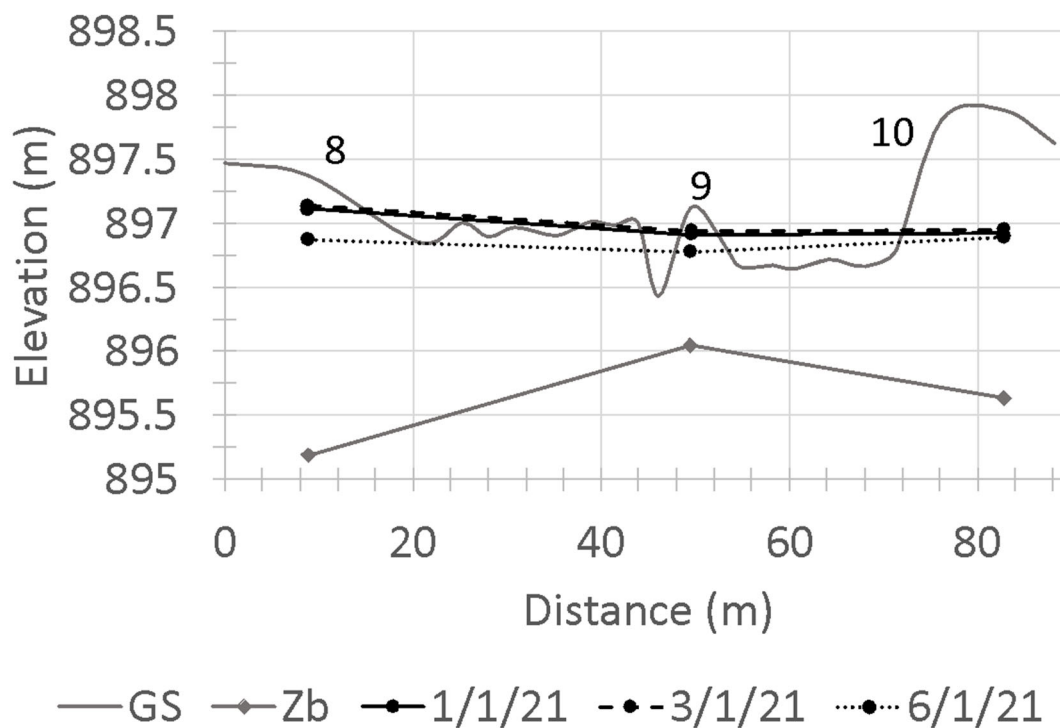


Figure 46. Cross section of Transect 3 water surface elevation at each well (8,9,10), ground surface (GS) and boundary layer Zb. Flow would be going into the page and the overall cross-sectional gradient is from RL and RR wells to the stream. Well 9 is instream proximal and is assumed to closely resemble river stage.

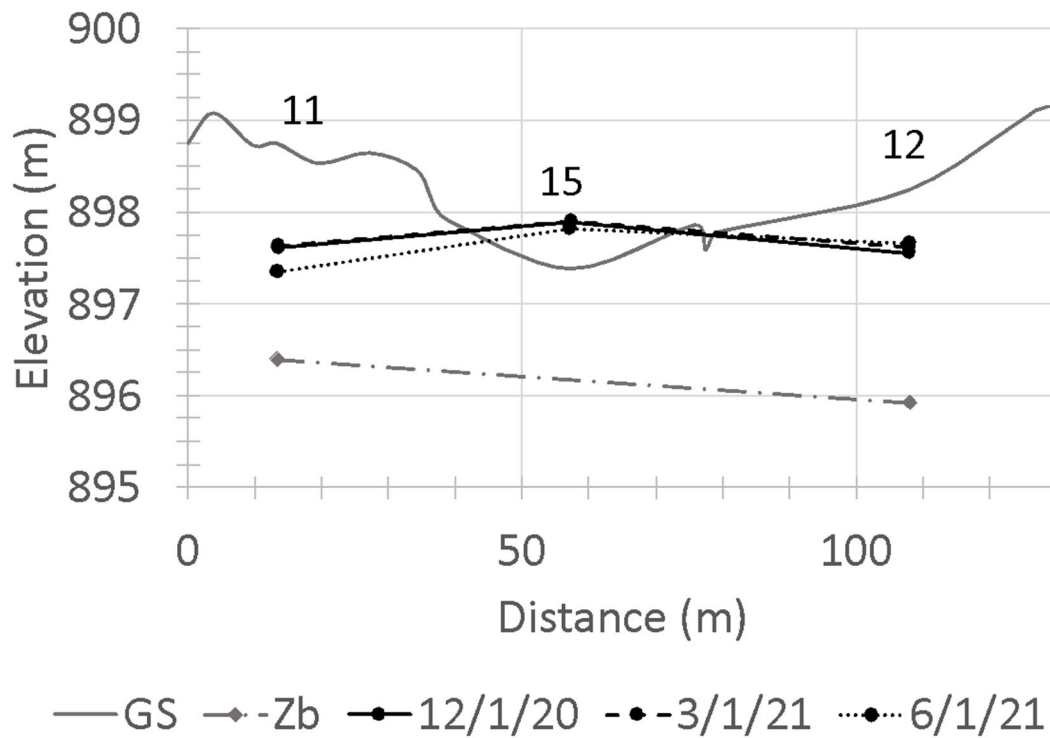


Figure 47. Cross-section of transect 4 water surface elevation at each well (11,15,12), ground surface (GS) and boundary layer Zb. Flow would be going into the page and the overall cross-sectional gradient is from the stream to RL and RR wells. Well 15 is instream stilling well, therefore, there is no estimate of Zb associated with this well.